In compliance with the
Canadian Privacy Legislation
some supporting forms
may have been removed from
this dissertation.

While these forms may be included
in the document page count,
their removal does not represent
any loss of content from the dissertation.

University of Alberta

Delineation of Structural Domains and Joint Sets at the Ekati™ Diamond Mine and Implications for Underground Mining

by

Michael William Martin ©

A thesis submitted to the Faculty of Graduate Studies and Research in partial fulfillment
of the requirements for the degree of Master of Science

in

Mining Engineering

Department of Civil and Environmental Engineering

Edmonton, Alberta

Fall, 2003

National Library
of Canada

Acquisitions and
Bibliographic Services

395 Wellington Street
Ottawa ON K1A 0N4
Canada

Bibliothèque nationale
du Canada

Acquisisitons et
services bibliographiques

395, rue Wellington
Ottawa ON K1A 0N4
Canada

Your file Votre référence
ISBN: 0-612-87827-9
Our file Notre référence
ISBN: 0-612-87827-9

The author has granted a non-exclusive licence allowing the National Library of Canada to reproduce, loan, distribute or sell copies of this thesis in microform, paper or electronic formats.

The author retains ownership of the copyright in this thesis. Neither the thesis nor substantial extracts from it may be printed or otherwise reproduced without the author's permission.

L'auteur a accordé une licence non exclusive permettant à la Bibliothèque nationale du Canada de reproduire, prêter, distribuer ou vendre des copies de cette thèse sous la forme de microfiche/film, de reproduction sur papier ou sur format électronique.

L'auteur conserve la propriété du droit d'auteur qui protège cette thèse. Ni la thèse ni des extraits substantiels de celle-ci ne doivent être imprimés ou aturement reproduits sans son autorisation.

Canada

University of Alberta

Library Release Form

Name of Author: Michael William Martin

Title of Thesis: Delineation of Structural Domains and Joint Sets at the Ekati™ Diamond Mine and Implications for Underground Mining

Degree: Master of Science

Year this Degree Granted: 2003

Permission is hereby granted to the University of Alberta Library to reproduce single copies of this thesis and to lend or sell such copies for private, scholarly or scientific research purposes only.

The author reserves all other publication and other rights in association with the copyright in the thesis, and except as herein before provided, neither the thesis nor any substantial portion thereof may be printed or otherwise reproduced in any material form whatever without the author's prior written permission.

Date: 17 July 2003

University of Alberta

Faculty of Graduate Studies and Research

The undersigned certify that they have read, and recommend to the Faculty of Graduate Studies and Research for acceptance, a thesis entitled Delineation of Structural Domains and Joint Sets at the Ekati™ Diamond Mine and Implications for Underground Mining submitted by Michael William Martin in partial fulfillment of the requirements for the degree of Master of Science in Mining Engineering.

Dr. D.D. Tannant (Supervisor)

Dr. C.D. Martin

Dr. M.H. Heimpel

Date: 17 July 2003

Abstract

Rock mass stability is of critical importance to the safety and economic viability of underground hard rock mining operations. Evaluation of discrete failure mechanisms requires that the structural geology of the area be well understood. Interpretation of structural data is often subjective; a quantitative approach is desired.

In the fall of 2001 a joint research project between BHP Billiton Diamonds Inc. and the University of Alberta was initiated to evaluate structural geology features at the Ekati™ Diamond Mine. The end objective of the project was to predict structurally controlled problems that may prohibit successful employment of the open bench underground mining method on the Koala North kimberlite pipe.

Structural geology data from a variety of sources was collected, manipulated and modelled into structural domains using statistical tools. It was determined that joint controlled instability mechanisms would not be sufficient to seriously jeopardize an operation at Koala North.

Acknowledgements

I would like to acknowledge the efforts of those people who assisted in the successful completion of the thesis. Many thanks go to my supervisor Dr. Dwayne Tannant whose guidance, help, and insight were essential in the completion of this thesis. I particularly enjoyed and learned much from our brainstorming sessions. Dr. Clayton Deutsch also provided valuable input in the thesis development, and Doug Booth kept all computer systems and applications running smoothly throughout.

Gratitude is also extended to the engineering and geology staff at the Ekati™ Diamond Mine for their significant assistance during the data collection stages of the program. Jody Todd, Darin Anonby and Gary Baldwin granted access to geotechnical data. Larry Long provided tours and computer models of underground mining operations. Dave Gill of Connors Drilling kindly answered any questions pertaining to diamond drilling. All efforts greatly added to the practical development of the thesis. Lastly, Scott Williams was instrumental in getting the project started.

The University of Alberta provided financial support for this thesis, which was greatly appreciated, as without I would be deeply in debt.

Finally, I would like to thank my family, friends and colleagues for their support during my time in the master's program. Graduate studies at the University of Alberta has been a very positive experience, and I would again like to thank all those who made it possible.

Table of Contents

CHAPTER 1 INTRODUCTION **1**

1.1 THESIS OBJECTIVES 1
1.2 SCOPE OF WORK 2
1.3 THESIS ORGANIZATION 3

CHAPTER 2 THE EKATI™ DIAMOND MINE **5**

2.1 LOCATION AND TOPOGRAPHY 5
2.2 CLIMATIC FACTORS 6
2.3 GEOLOGIC OVERVIEW 8
2.3.1 Regional Geology *8*
2.3.2 Diamond Genesis *8*
2.3.3 Local Geology *9*
2.3.4 Discontinuities *11*
2.4 KOALA, KOALA NORTH AND PANDA MINING AREAS 12

CHAPTER 3 ROCK MASS STABILITY AND MINING METHODS **14**

3.1 ROCK MASS STABILITY 14
3.2 SURFACE MINING METHODS 15
3.3 UNDERGROUND MINING METHODS 18

CHAPTER 4 COLLECTION OF STRUCTURAL GEOLOGY DATA **23**

4.1 SOURCES AND PROCESSING OF STRUCTURAL DATA 23
4.2 DIAMOND DRILL CORE LOGGING 24
4.2.1 Diamond Drilling *24*
4.2.2 Oriented Core Logging *25*
4.2.3 Geotechnical Rock Mass Logging *27*
4.2.4 Transformations *29*
4.3 LARGE AND SMALL-SCALE CELL MAPPING 32
4.3.1 Data Collection *32*
4.3.2 Transformations *34*
4.4 VIRTUAL CELL MAPPING 34
4.4.1 Data Collection *34*
4.4.2 Transformations *36*
4.5 CORRECTING FOR BIAS IN ORIENTATION DATA 36

CHAPTER 5 ROCK MASS STRUCTURAL DOMAINS DETERMINED FROM STRUCTURAL DATA **42**

5.1 REVIEW OF STRUCTURAL DOMAIN IDENTIFICATION 42
5.1.1 Importance of Domains *42*
5.1.2 Tests of Similarity *43*
5.2 STEREONET REPRESENTATION OF DATA 45

5.3 DETERMINING SPATIAL SIMILARITY OF JOINT ORIENTATIONS FROM THE COEFFICIENT OF CORRELATION 47
5.3.1 Definition of Coefficient of Correlation *47*
5.3.2 Stereonet Sensitivity and Comparison of Open Pits *49*
5.3.3 Similarity of Data from Different Sources *50*
5.4 STRUCTURAL DOMAIN DELINEATION 52
5.4.1 Correlogram with Depth *52*
5.4.2 Vertical Correlations *55*
5.4.3 Radial Correlations *57*
5.4.4 Prediction of Structural Domains at Distant Locations *62*

CHAPTER 6 JOINT SET SPACING AND SHEAR STRENGTH PROPERTIES. 67

6.1 REVIEW OF JOINT SET IDENTIFICATION 67
6.1.1 Importance of Joint Sets *67*
6.1.2 Tests of Similarity *68*
6.2 JOINT SETS AT EKATI™ MINE 69
6.2.1 Joint Set Identification and Characteristics *69*
6.2.2 Using Coefficients of Correlation to Help Identify Spatial Continuity of Joint Sets *74*
6.2.3 Determination of Structural Domain RQD *75*
6.3 SHEAR STRENGTH OF JOINTS 77
6.3.1 Empirical Analysis of Joint Shear Strength *77*
6.3.2 Lab Results and Comparison from Joint Shear Strength Testing *79*
6.4 SUMMARY OF STRUCTURAL DOMAINS AND MAJOR JOINT SETS AT THE EKATI™ DIAMOND MINE 82

CHAPTER 7 POTENTIAL ROCK MASS INSTABILITIES AT EKATI™ MINE 87

7.1 SURFACE TO UNDERGROUND TRANSITION 87
7.2 CAUSES OF INSTABILITY AND CONSEQUENCES OF FAILURE 89
7.2.1 Effects of Surface Mining on Underground Operations *89*
7.2.2 Gloryhole Conditions *92*
7.2.3 Underground Development *94*
7.3 HAZARD MITIGATION 95
7.3.1 Gloryhole Stability *95*
7.3.2 Development Stability *96*

CHAPTER 8 STABILITY ANALYSIS OF KOALA NORTH GLORYHOLE....... 97

8.1 RELEVANT FAILURE MECHANISMS AND REQUIRED INPUT 97
8.2 ANALYSIS METHODOLOGY 98
8.2.1 Wedge Failures *98*
8.2.2 Toppling Failures *101*
8.3 STABILITY INVESTIGATIONS 104
8.3.1 Structural Domain 1 Analysis *104*
8.3.2 Structural Domain 2 Analysis *106*
8.3.3 Structural Domain 3 Analysis *108*
8.3.4 Summary of Kinematic Failures *109*
8.4 DISCUSSION OF POTENTIAL FAILURE MECHANISMS 110

8.4.1 Failure Sizes *110*
8.4.2 Groundwater *112*
8.4.3 Blasting *113*
8.4.4 Implications of Stress *113*
8.5 Structural Implications for Development in Koala North 117
8.5.1 Recommended Cross-Cut Orientations for Kimberlite Pipe Access *117*
8.5.2 Gloryhole Support Issues *118*
8.5.3 Gloryhole Monitoring Issues *119*
8.5.3.1 Access 119
8.5.3.2 Instrumentation 121

CHAPTER 9 KOALA NORTH UNDERGROUND DEVELOPMENT STABILITY 124

9.1 Relevant Failure Mechanisms and Required Input 124
9.2 Stability Analysis 125
9.2.1 Methodology *125*
9.2.2 Investigation *128*
9.2.3 Discussion of Results *130*
9.3 Development Optimization 131
9.3.1 Drift Shape and Size *131*
9.3.2 Drift Support *132*

CHAPTER 10 SUMMARY AND RECOMMENDATIONS 137

10.1 Summary 137
10.2 Recommendations 141
10.2.1 Data Collection and Processing *141*
10.2.2 Determining Structural Domains and Joint Sets *142*
10.2.3 Stability Analysis for Underground Excavations *143*

CHAPTER 11 REFERENCES 144

CHAPTER 12 APPENDICES 150

12.1 Joint Roughness Table and Figures 150
12.2 Vector Mathematics for Joint Orientation Determination 153

Table of Tables

Table 4-1 Structural Geology Data Sources 24
Table 4-2 Oriented Core Logging Sheet 27
Table 4-3 Geotechnical Logging Sheet 27
Table 4-4 Diamond Drill Holes 28
Table 4-5 Database Header Fields with Associated Data Type 32
Table 4-6 Cell Mapping Log Sheet 33
Table 4-7 Modified Structural Dataset 41
Table 5-1 Lower Hemisphere Division Schemes 49
Table 5-2 Correlation Between Data Types 51
Table 5-3 Vertical Slices For Each Open Pit 52
Table 5-4 Correlations with Depth 53
Table 5-5 Koala Radial Correlation Results 58
Table 6-1 Joint Set Orientations 71
Table 6-2 Joint Set Spacing and Roughness Characteristics 73
Table 6-3 Structural Domain RQD Values 76
Table 6-4 Direct Shear Test Results 80
Table 6-5 Summary of Structural Domains and Joint Sets at Ekati™ Mine 86
Table 8-1 Summary of Wedge Failures in Koala North Gloryhole Wall 109
Table 8-2 Summary of Toppling Failures in Koala North Gloryhole Wall 110
Table 9-1 Potential Wedge Failures in Excavation Back 129
Table 9-2 Rock Bolt Support Attributes 135
Table 12-1 Alphanumeric to Numeric Laubscher Parameter Conversions (modified from Anonby, 2002) 150
Table 12-2 Vector Solution to Determine Fracture Orientation from Goniometer Measurements (from Call et al., 1981) 153

Table of Figures

Figure 2-1 Ekati™ and Area Map (modified from Mining Technology, 2002) 5
Figure 2-2 Permafrost and Ground Ice Conditions (modified from Andersland and Ladanyi, 1994) 7
Figure 2-3 Diamond Genesis Model (modified from Ashton Mining of Canada Inc., 2002) 9
Figure 2-4 Model of a Kimberlite Pipe (modified from De Beers Canada, 2003) 10
Figure 2-5 Plan View of Koala, Koala North and Panda Open Pits 13
Figure 3-1 Fault and Joint Structures in Panda Pit West Wall 15
Figure 3-2 Open Pit Mining of a Kimberlite Pipe (modified from Peterson and Tannant, 2001) 16
Figure 3-3 Panda Pit in Fall 2002 (photo courtesy of Darin Anonby) 17
Figure 3-4 Surface Mining Completed at Koala North Pit in 2001 (modified from Werniuk, 2003) 17
Figure 3-5 Koala North Underground Development 19
Figure 3-6 Sub-level Caving Mining Method Layout (modified from Mery, 2002) . 20
Figure 3-7 Plan View of Open Bench Layout 21
Figure 3-8 Koala North Level Cross-cuts 22
Figure 4-1 Core Orienting Goniometer (modified from Call et al., 1982) 25
Figure 4-2 "B" or "T" Core Designations (modified from Call et al., 1982) 26
Figure 4-3 Core Box Photograph 28
Figure 4-4 Goniometer Measurements (modified from RocScience geomechanics software and research, 2003) 29
Figure 4-5 Oriented Joint Data Locations 31
Figure 4-6 3D Image of Koala NW Benches 35
Figure 4-7 Sample Line Bias (modified from RocScience geomechanics software and research, 2003) 37
Figure 4-8 Correction Angle (modified from RocScience geomechanics software and research, 2003) 38

Figure 4-9 KGT-10 Diamond Drill Hole Blind Zone 40
Figure 5-1 Division of Hemispherical Surface into 100 Equal-Area Windows (modified from Mahtab and Yegulalp, 1984) 46
Figure 5-2 Values of ρ and Their Implications (modified from Scheaffer and McClave, 1995) 48
Figure 5-3 Vertical Correlogram of DDH Data 54
Figure 5-4 Koala Vertical Correlation 56
Figure 5-5 Koala Radial Correlations 59
Figure 5-6 Koala North Radial Correlations 60
Figure 5-7 Panda Radial Correlations 61
Figure 5-8 Summary of Quantified Structural Domains 62
Figure 5-9 Koala Directional Correlogram 63
Figure 6-1 Pole Plot Overlaid with Contour Plot Depicting Set Windows 70
Figure 6-2 Direct Shear Testing of Joints (modified from Mathis, 2002) 80
Figure 6-3 Stereonet of Contoured Joint Poles (A) and Joint Set Windows (B) in Koala Structural Domain 1 82
Figure 6-4 Stereonet of Contoured Joint Poles (A) and Joint Set Windows (B) in Koala Structural Domain 2 83
Figure 6-5 Stereonet of Contoured Joint Poles (A) and Joint Set Windows (B) in Koala North Structural Domain 1 83
Figure 6-6 Stereonet of Contoured Joint Poles (A) and Joint Set Windows (B) in Koala North Structural Domain 2 84
Figure 6-7 Stereonet of Contoured Joint Poles (A) and Joint Set Windows (B) in Koala North Structural Domain 3 84
Figure 6-8 Stereonet of Contoured Joint Poles (A) and Joint Set Windows (B) in Panda Structural Domain 1 85
Figure 6-9 Stereonet of Contoured Joint Poles (A) and Joint Set Windows (B) in Panda Structural Domain 2 85
Figure 7-1 Surface to Underground Transition at Koala North 88
Figure 7-2 Multiple Bench Planar Failure in Koala Pit, Spring 2002 (photo courtesy of Gary Baldwin) 89

Figure 7-3 Catchment Width Achievement on Panda 300 Bench 90
Figure 7-4 Unstable Section in Koala Pit West Wall 91
Figure 7-5 Kimberley Gloryhole, South Africa (modified from Aviation Adventure Tours, 2002) 92
Figure 7-6 Cross-cut Drawpoint 94
Figure 8-1 Wedge Undercutting in Panda Pit NW Wall 98
Figure 8-2 Wedge Formed by Intersection of Three Discontinuities with Gloryhole Wall (modified from Norrish and Wyllie, 1996) 99
Figure 8-3 Stereonet Wedge Failure Identification (modified from Norrish and Wyllie, 1996) 100
Figure 8-4 Block Toppling in a Hard Rock Mass with Widely Spaced Orthogonal Joints (modified from Hudson and Harrison, 1997) 102
Figure 8-5 Stereonet Toppling Failure Identification (modified from Norrish and Wyllie, 1996) 102
Figure 8-6 Stereonet Identification of Failures in Koala North Domain 1 (A – Wedge Failures, B – Toppling Failures) 104
Figure 8-7 Wedge Failures in Domain 1 105
Figure 8-8 Stereonet Identification of Failures in Koala North Domain 2 (A – Wedge Failures, B – Toppling Failures) 106
Figure 8-9 Wedge Failure in Domain 2 107
Figure 8-10 Centre of Gravity Influence on Stability 107
Figure 8-11 Stereonet Identification of Failures in Koala North Domain 3 (A – Wedge Failures, B – Toppling Failures) 108
Figure 8-12 Wedge Failures in Domain 3 109
Figure 8-13 Koala North Wedge in North Wall 111
Figure 8-14 Elemental Stress Distribution about a Circular Excavation (modified from Brady and Brown, 1993) 114
Figure 8-15 Boundary Stress Distribution around a Circular Excavation in a Hydrostatic Stress Field (modified from Brady and Brown, 1993) 114
Figure 8-16 Stressed Zones around an Elliptical Opening in a Hydrostatic Stress Field (modified from Brady and Brown, 1993) 115

Figure 8-17 Model of a 2D Rock Wedge 116
Figure 8-18 Plan View of Area in Domain 2 Possibly Requiring Artificial Support 118
Figure 8-19 Section Depicting Cable Bolt Gloryhole Wall Support 119
Figure 8-20 Plan View of Instrumentation Drift 120
Figure 8-21 Section of Instrumentation Installation 122
Figure 9-1 Kinematic Identification of a Falling Wedge (modified from Hudson and Harrison, 1997) 125
Figure 9-2 Kinematic Identification of Sliding Wedges (modified from Hudson and Harrison, 1997) 126
Figure 9-3 Slab Failure Due to Relief Along Sub-Horizontal Joint Set (modified from Hudson and Harrison, 1997) 127
Figure 9-4 Plan View of Development Drift and Cross-Cut Intersection 128
Figure 9-5 Modes of Failure (A - Falling, B - Sliding) 129
Figure 9-6 Slab Failure Example 130
Figure 9-7 Rock Bolt Wedge Reinforcement (modified from Brady and Brown, 1993) 133
Figure 9-8 Long Section of Development Drift Showing Rock Bolt Support of Wedge 135
Figure 9-9 Plan View of Rock Bolt Pattern 136
Figure 12-1 Laubscher B Parameter Small-Scale Roughness Profiles (modified from Laubscher, 1990) 151
Figure 12-2 Barton JRC Roughness Profiles (modified from Beer, 2002) 152

Table of Symbols

Orient1	Goniometer dip angle	=	degrees
Orient2, O2	Goniometre circumference angle	=	degrees
Orient3	Orient2 corrected for B/T	=	degrees
B/T	Bottom/top of top/bottom stick	=	-
RQD	Rock quality designation	=	%
P.L.	Compressive strength from Point load test	=	MPa
X	Easting	=	m
Y	Northing	=	m
Z, z	Elevation	=	m
l	direction cosine	=	dimensionless
m	direction cosine	=	dimensionless
n	direction cosine	=	dimensionless
r	radial distance (cylindrical coordinate)	=	m
θ	angle in horizontal plane (cyl. coord.)	=	degrees
JRC	Barton joint roughness coefficient	=	-
δ	Angle of intersection	=	degrees
D	True joint spacing	=	m
D'	Apparent joint spacing	=	m
α	Trend of line	=	degrees
β	Plunge of line	=	degrees
TCF	Terzaghi correction factor	=	-
X_i	Random variable at i^{th} location	=	-
Y_i	Random variable at i^{th} location	=	-
Z_i	Random variable at i^{th} location	=	-
n	Variable	=	-
ρ	Coefficient of correlation	=	dimensionless
h	Separation vector	=	m
C(0)	Variance	=	-

C(h)	Covariance	=	-
$\gamma(h)$	Variogram value	=	-
C	Covariance matrix between samples	=	-
d	Covariance sample estimator matrix	=	-
vo	Simulated value	=	-
wi	Kriging weights	=	-
vi	Value at ith location	=	-

τ	Shear strength	=	kPa
σ'_n	Effective normal stress	=	kPa
ϕ'	Total friction angle	=	degrees
ϕ'_r	Residual friction angle	=	degrees
i	Asperity friction angle	=	degrees
JCS	Barton's joint wall compressive strength	=	MPa
p	Far field stress	=	MPa
K	Stress ratio	=	-
σ_{rr}	Radial stress around normal to a boundary	=	MPa
$\sigma_{\theta\theta}$	Tangential stress parallel to a boundary	=	MPa

b	Wedge apex height	=	m
a	Half wedge face length	=	m
L	Length	=	m
λ	Half wedge apex angle	=	degrees

FS	Factor of safety	=	-
W	Wedge weight	=	tonnes
ψ	Sliding plane dip	=	degrees
γ	Angle between sliding plane and bolt	=	degrees
t	Force from rock bolt	=	kN
β	Dip direction of plane	=	degrees

Chapter 1

Introduction

1.1 Thesis Objectives

Presently the BHP Billiton operated Ekati™ Diamond Mine is entering a new phase of development. Mining of kimberlite pipes is now being planned to continue on via underground methods after the open pit phases have been completed. The first production from underground methods was realized in the fall of 2002 from a small test pipe – Koala North.

Of critical importance to the safety and economic viability of underground operations will be stability of the open pit walls and exposed gloryhole that lie above. Proper design, monitoring and stabilization methods for these exposed faces will be required. Design and development of underground workings must be done with structural features in mind.

To satisfy the above requirements it is necessary that the structural geology of the area be well understood. As such, the objectives of this thesis are as follows:

1) Collect and amalgamate existing structural geology data at the Ekati™ mine into one database,
2) Use statistical techniques to analyze the structural database to determine the spatial boundaries (structural domains) between zones of the rock mass that possess joints with different orientation characteristics,
3) Determine the orientation and strength properties of dominant joint sets within each structural domain,

4) Use knowledge of the structural domains and associated joint set characteristics to analyze the stability of gloryhole walls created at Koala North by underground mining.

5) Use the structural model to assess the stability of underground development drifts at the Koala North operation.

Completion of these objectives will allow a better understanding of the geologic structure and its implications for stability at the Ekati™ Diamond Mine.

1.2 Scope of Work

Structural geology information is needed for analysis of excavation behaviour. Accordingly, much fieldwork performed in the summer and fall of 2002 involved the logging of diamond drill core to delineate geologic structures, primarily joints, around and beneath existing open pit operations. This information in combination with consulting reports, surface discontinuity mapping, and diamond drill hole core logs from the previous eight years was used to create a structural geology database of the region.

Statistical tools were utilized on the structural geology database to identify structural domains around three existing open pit operations. Joint sets and their associated characteristics were extracted from the domains. Practical problems associated with underground mining at Koala North were then addressed using the information extracted from the database.

In the underground environment, gloryhole stability will be assessed in the context of the structural geology coupled with an assumed stress analysis. Optimal orientations for underground development, particularly the cross-cuts used to directly access the kimberlite pipe, are recommended. Various software packages were used to perform this analysis.

Possible support of the gloryhole wall via cable bolting is addressed. Appropriate systems for rock mass monitoring are proposed given the challenging geologic and climatic conditions at Ekati™.

The stability of underground development drifts was analysed using computer software. Finally, rock bolt support was designed to mitigate potential wedge failures in the drifts.

1.3 Thesis Organization

Site features of the Ekati™ Diamond Mine are introduced in Chapter 2 to give the reader a framework for the environment in which the site is situated. Geology and geotechnical features are briefly touched upon and serve to introduce the reader to some of the particular challenges encountered at this mine.

In Chapter 3, stability issues at the Ekati™ mine are discussed within the geologic framework introduced in Chapter 2. The current state of surface mining operations is also addressed in conjunction with the underground mining method to be employed upon completion of the open pit operations.

Chapter 4 describes the different sources of data available from which a structural model was created. The collection procedures for the data types are discussed, as are any transformations that where made to the raw data. Finally, the correction of sampling bias invoked by the different collection procedures is examined.

Chapter 5 involves a statistical analysis of the dataset. Issues to be addressed include: quantifying the similarity of data collected via different methods, assessing the sensitivity of results from analysis procedures, and creating structural domains at the Ekati™ Diamond Mine.

Chapter 6 looks in detail at the characteristics of dominant joint sets within the structural domains identified in Chapter 5. A summary of all structural information is presented which will be used to evaluate specific stability issues that are addressed in the remainder of the thesis.

In Chapter 7, particular areas of concern pertaining to mining operations outlined in Chapter 3 are elaborated upon. The causes and consequences of instability in these areas are focused on. Methods available for managing these hazards, which the remainder of the thesis will evaluate, are also proposed at this time.

Chapter 8 utilizes the findings of Chapter 6 to assess the stability of the Koala North gloryhole, which will be created by underground mining activities. Specifically, wall failure mechanisms and their impact on underground developments will be addressed. Support methods and instrumentation options are detailed as well.

Chapter 9, also utilizing the findings of Chapter 6, assesses the stability of the underground developments at Koala North. Rock bolting for underground support is examined.

Chapter 10 provides a summary of the work performed during the course of the thesis work. Any recommendations for future fieldwork and/or analysis procedures at the Ekati™ Diamond Mine are restated.

The Appendices follow the list of References and provide figures and tables referred to, but not included in, the main body of the thesis.

Chapter 2

The Ekati™ Diamond Mine

2.1 Location and Topography

The Ekati™ Diamond Mine is located approximately 300 km NE of Yellowknife in the Northwest Territories (NWT) of Canada. The geographic coordinates are 7,177,500 N and 520,000 E, roughly 100 km north of the treeline and 200 km south of the Arctic Circle. The map in Figure 2-1 depicts the proximity of the mine to the nearest communities and major bodies of water.

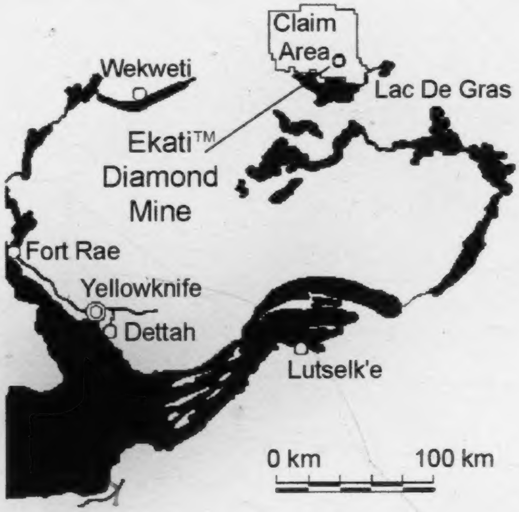
Claim Area
Wekweti
Lac De Gras
Ekati™ Diamond Mine
Fort Rae
Yellowknife
Dettah
Lutselk'e
0 km
100 km

Figure 2-1 Ekati™ and Area Map (modified from Mining Technology, 2002)

The Lac de Gras is the nearest large surface water deposit. On a more localized scale the area is pockmarked with small lakes and many interconnecting streams as the landscape, while undulating, is relatively flat. This terrain was formed by the retreat of glaciers at the end of the last ice age some 10,000 years ago.

2.2 Climatic Factors

The area generally receives an average annual precipitation of 400 mm with 50% occurring as snow. These figures would classify the region as a semi-arid desert, or tundra as it is termed in the north. However, water control is still a major issue as most of the surface moisture is stored in lakes or within the active layer (i.e. the depth down to which the ground annually undergoes freeze/thaw cycles). The nature of the terrain is such that many potential conduits exist for this water to infiltrate active mining areas.

In winter months temperatures reaching –40° C (without wind chill) are often encountered. Whiteouts, where diffuse light conditions make depth perception impossible, and blizzards are also frequent events. Thus, the installation and reading of rock mass monitoring equipment can be particularly challenging from an operational standpoint.

Temperatures in the summer months may reach 30° C. During this time various grasses, mosses/lichens, and shrubs grow over the rocky ground surface.

The project site is located in the continuous permafrost region of Canada (see Figure 2-2). Permafrost is defined as soil or rock having temperatures below 0° C over at least two consecutive winters and the intervening summer; moisture in the form of water and ground ice may or may not be present (Andersland and Ladanyi, 1994).

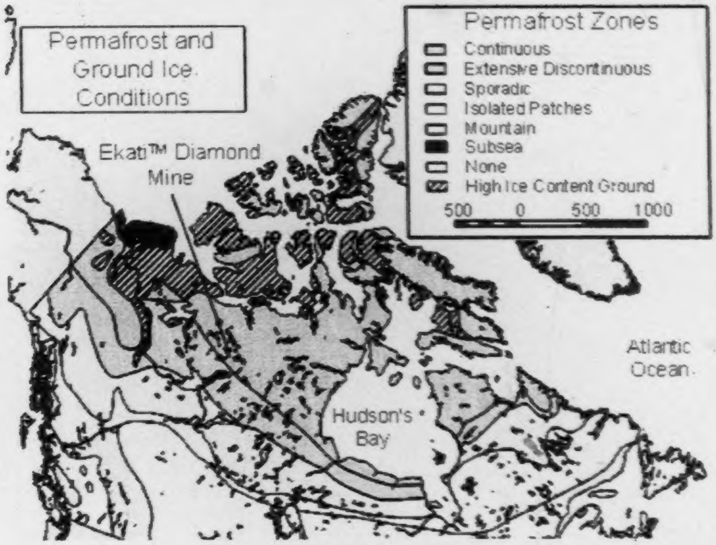
Permafrost and Ground Ice Conditions
Ekati™ Diamond Mine
Permafrost Zones
Continuous
Extensive Discontinuous
Sporadic
Isolated Patches
Mountain
Subsea
None
High Ice Content Ground
500
0
500
1000
Atlantic Ocean
Hudson's Bay

Figure 2-2 Permafrost and Ground Ice Conditions (modified from Andersland and Ladanyi, 1994)

Most kimberlite deposits are overlain by lakes, which act as thermal reservoirs thereby keeping the ground temperature above 0°C in winter months. Thus, permafrost is only encountered once into the host country rock, or at great depth into the kimberlite pipe itself.

Experience at Ekati™ shows that the extent of annual freeze/thaw is much more significant on south facing walls due to their increased exposure to sunlight in the spring. It was observed that ice-jacking caused instability problems perpetuate this area in the fall while ravelling of loose blocks is more common during spring freshet (i.e. annual snow melt) where washout of gouge material will initiate failures.

At the Ekati™ operation, terrain features in conjunction with climatic factors such as freeze/thaw cycles and eroding permafrost present unique geotechnical challenges encountered in few other mining environments.

2.3 Geologic Overview

2.3.1 Regional Geology

The area is located in what is known as the Slave Structural Province of the Canadian Shield. The Slave is a relatively small, although old, portion of Precambrian Shield totalling approximately 200,000 km^2 in area. It is composed of granites, gneisses, and supracrustal rocks (Pell, 1995).

The Slave Province is a classical setting for diamondiferous kimberlites - a stable Archean craton with, as suggested by seismic tomography, a cool mantle root (Anderson et al., 1992). The Ekati™ deposits are specifically located in a country rock deposit of granite. The kimberlite formations themselves are much younger than the host rock, being extruded some 52 million years ago.

2.3.2 Diamond Genesis

The kimberlite deposits in the Lac de Gras region are relatively young and occur in old hardrock formations. However, the diamonds themselves are generally much older than the host kimberlite pipe, which is the transportation system for the diamonds and not the actual source rock where their formation occurs (Ashton Mining of Canada Inc., 2002).

Diamond formation originates at depths of 150 km or more below the Earth's surface in the upper mantle. Depending upon temperature and pressure, carbon may form either graphite or diamond. The high-pressure region at the base of a craton is critical to diamond formation (shown in Figure 2-3).

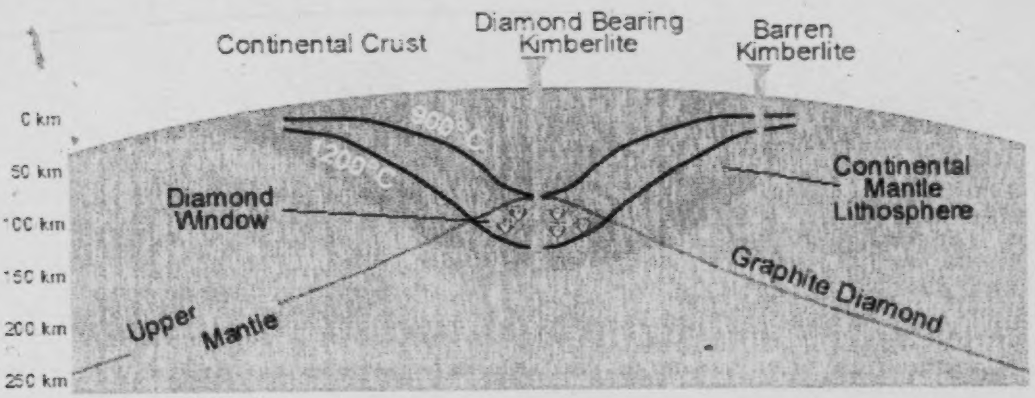
Continental Crust
Diamond Bearing Kimberlite
Barren Kimberlite
0 km
50 km
100 km
150 km
200 km
250 km
900°C
1200°C
Diamond Window
Continental Mantle Lithosphere
Graphite Diamond
Upper Mantle

Figure 2-3 Diamond Genesis Model (modified from Ashton Mining of Canada Inc., 2002)

Transportation of these diamonds to the surface is only possible in the case of an overlying archean craton, as this crustal structure extends to sufficient depth to provide a link to the surface. When kimberlite magma is forced through the crust by high internal pressures, the magma will sometimes carry with it diamonds. Figure 2-3 also illustrates this process.

2.3.3 Local Geology

A kimberlite pipe is generally subdivided into three regions (depicted in Figure 2-4); the crater facies - the surface expression of the pipe; the diatreme facies - the main body of the pipe; and the root facies, which go to great depth (Pell, 1995). Much of the crater facies zone in the Ekati™ deposits has been eroded away and so is not easily distinguishable from the lower diatreme region. The remaining crater facies region in these pipes along with the uppermost diatreme facies is where surface mining has been occurring. Below that, still in the diatreme facies, underground mining operations are planned to take place after surface operations have been completed.

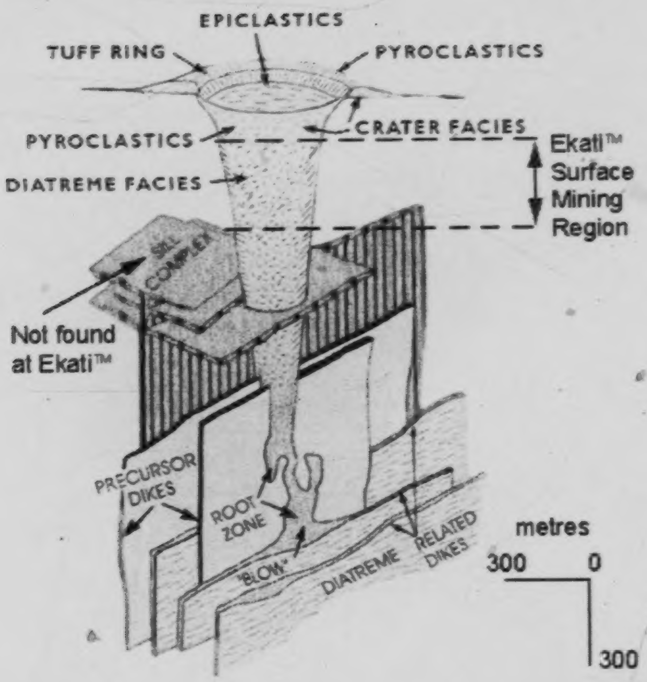
EPICLASTICS
TUFF RING
PYROCLASTICS
PYROCLASTICS
CRATER FACIES
DIATREME FACIES
Ekati™ Surface Mining Region
SILL COMPLEX
Not found at Ekati™
PRECURSOR DIKES
ROOT ZONE
"BLOW"
DIATREME
RELATED DIKES
metres
300
0
300

Figure 2-4 Model of a Kimberlite Pipe (modified from De Beers Canada, 2003)

The size of the kimberlite pipe itself can be quite variable. Small pipes have been found in the Ekati™ area with surface diameters in the 10's of metres. The next pipe to be mined at Ekati™, Fox pipe, has a surface diameter approaching 475 m.

The kimberlite itself is a rare variety of ultrabasic igneous rock consisting primarily of olivine, which upon increasing depth and under the proper conditions alters to serpentine. Note that a volume change of +90% is associated with this reaction, thus generating internal stresses within the pipe (Mathis, 1998). These stresses will generate internal shears within the pipe itself (Mathis, 1998); it is not known to what extent the host rock is affected by this activity.

The predominant host rock type is granitic. Certain areas may be predominantly composed of biotite granite or granodiorite (also referred to as quartz diorite), occasionally showing gneissose texture. Where a gneissic texture is dominant (i.e. segregation and alignment of biotite micas or chlorite), the rock will be weaker with a more pronounced strength anisotropy (Mathis, 1998).

Other lithologies in the vicinity include other varieties of granitods. For the purposes of this thesis, the term granite will be used to refer to all host rock in the Ekati™ region. Generally, the host rock is quite unaltered.

Near the surface, gravel and lesser amounts of sand and silt overlie the kimberlite pipes. Due to the erodable nature of kimberlite material, all pipes in the vicinity were at one point submerged beneath small lakes. These small bodies of water have since been drained and diverted to allow for mining activities to take place.

2.3.4 Discontinuities

Rock masses usually contain many structural features such as bedding planes, faults, fissures, fractures, joints and other mechanical defects which, although formed from a wide range of geological processes, possess the common characteristics of low shear strength, negligible tensile strength and high fluid conductivity compared to the surrounding rock material (Priest, 1993). The term discontinuity is used to cover the above mechanical defects without making any inferences about their geologic origins.

At the Ekati™ mine, both joints and faults are distinctly evident. Joints may best be described as fractures in rock along which there has been extremely little or no movement. A fault is a plane of shear failure where movement of the rock mass on either side of the plane has occurred. Priest (1993) notes that the characteristics of joints and faults from a geological perspective may have a long and complex history of changing stress, temperature, strain rate, materialization and recrystallization. In this thesis, no effort is made to deduce the history of any joint features from this perspective.

From Priest (1993), discontinuity properties that have the greatest influence at the design stage, of a surface or underground excavation, are:

- Orientation,
- Size,
- Frequency,
- Surface geometry,

- Genetic type, and
- Infill material.

To this end, joint information was collected at Ekati™ by various means; the end goal being to identify systematic joint sets (i.e. those occurring in planar, sub-parallel groups) which could be spatially assigned over certain areas, or domains, of the various mining areas. With this information, it is then possible to address more specific stability issues.

2.4 Koala, Koala North and Panda Mining Areas

The Ekati™ operation currently consists of five open pit developments (Panda, Koala, Koala North, Fox and Misery), with at least three more (Beartooth, Sable, Lynx) in the permitting process. Surface mining has been completed at Koala North where underground operations have already begun. These underground operations will ultimately branch off to Koala and Panda once their open pit phases have concluded.

Three of the aforementioned pits – Koala, Koala North, and Panda – are in close proximity, sharing similar geologic domains. Figure 2-5 is a plan view showing their location. Note that the depicted area is approximately 4 km^2. These three developments will be the focus of this thesis.

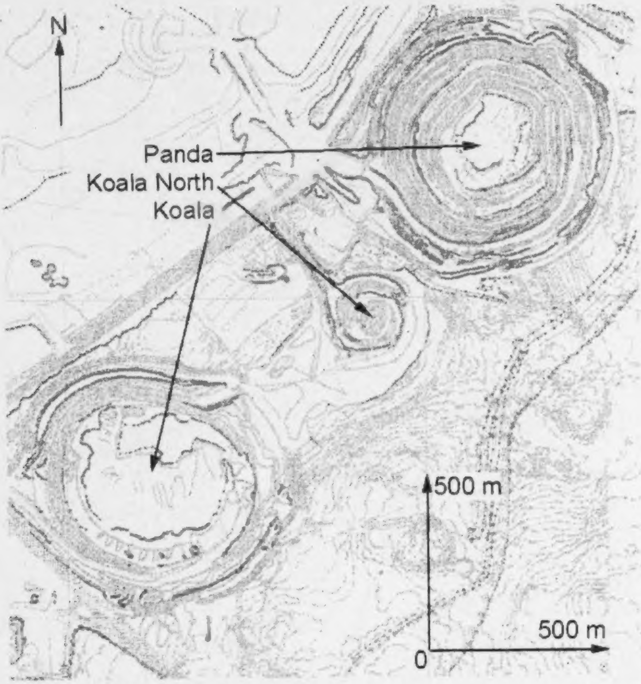
N
Panda
Koala North
Koala
500 m
500 m
0

Figure 2-5 Plan View of Koala, Koala North and Panda Open Pits

Chapter 3

Rock Mass Stability and Mining Methods

3.1 Rock Mass Stability

For both surface and underground mining methods, it is necessary to establish if structural features (i.e. discontinuities) will control wall stability or if failure is more likely to occur through intact sections of rock. As all kimberlitic material is extracted only properties of the host granite rock type need to be discussed.

The average density of the granite is around 2700 kg/m^3. From uniaxial compression tests, the granite has been found to be quite strong, with a compressive strength averaging 150 MPa (Mathis 2001) at atmospheric pressure.

Joint sets in the region have been found to be quite planar and continuous with minimum undulation, minor locking of asperities and minimal joint aperture. Thus, it is likely that while joints will be difficult to initially displace, once movement is initiated subsequent movement will occur relatively easily (Mathis, 1998).

It is observed that the majority of rock slope instability is caused by individual discontinuities. This is because the strength of the intact rock is usually quite high, with the result that the pre-existing discontinuities are the weakest link (Hudson and Harrison, 1997). Such is the case at Ekati™. However, it still must be determined whether structural failures will be discrete, or if a rock mass failure (i.e. more soil-like failure mechanism) is more probable. In other words, it must be determined if the rock mass is behaving as a discontinuum or a continuum.

Mathis (1998) used Bieniawski's rock mass rating (RMR) system, which takes into account rock strength, rock quality designation (RQD), discontinuity spacing, and groundwater effects, and determined that the majority of the host rock falls into the fair to good category (RMR = 40 to 80). An RMR < 40 is generally considered the point at which rock mass failure will substantially contribute to pit slope instability.

Thus, at the Ekati™ operation discrete structurally controlled failure mechanisms will dictate the stability of open pit slopes, as well as of any faces exposed through underground mining activities. The exact nature of these failure mechanisms is discussed in Chapter 7.

3.2 Surface Mining Methods

The Ekati™ Diamond Mine has to date used traditional open pit methods for mining, making use of the latest in truck-shovel technology. Due to the high strength of host granite, the pit designs have been based upon structurally controlled modes of failure (as opposed to rock strength parameters). The two classes of rock structure of concern are joints and faults. Figure 3-1 is a photograph in Panda pit showing fault and joint features quite clearly on a bench face.

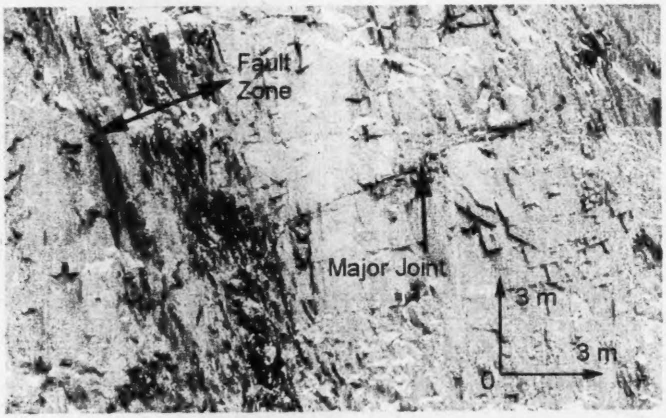

Figure 3-1 Fault and Joint Structures in Panda Pit West Wall

Due to generally favourable orientations of the above features bench angles to date have been close to 90 °. A 3 m spall allowance is allotted for in the design of most of the 14 m wide benches.

Benches are mined out in 15 m lifts with double benching utilized against the final wall such that a 30 m sheer face is left. This serves to increase the inter-ramp angle to approximately 70° and the overall pit slope to 45°. A steep overall pit slope is desired as the waste:ore extraction ratio is reduced, thereby improving economics and allowing surface mining to continue to greater depths. The surface mining of a typical kimberlite pipe is given in section in Figure 3-2.

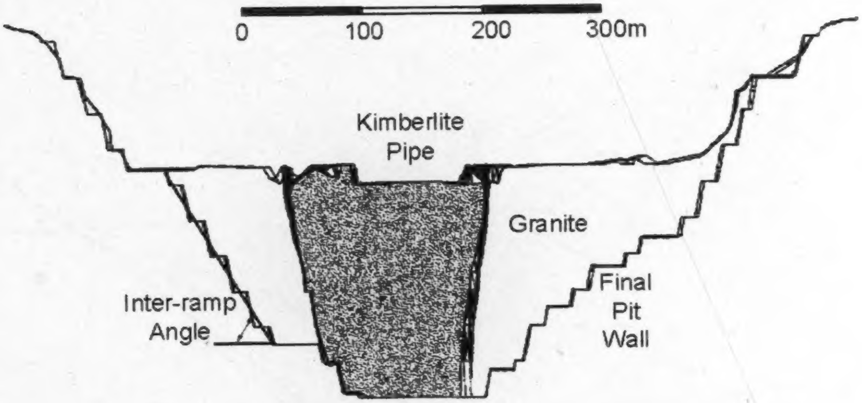

Figure 3-2 Open Pit Mining of a Kimberlite Pipe (modified from Peterson and Tannant, 2001)

The Panda pit will be the deepest operation terminating at approximately 165 m above sea level. Surface elevation of this pipe is 465 m above sea level, making the final pit 300 m deep. Commercial production at Panda started in the fall of 1998 and it is expected that surface mining will be completed in mid 2003. Underground operations are planned to come online sometime in 2004. Figure 3-3 depicts Panda pit in the fall of 2002, when the pit floor was already quite deep at 240 m above sea level.

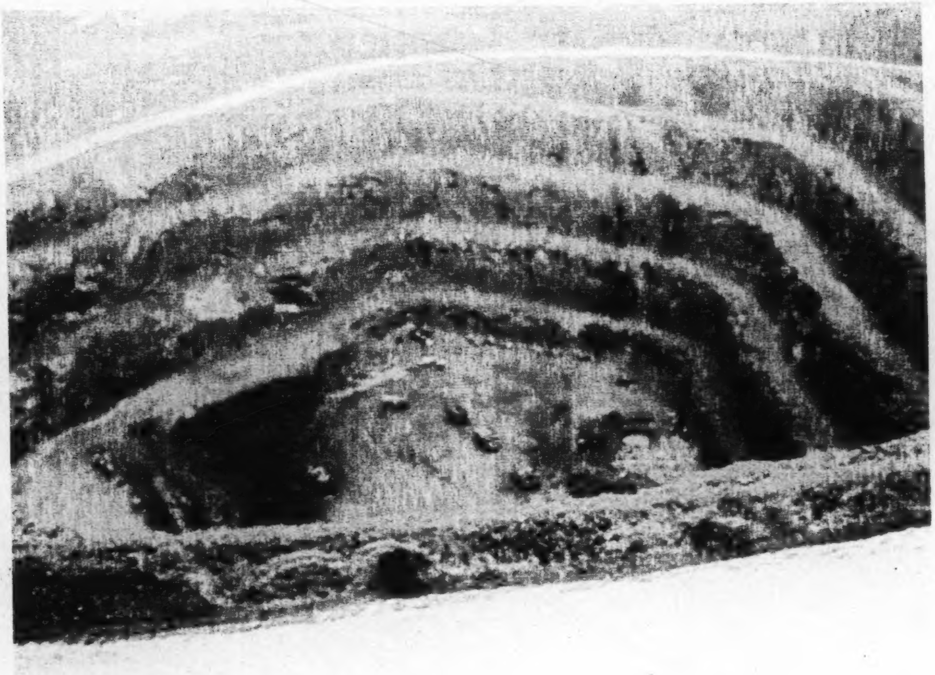

Figure 3-3 Panda Pit in Fall 2002 (photo courtesy of Darin Anonby)

As stated previously, Koala North is already in the underground mining stage. Open pit mining from 2000-2001 removed the top 70 m of ore from the Koala North pipe, ending at 405 m above sea level where the pipe is only 75 m in diameter (Werniuk, 2003). The state of the pit at this time is shown in Figure 3-4.

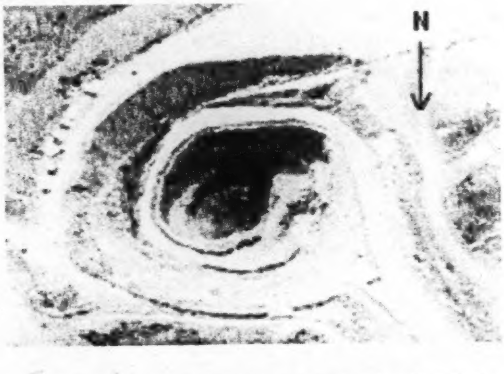

Figure 3-4 Surface Mining Completed at Koala North Pit in 2001 (modified from Werniuk, 2003)

The Koala pipe is larger in diameter than Panda, but operations will not proceed as deep due to less favourable economics. It is projected that underground development will start in late 2005.

To date, relatively minor geotechnical problems have been encountered in the open pits; the bulk of which stem from issues pertaining to permafrost degradation and freeze/thaw cycles. However, in some sectors of the open pits unfavourable joint orientations have necessitated the use of extensive cable bolting along with rock mass monitoring systems.

3.3 Underground Mining Methods

Underground development was initiated at Koala North with the excavation of a decline and ramp from which development drifts can be driven to access the kimberlite pipe. The underground mine will eventually include 11 levels over a vertical depth of 200 m to reach the 205 m above sea level elevation (Werniuk, 2003).

Ultimately adits will be driven off the decline to access the Panda and Koala pipes when their surface mining operations are completed. The layout for a completed Koala North underground mine is shown in Figure 3-5.

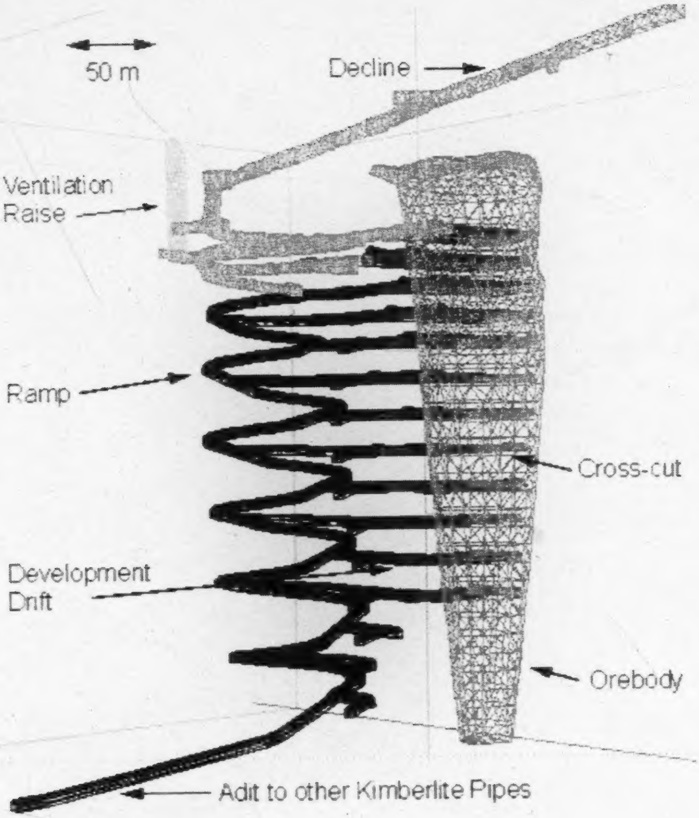
50 m
Decline
Ventilation Raise
Ramp
Cross-cut
Development Drift
Orebody
Adit to other Kimberlite Pipes

Figure 3-5 Koala North Underground Development

The decision to select an underground mining method for the Koala North pipe was based on technical, safety and economic constraints. Some of the most relevant features concerning kimberlite pipes are: hydrogeology, rock mass quality and strength, xenoliths, grade and grade distribution (SRK, 1995). Open benching, sub-level caving and benching with cemented fill were all considered as viable mining methods. In the end, it was concluded that open benching was the most practical and economic choice for Koala North (SRK, 2000).

Open benching was used successfully at De Beers' very large Finsch diamond mine in South Africa in the early years of its underground life during the 1990's (Werniuk, 2003). De Beer's Koffiefontein diamond mine also employs open benching (Harvey, 2003).

The open benching method is very similar to sub-level caving; the primary difference is that with open benching the drawpoints are pulled empty after every blast. In sub-level caving, some broken material is left behind to create a choke, thereby confining future blasts and keeping the ore near to the drawpoint. A hypothetical sub-level cave operation depicting various stages in the mining sequence is shown in Figure 3-6.

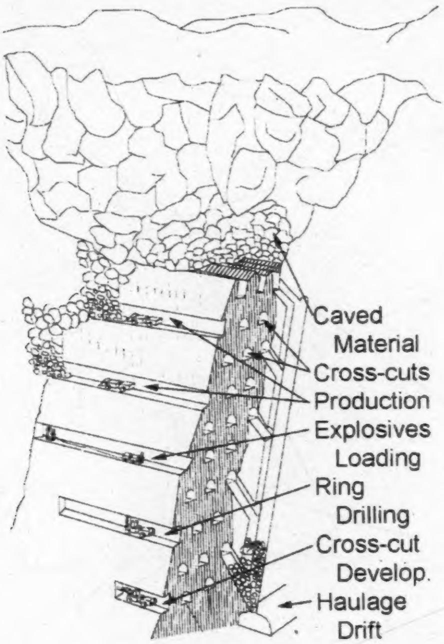

Figure 3-6 Sub-level Caving Mining Method Layout (modified from Mery, 2002)

As can be seen in Figure 3-5, a ramp is excavated adjacent to the kimberlite orebody. One development drift per level will be then be accessed from the ramp. The drift is then connected to three cross-cuts, likely reducing to two as the orebody narrows with depth. Cross-cuts are on 17.5 m centres, and from one level to the next are offset by half this in order to produce a typical diamond shaped draw cone. Levels are separated by a 15 m to 20 m difference in elevation; width and height dimensions for a cross-cut with an arched back are roughly 3.8 m by 4 m.

A slot raise is developed to connect the three cross-cuts as a free face before production blasting occurs. Fans of blastholes are drilled upwards from the cross-cut drifts. Production shots will be taken on alternating cross-cuts, all retreating back towards the development drift. As one sublevel is finishing up the next level will be starting. Figure 3-7 is a plan view of the operation on one sub-level.

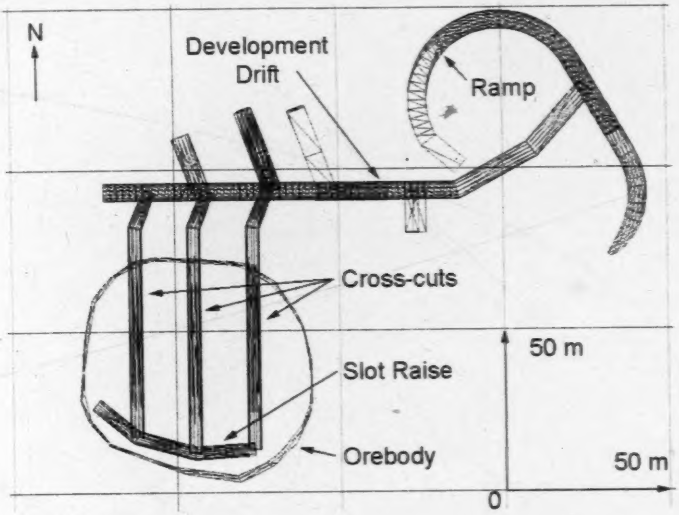

Figure 3-7 Plan View of Open Bench Layout

The orebody is currently mined out by retreating to the north. Of particular concern will be stability of the brow of each cross-cut at the kimberlite/granite interface. As scoops are remotely operated human injury is not likely, however, damaged equipment stranded out in the stope or large fragments of waste material requiring secondary blasting will call for mining personnel to be in the area.

If the brow is located in poor quality rock mass, reinforcement and additional ground support will be necessary. Rock bolts, wire mesh, shotcrete and possibly spray-on liners could all be employed. The optimal cross-cut orientation can be determined from examination of the structural geology in the area (Chapter 7), thereby reducing the need for ground support and diminishing the safety hazard to miners and equipment alike. Figure 3-8 depicts the beginning of underground mining at Koala North.

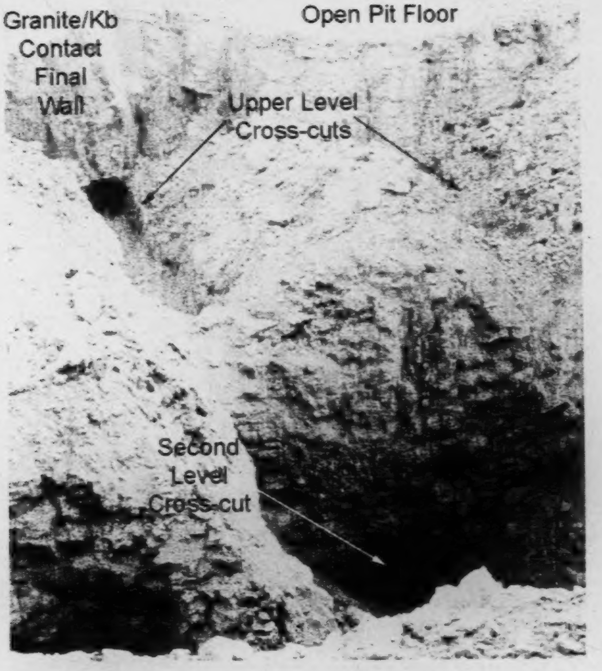
Granite/Kb Contact Final Wall
Open Pit Floor
Upper Level Cross-cuts
Second Level Cross-cut

Figure 3-8 Koala North Level Cross-cuts

Note that no crown pillar will be left; eventually the mined-out pipe will be a very steep-sided gloryhole in essentially the shape of the kimberlite pipe. Long-term reclamation calls for the gloryhole to fill with water to form a very deep lake.

Ultimately, if open benching works well at Koala North there is a good possibility that it will be the underground mining method employed on the Panda and Koala pipes. Before stability issues associated with mining activities are analyzed, information on structural features is required. The collection of this data is discussed next.

Chapter 4

Collection of Structural Geology Data

4.1 Sources and Processing of Structural Data

Geologic structure characteristics and the orientation of the pit wall relative to the structure orientations usually determine the attainable slope angle on rock (Nicholas and Sims, 2000). These same structures have an equally significant impact on the stability and safety of underground openings and excavations. This chapter deals with the characterization of geologic structures.

A variety of sources were available from which structural data could be extracted. The most important of these sources included diamond drill core logging, large-scale cell mapping, small-scale cell mapping and virtual cell mapping data.

The focus of this chapter will be the collection, manipulation, and correction of joint orientation data. While strength parameters are collected, they are dealt with in more detail in Chapter 6.

As it is desired to create one large database from which a structural geology model can be generated, it is important to keep in mind that when dealing with different datasets statistical similarity must be proven; otherwise amalgamation may produce meaningless results. Table 4-1 shows the number of data points (all containing joint orientations) collected from the four available sources. Each of these sources will be discussed in turn.

Table 4-1 Structural Geology Data Sources

Pit	Data Source	# Data
Koala	Diamond Drill Hole	5889
Koala North	Diamond Drill Hole	1220
Panda	Diamond Drill Hole	1469
	Sum	*8578*
Koala	Large-scale Cell Mapping	751
Koala North	Large-scale Cell Mapping	0
Panda	Large-scale Cell Mapping	373
	Sum	*1124*
Koala	Small-scale Cell Mapping	834
Koala North	Small-scale Cell Mapping	0
Panda	Small-scale Cell Mapping	0
	Sum	*834*
Koala	Virtual Cell Mapping	156
Koala North	Virtual Cell Mapping	0
Panda	Virtual Cell Mapping	0
	Sum	*156*
	TOTAL	10692

4.2 Diamond Drill Core Logging

4.2.1 Diamond Drilling

By far the most abundant form of data collected, the logging of the core collected from diamond drill holes (DDH) was also the only method employed capable of determining structures not daylighting on exposed faces. Consequently, data collected via this method is the only type that gives information on structures existing at depth (i.e. below current open pit operations).

Triple-tube core barrels were utilized when drilling to maximize core recovery. This is especially important when looking for in-filled joints (i.e. clay, calcite) or fault gouge. Triple-tube core barrels also minimize disturbance to the core, thus making it easier to determine its orientation. Both HQ and NQ core was drilled; HQ core indicates a nominal diameter of 65 mm while NQ indicates a nominal diameter of 50 mm.

A clay imprint of the bottom of the hole is taken every 9.1 m (30 ft or every 3rd run). This imprint is matched to the top of the succeeding core run, the drill core is pieced together, and a reference line representing the drill hole is scribed on each core (Call et al., 1982). Fracture orientations are then measured relative to the reference line and core axis. Unfortunately, in areas of highly fractured core and/or poor recovery this reference line is frequently lost. Also note that with the clay imprint method vertical holes cannot be used, as reference line placement relies on the force of gravity positioning an eccentric weight.

Upon completion of the hole, electronic instrumentation such as a Maxibore (optical instrument) or Gyroscope (rotational instrument) was lowered down the hole to determine the actual orientation of the drill hole itself. The drill hole survey information is required when determining joint orientations. The survey is also used to check the amount of drill hole deviation occurring.

4.2.2 Oriented Core Logging

The recovered core is logged for certain geotechnical parameters. The depth along the drill hole of joint features is noted. Orientations of joints in the drill core are then measured relative to the core axis and the reference line using a goniometer, as shown in Figure 4-1.

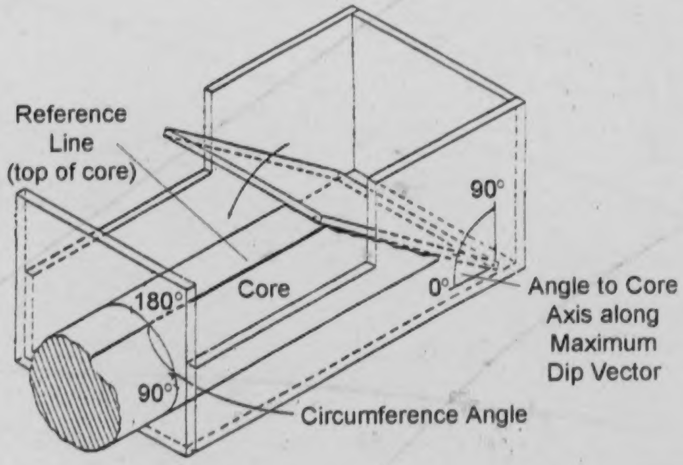
Reference Line (top of core)
90°
Core
180°
0°
Angle to Core Axis along Maximum Dip Vector
90°
Circumference Angle

Figure 4-1 Core Orienting Goniometer (modified from Call et al., 1982)

The core axis angle is recorded as *Orient1* and the circumference angle as *Orient2*. It is also important to specify which side of the fracture is measured. General convention is to measure the *B* end of the top stick as shown in Figure 4-2.

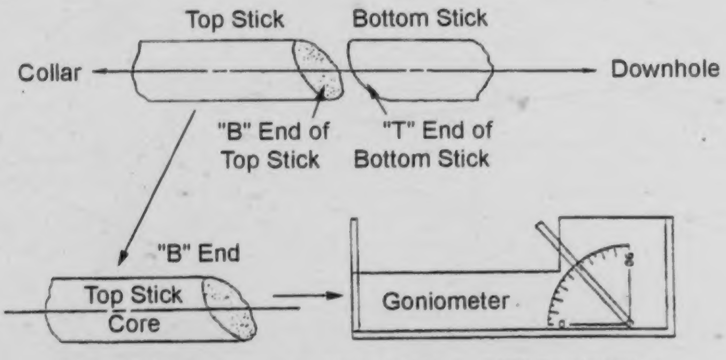

Note: This Measurement Would Have a "B" Designation

Figure 4-2 "B" or "T" Core Designations (modified from Call et al., 1982)

In conjunction with the drill hole orientation (from Maxibore or Gyroscope instrumentation) it is now possible to determine the true dip and dip direction of the discontinuity.

Goniometer measurements are of particular importance. In a structurally controlled environment, it is difficult to assess the risk for failure on a given bench if the joint orientations are unknown. As Ekati™ pit stability is structurally controlled, structural information is necessary such that kinematic modes of failure can be analyzed. With this in mind, only joints with orientations were selected for inclusion in the database (see Table 4-1).

After orientation measurements, the Laubscher (1990) mining rock mass rating (MRMR) system is used to characterize the joint conditions. Characters A through D represent the Laubscher parameters of large-scale joint roughness, small-scale joint roughness, joint wall alteration and joint filling respectively. A figure used for estimating the small-scale roughness parameter is located in the Appendices.

The type of fill and the presence or absence of water, as well as any other comment the logger wishes to make, can be noted. All depth, orientation and joint parameters are recorded on a core-logging sheet as shown in Table 4-2.

Table 4-2 Oriented Core Logging Sheet

Date: 10 July 2002 ***Hole ID:*** KGT-XX
Project: Koala ***Logged By:*** MM ***Core Dia.:*** HQ ***Page:*** 1/10

B/T	**Joint Depth (m)**	**Orient1 (°)**	**Orient2 (°)**	**Laubscher MRMR Parameters**				**Fill Type**	**Comments**
				A	**B**	**C**	**D**		
B	10.48	54	010	80	85	100	100	-	
B	15.53	30	170	75	75	100	90	Ca	
T	15.58	72	350	60	60	100	60	Cy	1 cm gouge
	... etc.								

4.2.3 Geotechnical Rock Mass Logging

Details regarding the condition of the rock mass are recorded on a different form. A sample of this form, a geotechnical-logging sheet, is shown in Table 4-3.

Table 4-3 Geotechnical Logging Sheet

Date: 10 June 2002 ***Hole ID:*** KGT-XX
Project: Koala ***Logged By:*** MM ***Core Dia:*** HQ ***Page:*** 1/4

Rock Mass Paramters				**Intact**	**Average Joint Conditions**						
				P.L.	Natural	Mech.	Ave. MRMR Values				
From	To	Length	RQD	(MPa)	Fractures	Fractures	A	B	C	D	Comments
10.48	12.53	3.05	100%	150	4	5	80	85	100	100	
13.53	16.58	3.00	90%	140	6	6	75	75	100	95	
16.58	19.62	2.83	80%	155	12	7	75	65	100	65	
	..etc.										

As a drilling run is 3.1 m (10 ft) long, the RQD is conveniently calculated over this distance to establish the competency of the rock. The measured core length over a run can then be used to calculate core recovery. Note that mechanical fractures (i.e. those caused during the drilling process) must not come into the RQD calculation and are also not logged. Misclassification of fractures can be a problem and is a source of error. Rock strength is typically estimated either by hammer blows or by the point load test. Average Laubscher parameters are also assigned over the run.

After logging is completed, samples may be vacuum sealed and sent off to a laboratory if information that is more precise is required (i.e. moisture content, bulk density, shear strength of discontinuities, compressive strength of intact rock). The core boxes are then photographed, as in Figure 4-3, and stored. On each photograph the hole identification, date, box number and core location is noted for future reference.

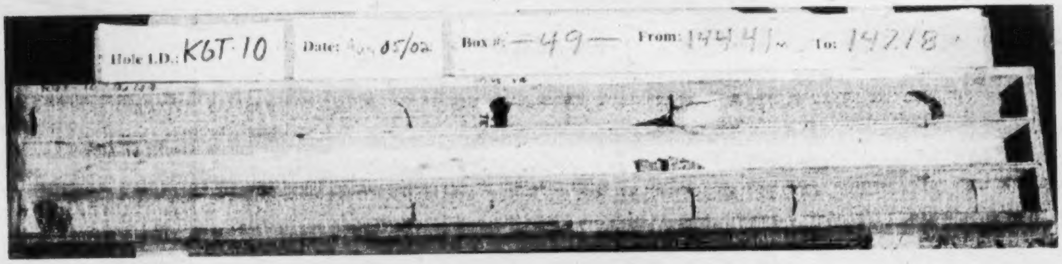

Figure 4-3 Core Box Photograph

In total, geotechnical information was gathered from forty-five different oriented diamond drill holes; these are grouped in Table 4-4 according to which mining area the data pertain to.

Table 4-4 Diamond Drill Holes

PIT	Koala		Koala North	Panda
DRILLHOLE I.D.	KDC-03	KGT-04	KDC-15	PDC-03
	KDC-04	KGT-05	KDC-16	PDC-04
	KDC-05	KGT-06	KDC-17	PDC-07
	KDC-08	KGT-07	KDC-18	PDC-08
	KDC-10	KGT-08	KNGT-08	PDC-09
	KDC-11	KGT-09	KNGT-09	PUC3-1
	KDC-12	KGT-10	KNGT-10	PGT-01
	KDC-13	KGT-11	KNGT-11	PGT-02
	KDC-19	KGT-12		PGT-03
	KGT-01	KGT-13		PGT-04
	KGT-02	KGTS-01		PGT-05
	KGT-03	KGTS-02		PGT-34
				PGT-36

These core logs span a period of eight years and consequently many core loggers have been utilized in the process. While efforts are made to ensure consistent reporting, different instructions and changing reporting systems have led to variable data quality and accuracy. However, for this thesis the joint orientation values made by the goniometer are the most critical. As these are somewhat less subjective, it is hoped that this variability is reduced.

4.2.4 Transformations

Once collected, the drill hole core logging files must be modified to be in a consistent format with one another such that they can be amalgamated and one database constructed. As much of the raw data is in different formats, it is necessary to transform some variables.

Firstly, note that goniometers are not all the same and may measure from different reference points. It is necessary to confirm what device was used to record the readings so that all can be transformed to a common system. The readings obtained from Ekati™ were all made with one type of goniometer device (which was shown in Figure 4-1) and using the conventions previously discussed. Certain software packages in use at the Ekati™ mine such as the RocScience program DIPS require a different convention. The DIPS convention is depicted in Figure 4-4.

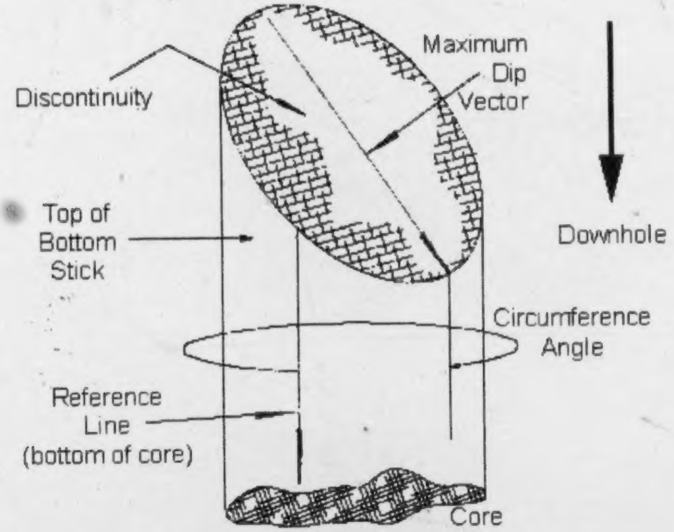

Figure 4-4 Goniometer Measurements (modified from RocScience geomechanics software and research, 2003)

A simple angle correction was performed based on the *B/T* and *Orient2* variables in Table 4-2 to convert to the DIPS format. Only measurements made on the *T* stick need correcting. In Eqn 4-1 *Orient3* represents the corrected *Orient2* (*O2*).

$$Orient3 = If(O2 < 180^{o}, then = 180^{o} - O2, else = 540^{o} - O2) \qquad \text{Eqn 4-1}$$

The conversion is necessary for DIPS to correctly calculate the true dip and dip direction of discontinuities, given the relative measurements from the goniometer and the orientation of the drill hole from Maxibore or Gyroscope instruments. Manual conversions were also performed such that DIPS was not needed to determine the true orientation of features. The vector mathematics are given in the Appendices.

Concerning rock mass classification schemes, the use of Laubscher's MRMR system at Ekati™ mine has evolved over the years. In earlier logs, an alphanumeric legend was used to assign values to the A, B, C, and D fields of Table 4-2. The latest system is numerical and assigns a value of 0 to 100 for each of the fields. The alphanumeric to numeric conversion chart used is given in the Appendices.

Spatial coordinates (*X*, *Y* and *Z*) for each measurement were also computed from the orientation and collar coordinates of each drill hole. Clustering of data sampling can be seen in Figure 4-5, where all 8,578 drill hole sample points are plotted. The 2212 mapping points are also shown and are distinguished by being located near the top of sample clustering and by occurring in horizontal arcs. The points in Figure 4-5 define the open pits quite well.

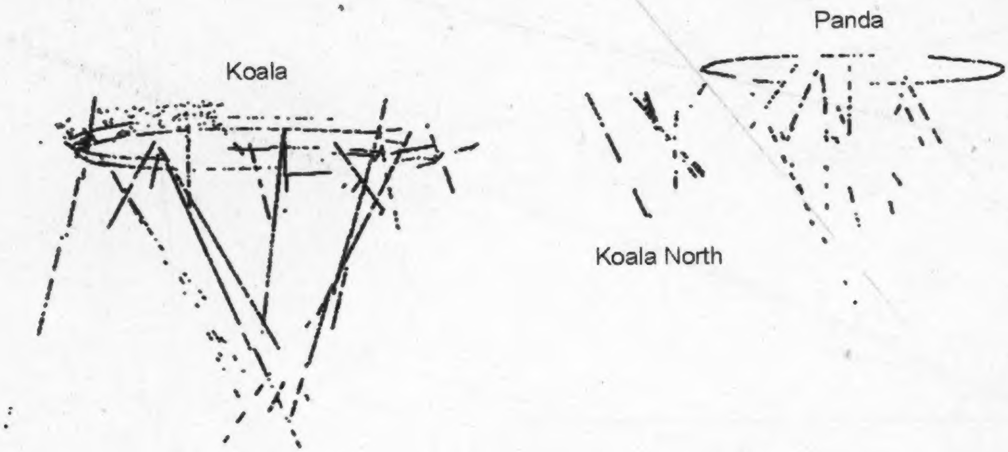

Figure 4-5 Oriented Joint Data Locations

As stereonets will be a useful tool when dealing with orientation data, the plunge and trend of each plane's pole was calculated. From the trend and plunge values direction cosines were determined.

It is common for open pits to be separated into pie-like pieces that represent different structural domains. In order for structural domains to be analyzed later, a central reference point was therefore assigned to each open pit and all nearby data points assigned cylindrical coordinates (i.e. radial distance, angle, and elevation).

Completed conversions and transformations were then placed in a database, with header fields as shown in Table 4-5. Note that not all fields apply to discussions under drill hole data; a 1 in Table 4-5 indicates applicable fields, a 0 indicates a non-populated field for that data type.

Table 4-5 Database Header Fields with Associated Data Type

Field Data Type	Diamond Drill Hole	Small Scale Map	Large Scale Map	Virtual Map
Orient 1	1	1	1	1
Orient 2	1	1	1	1
Traverse	1	1	1	1
DH Distance	1	0	0	0
Laubscher A	1	0	0	0
Laubscher B	1	1	1	0
Laubscher D	1	1	1	0
Code	0	1	1	0
X Coord.	1	1	1	1
Y Coord.	1	1	1	1
Z Coord	1	1	1	1
Ends	0	1	0	0
Pole plunge	1	1	1	1
Pole trend	1	1	1	1
l dir. cosine	1	1	1	1
m dir. cosine	1	1	1	1
n dir. cosine	1	1	1	1
r (cyl. coord.)	1	1	1	1
θ (cyl. coord.)	1	1	1	1
Data type	1	1	1	1
Pit domain	1	1	1	1

4.3 Large and Small-Scale Cell Mapping

4.3.1 Data Collection

Scan-line mapping is a systematic spot sampling method in which a measuring tape is stretched along the bench face or outcrop to be measured. For all fractures along the tape, orientation, length, roughness, filling type and thickness are recorded (Nicholas and Sims, 2000). Cell mapping is similar to the above but involves identifying the above discontinuity features within a window on the bench face. This method is sensitive to the condition of the exposed bench faces (i.e. muck obscuring face, obstruction due to ravelled material, degree of damage from blasting, etc.).

In large-scale cell mapping only larger discontinuities that extend for the full height of the bench (15 m) or longer are recorded. In small-scale mapping a window on the bench face 1.5m up from the bench floor and extending horizontally is mapped for all joint features (measurements made at mid-height). A sample log sheet is shown in Table 4-6.

Table 4-6 Cell Mapping Log Sheet

Start X,Y, Z Coord.	**Bearing**	**Distance**	**Strike**	**Dip**	**JRC**	**Infill**	**Code**	**Rock Type**	**Ends**
0,0,0	54 deg.	5 m	170	75	11	Ca	Joint	GD	0
		5.25	155	56	9	Cb	Fault	GD	1
		5.45	160	54	9	Cb	Fault	GD	1
	... etc.								

The strike and dip of a discontinuity are measured with a compass. Any infilling is noted and the roughness is estimated using the Barton (1985) joint roughness coefficient (JRC). A figure used for estimating JRC is located in the Appendices.

If the discontinuity is a fault, this is noted under the Code field. In small-scale mapping the Ends field is used to indicate if the discontinuity crosses completely through the window or terminates inside, thus giving a very rough indication of a joint's trace length (something not possible when logging diamond drill core). Another advantage cell mapping has over core logging is the identification of fault zones. At the Ekati™ mine these are fairly obvious when exposed on a bench face, yet interpreting them from drill core can be more challenging and is only obvious by looking for an extremely broken zone in the core. Due to this brokenness orientation is frequently not possible and thus a 3-point problem, needing two additional boreholes, is required to determine the orientation of a fault zone.

As with the diamond drill core logging, many different individuals completed cell map forms. In particular, small-scale mapping errors may be introduced by an inexperienced mapper that mistakes blast damage for in-situ joint features, much as the inexperienced core logger will record mechanical fractures. It is not possible to catch these mapping errors, however, data garnered from large-scale mapping and drill holes in the vicinity should support the small-scale data. Thus, a statistical analysis was performed as a check and the results are discussed in Chapter 5. For additional information on cell mapping, Nicholas and Sims (2000) provide an excellent overview.

4.3.2 Transformations

To make cell map data consistent with the transformed core logging data some modifications must be made. Firstly, strike is converted to dip direction. Secondly, the JRC parameter was used to classify joint roughness for cell mapping while the MRMR system (specifically the Laubscher B parameter identifying small scale joint roughness) was used when logging drill holes. JRC ranges from 0 to 20, while corresponding B values range from 55 to 95. A simple linear transformation, shown in Eqn 4-2, was used to convert JRC to B.

$$B = JRC * 2 + 55 \qquad \text{Eqn 4-2}$$

Recall that figures depicting roughness profiles for both systems are given in the Appendices. The rest of the applicable fields in Table 4-5 were then populated in similar fashion to the core logging data.

4.4 Virtual Cell Mapping

4.4.1 Data Collection

This form of joint mapping is done remotely. Joints may be mapped via a computer system without having to actually be out standing under the bench face.

This system makes use of photogrammetric tools. A high definition digital camera is used to take adjacent images of a bench face. The camera set-up position is then changed and the process repeated; this is similar to the procedures used to produce aerial photographs. Ultimately a 3-D spatial map of the bench is produced, from which a 3-D topographical map is generated (see Figure 4-6). This map may then be imported into a computer software program, SIROJOINT, for joint mapping and analysis. The Commonwealth Scientific & Industrial Research Organization (CSIRO) is the developer of SIROJOINT.

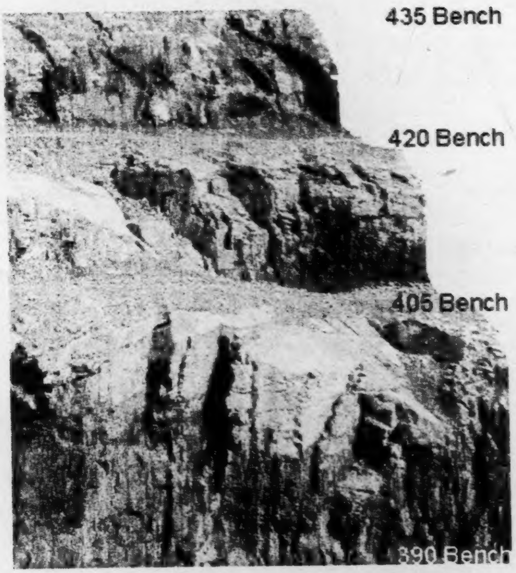

Figure 4-6 3D Image of Koala NW Benches

The demo version of the software was used; this version allowed determination of the spatial (3D) coordinates and orientation for a joint feature. The full version features additional components allowing the user to: identify and measure the orientation, area, and position of joint faces and joint traces; identify and measure geological features such as bedding planes and faults; classify joints according to orientation; calculate spacing for joint sets and bedding planes; calculate statistics of joint set spacing; annotate joints with termination information (Roberts and Poropat, 2002).

Digital mapping of this kind has some obvious advantages over more traditional means, namely the ability to map large and inaccessible areas. This method is also desirable from a safety perspective, as individuals are not placed at risk by being directly underneath bench faces. However, with this method little information can be gleaned concerning joint roughness, infilling and water conditions.

With the virtual mapping technique it was noted that features sub-parallel to the rock face where the easiest to pick up; in traditional mapping it is usually easier to identify features perpendicular to the rock face. As this method is relatively new and untested, the results of virtual cell mapping performed in Koala will be statistically compared to large and small-scale mapping done in Koala to see if they are comparable.

4.4.2 Transformations

Spatial coordinates and joint orientation data were read directly from SIROJOINT. The rest of the applicable fields in Table 4-5 were then populated in similar fashion to the large-scale and small-scale cell mapping data.

4.5 Correcting for Bias in Orientation Data

Before any analysis is performed on the Ekati™ dataset corrections must be applied to account for the bias owing to the orientation of the sampling line (be it from drill hole logging or any form of surface window and scan-line mapping).

This bias arises from the fact that the orientation of drill holes and of scan-lines commonly lacks sufficient variety to ensure a representative description of the relative abundance of several joint sets present in the domain (Terzaghi, 1965). Note also that data collected from surface mapping is often along a horizontal line, whereas drill holes commonly tend towards the vertical. This fact alone can lead to serious differences in measured orientation of dominant discontinuity sets (Park and West, 2002).

A linear sample line will tend to preferentially intersect those discontinuities that have a pole at the same orientation as the sample line, thereby tending to heavily bias the frequency of occurrence of those discontinuities. This is illustrated in 2D space in Figure 4-7 where even though joint sets A, B and C are of equal spacing, measurements along the scan-line will record many more joints in set A than in set C.

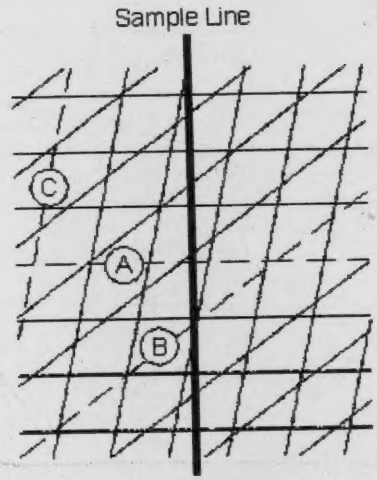

Figure 4-7 Sample Line Bias (modified from RocScience geomechanics software and research, 2003)

The bias can generally be reduced to a tolerable level by correcting for the effects of non-random orientation of exposed rock surfaces, by making observations in an adequate number of appropriately orientated boreholes, and by plotting the result of the survey in polar diagrams which are corrected for the effect of the angle of intersection between the joints and the drill holes or exposed rock faces (Terzaghi, 1965). Figure 4-8 depicts the angle of intersection (δ) between scan-line and discontinuity normal, as well as the true and apparent spacing of the joint set (D and D' respectively). Note that Figure 4-8 is representative of 2-D space and that the dips of the discontinuities are at 90° to the page (i.e. going straight into the page) such that the angle of intersection is a minimum value.

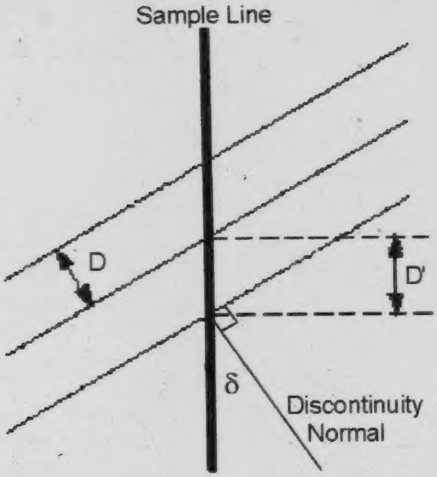

Figure 4-8 Correction Angle (modified from RocScience geomechanics software and research, 2003)

In order to reduce the bias introduced by the sampling method all joints are corrected according to the value of δ. Essentially this is a declustering procedure whereby each joint orientation is assigned a weight based on its probability of occurrence. The angle of intersection δ can be determined via Eqn 4-3 (Priest, 1993).

$$\cos\delta = \left|\cos(\alpha_n - \alpha_s)\cos\beta_n\cos\beta_s + \sin\beta_n\beta_s\right| \qquad \text{Eqn 4-3}$$

Note that α_n/β_n is trend/plunge of the discontinuity normal and α_s/β_s represents the trend/plunge of the scan-line. Once δ is determined, the Terzaghi (1965) correction factor, given in Eqn 4-4, can be applied.

$$TerzaghiCorrection(TCF) = \frac{1}{\cos\delta} \qquad \text{Eqn 4-4}$$

Note that δ varies from 0° to 90°. By applying the correction factor to joint sets A, B and C in Figure 4-7, their adjusted frequencies of occurrence will be correctly shown as equal.

The correction factor could be applied in a number of ways. With the Ekati™ dataset the correction factor associated with a particular joint was rounded to the nearest integer; this integer represents the true occurrence of this particular joint. Thus, every recorded joint was reproduced such that the total number of occurrences equalled the correction factor. Rounding to the nearest integer introduces some error, but is obviously necessary as there cannot be half of a joint.

While spatially the duplicated joints cannot be used for spacing determination (as the X, Y and Z coordinates are the same as the original), the correct frequencies of occurrence and associated average roughness and infill values of joint sets are now known. Concerning joint spacing determination, the correction factor is used on the original joint coordinates to determine D, as was shown in Figure 4-8.

At the Ekati™ mine, the practice when logging drill core is to classify any joints with an angle of intersection (δ) greater than 70° as a core axis fracture. Reading the dip from the goniometer becomes unreliable at these angles. The maximum weighting factor applied to any joint set is approximately three (i.e. $1/\cos 70°$). This is also necessary as if the angle of intersection is allowed to approach 90° the correction factor will tend towards infinity. Therefore, the few logged joints having an angle of intersection greater than 70° are also given a weighting of 3.

Unfortunately, there is a negative side effect to the core axis classification, namely that certain subsets of joints (i.e. those with intersection angles greater than 70°) go unsampled. Thus, for every sample line there is an associated blind zone whereby virtually no poles are picked up in this region. As this data is effectively censored, or not sampled at all, weighting cannot restore the underlying population. The blind zone effect on a drill hole is shown in Figure 4-9.

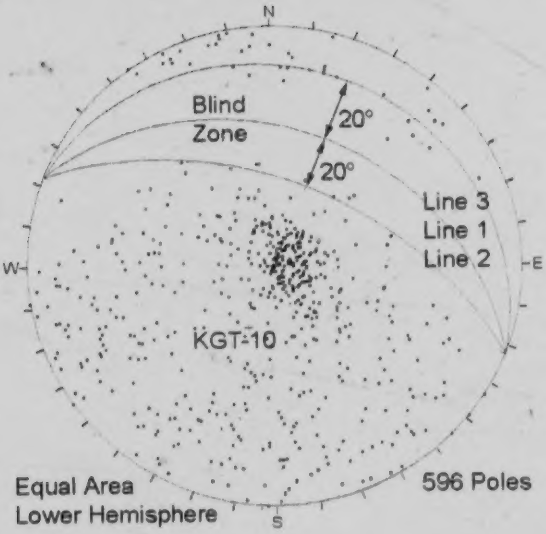

Figure 4-9 KGT-10 Diamond Drill Hole Blind Zone

The orientation of diamond drill hole KGT-10 is shown on a stereonet in Figure 4-9 along with the poles of all associated joint orientation measurements made. If KGT-10 is thought of as a pole, line 1 is the associated plane. Lines 2 and 3 have the same trend of line 1, but their plunge is plus or minus 20° from that of line 1. The area between lines 2 and 3 encompasses a region where poles to joints that are within 20° of the borehole would plot. In Figure 4-9 the weighting of poles would rise from 1 to 3 when moving away from the pole of KGT-10.

Any poles that occur in the blind zone (contained between lines 2 and 3) are generally not sampled. The only way to identify features located within the blind zone is to make observations in a nearby drill hole that is orientated such that their blind zones do not overlap.

This same size of blind zone was also assumed to apply to all surface mapping data. A maximum correction factor of 3 was assigned to any recorded data that happened to fall within the blind zone. Table 4-7 reflects the additional data points (the # correctors) added to the database.

Table 4-7 Modified Structural Dataset

Pit	Data Source	# Data	# Correctors	Total
Koala	Diamond Drill Hole	5889	2869	8758
Koala North	Diamond Drill Hole	1220	557	1777
Panda	Diamond Drill Hole	1469	492	1961
	Sum	*8578*	*3918*	*12496*
Koala	Large-scale Cell Mapping	751	601	1352
Panda	Large-scale Cell Mapping	373	322	695
	Sum	*1124*	*923*	*2047*
Koala	Small-scale Cell Mapping	834	648	1482
	Sum	*834*	*648*	*1482*
Koala	Virtual Cell Mapping	156	*N/A*	*156*
	Sum	*156*	*0*	*156*
	TOTAL	10692	*5489*	**16181**

Note that virtual cell mapping data was not corrected; in this case the Terzaghi correction is not appropriate. As mentioned previously, it was found that unlike the other forms of data collection, primarily sub-parallel features to the rock face were identified using the virtual mapping method due to the nature of the program. Thus, any correction applied to the data would tend to bias the results even further towards orientations in this area. It was therefore decided not to apply the Terzaghi correction. A statistical analysis will be performed to determine how similar the virtual cell map data is to the other forms, and if this new tool may be useful in a mining environment.

In summary for this chapter, a database has been constructed consisting of information collected via four different procedures. The database consists primarily of joint orientations, but tied to each may be other parameters such as joint roughness and infill. The database has been corrected for orientation bias such that the most accurate representation of the in-situ geologic environment is available. This data can now be used for determining structural domains in the region.

Chapter 5

Rock Mass Structural Domains Determined from Structural Data

5.1 Review of Structural Domain Identification

5.1.1 Importance of Domains

The delineation of structural domains and the definition of the structure characteristics within each domain are essential to ensure that the structure characteristics are applied only to those areas of the current and future pits where they will actually exist (Nicholas and Sims, 2000). This chapter covers the delineation of domains while Chapter 6 deals with the specific structure characteristics within each domain.

A variety of statistical techniques have been developed over the years with the intention of aiding in the division of a rock mass into domains. A domain represents an area with similar characteristics. In the case of a rock mass the defining characteristics may be joint features or rock types.

The recognition of separate domains in a rock mass is critical because changing geologic or hydrologic properties will effect how the rock mass responds to engineering activities (i.e. loading or excavating of the rock mass). When dealing with joints or other such discontinuity orientations the term structural domain is applied.

It is most common to characterize joints by their orientations, however, recall from Priest (1993) that the discontinuity properties that have the greatest influence at the design stage are: orientation, size, frequency, surface geometry, genetic type, and infill material. If desired, domains could also be created by considering the infilling, roughness or spacing of discontinuities. As the orientation of a discontinuity generally has a more pronounced effect on the behaviour of a rock mass it is usually structural domains that are created to characterize the rock mass. Seldom are the other properties taken into account.

As the rock mass at Ekati™ is structurally controlled, orientations are considered the most important joint characteristic. However, also tied to each joint is information concerning roughness, frequency, and infill. Though domains will not be created based on these parameters, their information will be quite valuable later when major joint sets within the domains are identified.

5.1.2 Tests of Similarity

Traditionally, domains were delineated from visually analyzing joint discontinuity orientations plotted on a stereonet. A stereonet is a projection of orientation data on a reference sphere such that the relative frequencies of joint orientations in an area can be evaluated. Experienced geologists or engineers then subjectively determine where sufficient differences exist between stereonets of adjacent regions in the rock mass to warrant the creation of a structural boundary. However, when fracture orientations appear dispersed and random on the plots, visual comparisons are not sufficient to determine whether the samples were obtained from the same structural domain (Miller, 1983).

Miller (1983) applied the chi-square (X^2) test to structural data. The procedure is based on a contingency table containing frequencies of fracture poles that occur in corresponding, equal-area patches on the stereonet plots being compared (Miller, 1983). Miller's method cannot be used in all cases though, as the X^2 test implicitly assumes independence (i.e. randomness) of data. Most geologic data are not independent.

Mahtab and Yegulalp (1984) developed a test that can handle non-random data; the data is modelled using the Poisson distribution. In constructing the similarity test, the mean orientation of a cluster being tested and the radius of the cone of confidence for the mean are used (Mahtab and Yegulalp, 1984). If two samples are shown to be similar they are grouped and the process repeated.

Kulatilake et al. (1989) review both of the aforementioned methods. They note that Mahtab and Yegulalp's procedure assumes two samples (i.e. stereonet plots) to be similar when only one cluster (i.e. joint set) from one sample is found to be similar with a cluster in the other sample. Thus, this procedure may group stereonets that contain only one similar joint set, but which otherwise are quite different. This limited degree of selectivity is not sufficient given the jointing conditions at Ekati™.

Cravero et al. (1991) reviewed five schemes, including both discussed above, for partitioning joint orientations into homogeneous domains. It was found that the simultaneous or sequential use of several schemes for a given site might be useful; the choice of a scheme may derive from the requirements of selectivity, the dispersion of the data, and the complexity of the site geology (Cravero et al., 1991). More specifically, Miller's method is suitable for a preliminary recognition of similar zones while Mahtab and Yegulalp's method is best used for the selective recognition of domains together with statistical parameters of clusters in the domains (Cravero et al., 1991).

All methods discussed so far determine fixed boundaries for structural domains, while in many cases it is more likely that there are gradual transitions in joint orientations occurring within the rock mass. Hume et al. (1982) recognized this and recommended that geostatistical tools such as the semivariogram be used to define the zone of influence of geologic variables. Unfortunately, this work was never done; however, the concept of the semivariogram is intriguing and will be looked at later.

No single method is suitable for identifying structural domains given the geologic conditions prevalent at the Ekati™ Diamond Mine. Use of multiple methods in conjunction is somewhat cumbersome. Thus, I propose a new method to accomplish domain identification in a quantitative manner.

The basis of this new method for domain identification involves plotting stereonets for various regions in space; then, looking for significant changes between stereonets that can be attributed to a structural change between the physical areas they represent (i.e. a structural boundary). A 3-stage process has been proposed for domain identification:

- Select data from a particular region in space. Regions may be blocks, pie slices, layers, or other somewhat arbitrary divisions of space. Using knowledge gathered from Section 2.3.3 (local geology) in conjunction with operational experience and desires at the mine site, appropriate divisions are proposed.
- Plot joint orientation data on a stereonet. An appropriate plotting scheme is proposed and a sensitivity analysis carried out to ensure that results are not a function of the plotting format.
- Identify significant differences on the stereonets that indicate the existence of structural boundaries and therefore justify the creation of domains.

The rest of this chapter will develop these elements. The results from this method will be compared to the domains currently in use at the mine.

5.2 Stereonet Representation of Data

When establishing structural domains, the joint orientations of two regions are analyzed to see if they are similar enough to be grouped into one region. As mentioned previously, the stereonet is a useful tool for displaying orientation data. An idea of the degree of similarity between two stereonets can be obtained by looking in a trend/plunge window and comparing the relative frequencies of occurrence of the measurements. If most windows between stereonets are quite similar, it is justifiable to include the two regions in the same domain. Note that it is important to normalize the data and compare frequencies, not the actual number of samples in a given orientation range.

Choosing the size of windows within the steronet can be difficult. Windows too large tend to overly smooth the data, thereby masking important trends. Windows too small inevitably contain few data, and any trends rendered unrecognizable due to noise.

The Ekati™ dataset has a large number of joint orientations to work with. A window that is 20° trend by 10° plunge should be acceptable. This would give 162 windows on the stereonet. However, the influence of joint orientations on rock slopes must be considered. Poles of joints clustered near the centre of a stereonet represent sub-horizontal sets. From an engineering behaviour point of view the trend of such shallow dipping features is not highly important; indeed, these features can all be grouped in the same set. On the other hand, poles near the perimeter of the stereonet represent sub-vertical features, the trends of which are very important with respect to the orientation of a bench face.

Thus, it is desired to have larger windows near the bottom/top of the sphere with the windows progressively becoming smaller towards the sides. Mahtab and Yegulalp (1984) used such a division of the upper hemispherical surface for their analysis; this division scheme is pictured in Figure 5-1.

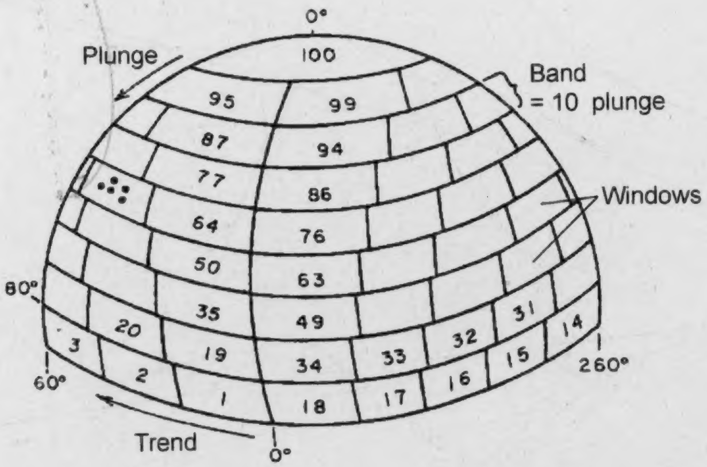

Figure 5-1 Division of Hemispherical Surface into 100 Equal-Area Windows (modified from Mahtab and Yegulalp, 1984)

While the window is larger on the hemisphere where poles are steeply plunging, when plotted on an equal-area stereonet the divisions shown in Figure 5-1 result in equal areas. This facilitates statistical comparison of the number of poles lying in each window on the stereonet. Specifically, this thesis will make use of a lower hemisphere stereographic projection divided into 100 equal-area windows.

It will be necessary to perform some sensitivity analyses on the data to ensure that the window size and 0° reference line do not unduly effect results. But first, it is necessary to introduce the tool for comparison.

5.3 Determining Spatial Similarity of Joint Orientations from the Coefficient of Correlation

5.3.1 Definition of Coefficient of Correlation

Of interest are the orientation differences between two regions in the rock mass; their data represented on stereonets divided into 100 equal-area windows. This comparison is a statistical and probabilistic problem.

A statistical parameter known as the covariance is used to assess the relationship between similar windows of the two regions in the following sense. The data is frequency of pole occurrence in a particular window; the data from two regions is represented by random variables X and Y. If X tends to be large when Y tends to be large, and X is small when Y is small, then X and Y will have a positive covariance. Alternatively, if X is large when Y is small, and small when Y is large, then X and Y will have a negative covariance. The covariance measures the direction of the association between two random variables. A covariance of zero represents no linear relation between the two variables.

The standardized covariance is the correlation coefficient. The correlation coefficient gives the strength of the association between the two variables. When determining the correlation between the stereonets of two regions there will be 100 X variables and 100 Y variables. The correlation coefficient, ρ, can then be calculated via Eqn 5-1 (where n is equal to 100).

$$\rho = \frac{\sum_{i=1}^{n} X_i Y_i / n - (\sum_{i=1}^{n} X_i / n)(\sum_{i=1}^{n} Y_i / n)}{\sqrt{[\sum_{i=1}^{n} X_i X_i / n - (\sum_{i=1}^{n} X_i / n)^2][\sum_{i=1}^{n} Y_i Y_i / n - (\sum_{i=1}^{n} Y_i / n)^2]}} \qquad \text{Eqn 5-1}$$

The covariance term is the numerator in Eqn 5-1. By dividing the covariance by the standard deviations of the two variables the correlation coefficient will always be between –1 and 1; providing an index that is independent of the magnitude of the data values.

Note that the correlation coefficient provides a measure of the linear relationship between two variables. If the relationship between the two variables is not linear, the correlation coefficient may be a very poor summary statistic (Isaaks and Srivastava, 1989). At the Ekati™ mine site the same variable is being compared (frequency of joint occurrence within a given orientation range) between two different regions; thus a linear relationship is appropriate. Figure 5-2 illustrates values of the correlation coefficient and their implications.

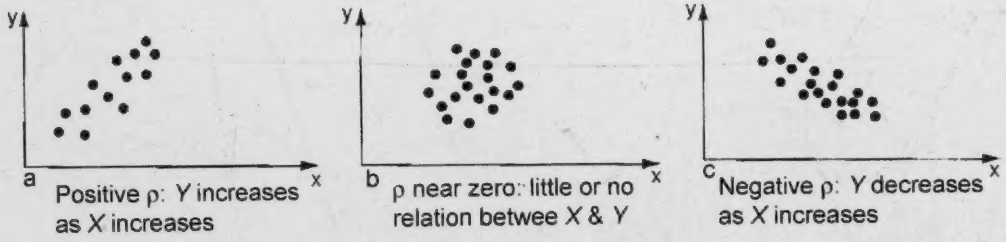

Figure 5-2 Values of ρ and Their Implications (modified from Scheaffer and McClave, 1995)

A ρ value of –1 entails perfect negative correlation, 0 entails no correlation, and 1 entails perfect positive correlation (Deutsch, 2002). In the latter case, the frequency value of every window in region 1 would be the same as the frequency value of every window in region 2 (i.e. the stereonets are identical). If these results were obtained it would obviously be justifiable to combine regions 1 and 2 into a single representative domain.

The same exercise also can be carried out between the different data types (i.e. diamond drilling information and surface mapping information). This will be useful to evaluate if the results obtained from virtual cell mapping agree with the more traditional forms of data collection.

Overall, this type of methodology will be applied when determining structural domains at the Ekati™ Diamond Mine.

5.3.2 Stereonet Sensitivity and Comparison of Open Pits

Section 5.2 discussed how to best represent orientation data by dividing the lower hemispherical projection into windows. The number and size of these windows can be varied to determine the effect on the correlation coefficient.

To test the sensitivity, the data are compared between the pits. Table 5-1 lists the correlation coefficients for four ways of dividing the lower hemisphere into windows. The comparison was done between open pits using only diamond drill core logging data.

Table 5-1 Lower Hemisphere Division Schemes

Pit Comparison	Data Source	X, Y, Z Coord.	Data Points	Classification			
				ρ_A	ρ_B	ρ_C	ρ_D
Koala Koala North	DDH DDH	all locations all locations	8758 1777	0.30	0.70	0.74	0.74
Koala Panda	DDH DDH	all locations all locations	8758 1961	0.47	0.82	0.86	0.87
Koala Panda	DDH DDH	all locations all locations	1777 1961	0.30	0.80	0.81	0.82

Classification A utilized a 20° trend by 10° plunge window division for a total of 162 windows. Note that the correlations obtained are quite low. For geologic data, it would be expected to have a higher correlation because all three pits are in the same vicinity and are located within the same rock type.

As previously discussed, from an engineering standpoint all sub-horizontal joints can be grouped in the same window. Classification B is identical to A except that the 80° to 90° plunge band is grouped as 1 window, not 18; thus having 145 windows in total. Note that the correlations have drastically increased, indicating that by segregating the sub-horizontal joints by trend, as in classification A, the correlation has been artificially lowered. Statistically the correlations in classification A are correct, but as far as rock mass behaviour is concerned classification B is more appropriate as the distinction between sub-horizontal joints does not need to be made.

Classification C is the 100 window division shown in Figure 5-1, except on the lower hemisphere. The correlations are marginally higher than found with classification B indicating that the larger windows are not contributing to substantial smoothing of data and masking of trends.

Classification D is the same as classification C, the only difference being the 0° reference line has been offset, in this case by 120°. The corresponding coefficients of correlation are almost identical to classification C, indicating that the location of this reference line will have a minimal effect on the outcome of results.

Therefore classification C will be used for all future analysis, with the 0° reference line corresponding to true north (i.e. 000°). Classification C was chosen over B as in future analyses not as many data points will be available for inclusion. A coarser grid of windows will result in fewer windows containing zero data points, reducing the level of noise and allowing a clearer visualization of trends. As well, the equal-area windows of classification C facilitate statistical comparison of the number of poles lying in each window on the stereonet.

5.3.3 Similarity of Data from Different Sources

The different data types (as discussed in Chapter 4) located within the same open pit will now be compared to identify anomalies that may indicate certain data types not being as reliable as others. All data points from a similar source were compared to all data points of other sources within each open pit. Table 5-2 is a summary table showing the correlation coefficients between various data types.

Table 5-2 Correlation Between Data Types

Pit	Data Source	X, Y, Z Coord.	Data Points	ρ
Koala	DDH LSCM	all locations all locations	8758 1352	0.61
Koala	DDH SSCM	all locations all locations	8758 1482	0.73
Koala	DDH VCM	all locations all locations	8758 156	-0.04
Koala	LSCM SSCM	all locations all locations	1352 1482	0.73
Koala	LSCM VCM	all locations all locations	1352 156	0.09
Koala	SSCM VCM	all locations all locations	1482 156	-0.04
Panda	DDH LSCM	all locations all locations	1961 695	0.59

Correlations between the traditional data collection methods (i.e. diamond drill hole data, large and small-scale cell mapping) are quite good, ranging from roughly 0.6 to 0.7. These data types appear to support one another, but they are not identical and will need to be treated separately. As diamond drill hole (DDH) data are by far the most abundant, they will be solely used when determining the structural domains in the region.

Since virtual cell mapping was just carried out in the northwest sector of Koala pit only, correlations might be expected to be somewhat lower. However, the virtual cell-map data in Koala appear to be completely uncorrelated to all other methods of collection. This is not surprising, as it was noted that virtual mapping almost exclusively identified features sub-parallel to the bench face. Additionally, only 156 points were sampled; given the 100 window stereonet used this is likely not sufficient to properly represent the geologic structures in a region.

It is now possible to delineate the domains within each open pit, making exclusive use of diamond drill hole data.

5.4 Structural Domain Delineation

5.4.1 Correlogram with Depth

Of particular importance to the mining operations at Ekati™ are changes in rock mass properties and joint orientations with depth. Will underground operations be working in a similar structural environment as surface operations, or will the environment be different due to geologic changes occurring with depth?

To determine if structural changes are occurring with depth, each open pit was analyzed independently. For all cases, horizontal slices encompassing all data at that level were used to vertically segregate each open pit. Table 5-3 depicts the vertical slices used for the Koala, Koala North and Panda mining areas.

Table 5-3 Vertical Slices For Each Open Pit

A. Koala

Slice	Depth Interval (60 m)		Data Points	Slice
	>=	<		(m)
X	435		326	
1	375	435	2001	60
2	315	375	2447	60
3	255	315	1036	60
4	195	255	749	60
5	135	195	746	60
6	75	135	638	60
7	15	75	401	60
8	-45	15	344	60
X		-45	70	
	data point used		8362	
		of	8758	
		% used	95.5	

B. Koala North

Slice	Depth Interval (50 m)		Data Points	Slice
	>=	<		(m)
1	400	450	620	50
2	350	400	387	50
3	300	350	373	50
4	250	300	381	50
X		250	16	
	data point used		1761	
		of	1777	
		% used	99.1	

C. Panda

Slice	Depth Interval (50 m)		Data Points	Slice
	>=	<		(m)
1	400	450	197	50
2	350	400	471	50
3	300	350	475	50
4	250	300	339	50
5	200	250	180	50
6	150	200	181	50
X		150	118	
	data point used		1843	
		of	1961	
		% used	94.0	

A given vertical distance was not considered if relatively few points occurred within it. This was usually the case at depth. As well, some very near surface data was not included in analysis. Over 94% of the data were utilized for each pit.

The next step involved calculating the correlation between vertical slices in the same open pit. In this way, it is possible to see if changes occur with depth, indicating perhaps a structural boundary. The results of this analysis are shown in Table 5-4. Note that *h* refers to the lag distances; correlations are given between slices located those distances apart. As *h* is a vector, it has both magnitude and direction, in this case the direction being vertical.

Table 5-4 Correlations with Depth

A. Koala

h (m)	60	120	180	240	300	360	420
	ρ_{12} 0.82	ρ_{13} 0.78	ρ_{14} 0.67	ρ_{15} 0.57	ρ_{16} 0.50	ρ_{17} 0.47	ρ_{18} 0.20
	ρ_{23} 0.84	ρ_{24} 0.70	ρ_{25} 0.62	ρ_{26} 0.51	ρ_{27} 0.59	ρ_{28} 0.21	
	ρ_{34} 0.78	ρ_{35} 0.67	ρ_{36} 0.56	ρ_{37} 0.56	ρ_{38} 0.28		
	ρ_{45} 0.70	ρ_{46} 0.58	ρ_{47} 0.55	ρ_{48} 0.28			
	ρ_{56} 0.67	ρ_{57} 0.49	ρ_{58} 0.30				
	ρ_{67} 0.48	ρ_{68} 0.23					
	ρ_{78} 0.29						
ρ_{ave}	0.654	0.575	0.542	0.481			

B. Koala North

h (m)	50	100	150
	ρ_{12} 0.63	ρ_{13} 0.72	ρ_{14} 0.41
	ρ_{23} 0.77	ρ_{24} 0.52	
	ρ_{34} 0.49		
ρ_{ave}	0.628	0.618	

C. Panda

h (m)	50	100	150	200	250
	ρ_{12} 0.70	ρ_{13} 0.72	ρ_{14} 0.57	ρ_{15} 0.66	ρ_{16} 0.47
	ρ_{23} 0.88	ρ_{24} 0.80	ρ_{25} 0.83	ρ_{26} 0.62	
	ρ_{34} 0.79	ρ_{35} 0.84	ρ_{36} 0.54		
	ρ_{45} 0.82	ρ_{46} 0.58			
	ρ_{56} 0.56				
ρ_{ave}	0.750	0.735	0.646		

The average correlations were also calculated for each lag distance. The relationship between the correlation coefficient of individual comparisons and lag distance is called the correlation function or correlogram (Deutsch, 2002). Note that these were not calculated over the entire range, as once the lag distance exceeds about half the range over which the data is located, not all slices are included. Figure 5-3 is a vertical correlogram of the data for all three mining areas.

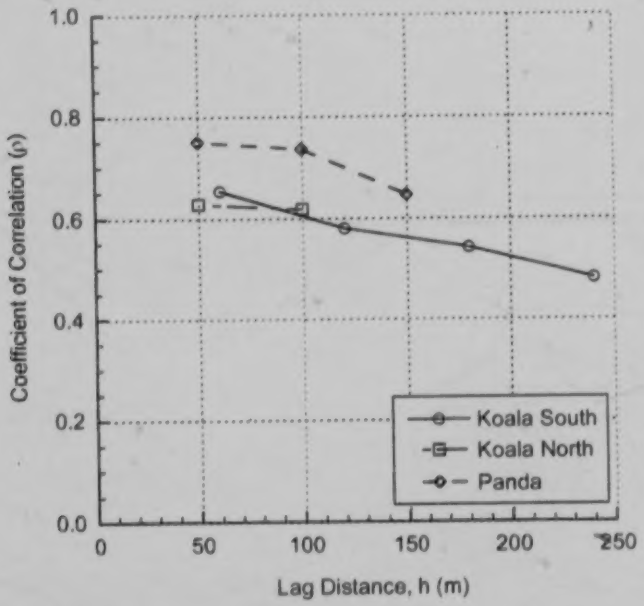

Figure 5-3 Vertical Correlogram of DDH Data

All three mining areas seem to have a similar vertical trend, though the correlations for Panda seem to be slightly higher than for the other areas. If the lines were extrapolated back to zero lag distance, correlations would be in the range of 0.65 to 0.85. This represents small-scale variability and is in the typical range for most geologic data. As the lines extend to increasing lag distances, the correlations tail off. This represents an increased change in geologic conditions the further apart data are located.

As changing geologic conditions with depth have been confirmed via the correlogram, the correlation coefficient can now be used to determine if an area of significant change exists such that it may be treated as a structural boundary. The correlogram will be revisited when the prediction of structural domains is touched upon at the end of this section.

5.4.2 Vertical Correlations

Table 5-4 indicates that for the Koala area correlations are lower for slices 7 and 8, thereby lowering the overall correlation. It is inferred that perhaps around 75 metres above sea level some structural change has occurred. Table 5-3 shows that slices 7 and 8 contain fewer data points than most others, so this difference could partially be attributed to lack of representative data. However, the amount of data contained is still substantial, and the change in correlation is significant enough to justify dividing the Koala area into two separate vertical domains.

From Table 5-4, Koala North and Panda are analyzed in similar fashion. The last slice in each appears to be substantially less correlated to those above. In the case of Koala North it may be premature to assume that a structural boundary exists at that depth due lack of information below. Once additional diamond drill hole data is available at lower depths, this decision can be made with more certainty. For now, it is assumed that only one vertical domain exists at Koala North.

Concerning the Panda data, lack of data below the last slice might lead to the same conclusion as at Koala North. However, the change in correlation is so drastic (occurring at approximately 200 m above sea level) that it cannot be ignored. Thus, it is suspected that two vertical domains exist in the Panda area. While the upper domain is well sampled, a relative lack of data in the supposed lower domain will preclude its analysis for the time being.

The Koala area contains more data than both Koala North and Panda combined, thus it is possible to more accurately place the structural boundary. The previous analysis was limited by the selection of static vertical slices (Table 5-3), thus a boundary could only be determined to the nearest pre-selected slice. Using what is known as a moving window analysis, the boundary will be determined to the nearest 15 m.

In the moving window analysis adjacent 60 m vertical slices were compared; these slices were offset 15 m vertically and thus overlapped by 30 m. The resultant correlations were then plotted in Figure 5-4 and the overall trends compared. Note that as the lowest correlations would occur when two slices straddled a boundary, the midpoint of the overlapping sections was taken to be the division line.

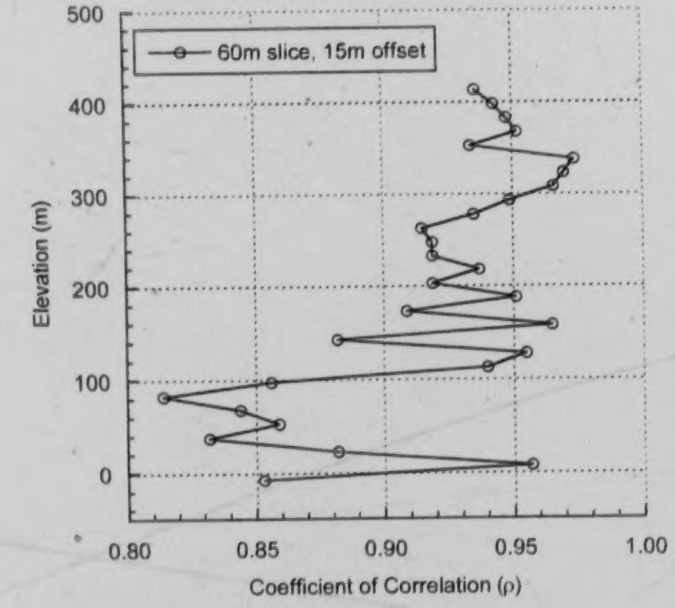

Figure 5-4 Koala Vertical Correlation

While quite variable, the overall trend is quite clear in Figure 5-4. It appears that around 75 m elevation (above sea level) the lowest correlation occurs, therefore indicating a vertical boundary. This agrees with the previous finding; therefore, it seems that the static windows were fortuitously chosen as they happened to bound the 75 m mark. Since there is good agreement, no further effort need be put into the moving window analysis (i.e. varying slice depths and offsets) in order to more clearly define the trends. In summary, the Koala area is subdivided into two vertical domains, separated at 75 m above sea level.

5.4.3 Radial Correlations

In current practice, the structural domains at the three open pit mining areas are divided into pie-shaped pieces. Due to the nature of kimberlite pipe emplacement where a weakness must have existed in the rock mass to allow transport to surface, as well as new jointing created upon emplacement, this pie-shaped division of domains seems reasonable. Practically speaking, domains whose boundaries are perpendicular to bench faces make stability analysis much easier to visualize and compute. As well, the sampling pattern conducted at Ekati™ suits this type of analysis (see Figure 4-5). Chapter 4 assigned each joint cylindrical coordinates, so it is now possible to create domains in the above fashion.

Taking an arc (i.e. pie piece) containing drill hole data, rotating it in increments to 360°, and comparing the coefficients of correlation between adjacent arcs enabled structural boundaries to be identified radially around the three open pits. The arc size and increment angle were chosen according to data spacing and their sensitivity on the results. The arc size and angle were then varied in order to smooth the data and identify the dominant changes in correlation.

Initially an arc angle of 120° was chosen. Smaller angles have problems picking up data due to the sampling distribution. The angle was also increased to 150° to see how sensitive the results are to the arc angle. Any arc larger than 150° and the data may be overly smoothed, therefore, potentially masking a domain boundary.

A rotation increment of 15° was initially tried. This was found to be too small and resulted in excessive noise on the plots. Once the increment was increased to 20° and 30°, the trends became progressively clearer. With increments larger than 30° the precision is lost when locating the domain boundary. Note that the optimal arc angles and increment angles are a function of the data quantity and spacing.

As before, this moving window analysis is considered superior to a static window analysis. In a static analysis, the pit is divided up into a number of pie slices and each slice is correlated to its neighbours. With a static window, the effects of drill hole blind zones may artificially reduce correlations. With a moving window, these effects are minimized, although not eliminated, by smoothing the data.

If relatively low correlations were found between two concurrent arcs, the bisector of the two mid-arc angles was taken to be the division line; the lowest correlation would be found when concurrent arcs were straddling the domain boundary. Results for one of the tests carried out on the Koala upper domain data (i.e. Z > 75 m) are shown in Table 5-5; all results for Koala are plotted in Figure 5-5.

Table 5-5 Koala Radial Correlation Results

Pit: **Koala**			Data: **ddh**			Depth: **> 75 m**	
Arc size:	**120** deg			Rotation increment:		**20** deg	
Slice (#)	Theta (deg)	Arc Boundary Angles (deg) >=	<	Data Points (#)	Correlation between Slices (ρ)		Boundary Angle (deg)
1	0	300	60	3326	$\rho_{1\,2}$	0.978	10
2	20	320	80	2840	$\rho_{2\,3}$	1.000	30
3	40	340	100	2840	$\rho_{3\,4}$	0.931	50
4	60	0	120	2665	$\rho_{4\,5}$	0.947	70
5	80	20	140	3019	$\rho_{5\,6}$	0.923	90
6	100	40	160	2187	$\rho_{6\,7}$	0.917	110
7	120	60	180	2093	$\rho_{7\,8}$	0.927	130
8	140	80	200	2873	$\rho_{8\,9}$	0.998	150
9	160	100	220	3007	$\rho_{9\,10}$	0.985	170
10	180	120	240	2640	$\rho_{10\,11}$	0.970	190
11	200	140	260	2258	$\rho_{11\,12}$	0.971	210
12	220	160	280	2727	$\rho_{12\,13}$	0.960	230
13	240	180	300	2524	$\rho_{13\,14}$	0.854	250
14	260	200	320	2230	$\rho_{14\,15}$	0.992	270
15	280	220	340	2096	$\rho_{15\,16}$	0.936	290
16	300	240	360	2648	$\rho_{16\,17}$	0.976	310
17	320	260	20	2666	$\rho_{17\,18}$	0.951	330
18	340	280	40	3029	$\rho_{18\,1}$	0.966	350

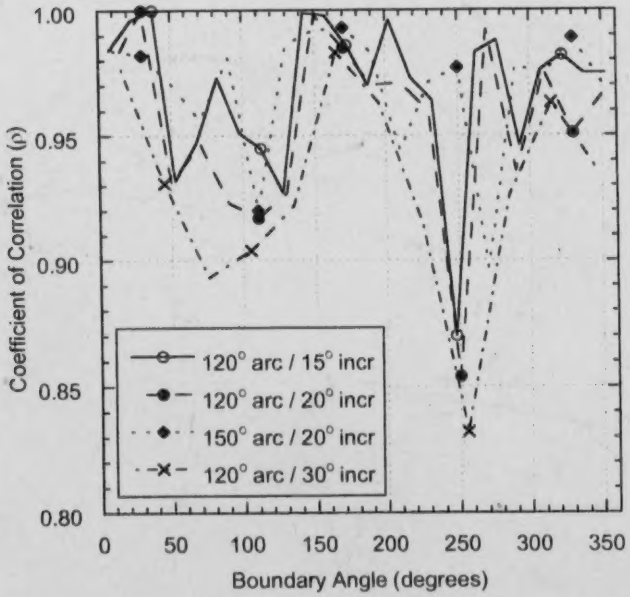

Figure 5-5 Koala Radial Correlations

Correlation occurring around 245° to 270° is low, leading to the belief that a structural boundary exists in this area. The correlation in the vicinity of 75° to 130° is also quite low, although to a lesser extent than the previous case. Thus, it was determined that structural boundaries exist at around 90° and 255°. Note that there is no correlation threshold that dictates where a structural boundary occurs; rather, the overall trends of the correlations are observed, and major troughs identified as boundaries. In the case of Koala a minor boundary is evident around 0°, however, compared to the other two boundaries this is not significant and so will not be used to create a third radial domain. The correlation coefficient between the data lying in the two radial domains is 0.58, confirming the distinct zones. Static comparison here is valid due to the large sections being compared, thus blind zones should not significantly affect results.

These findings agree quite favourably with domains currently in use at Koala, where boundaries are located at approximately 100° and 260°. Insufficient information is available to analyze the lower domain located below 75 m above sea level, although a preliminary analysis shows that two major boundaries still exist but are offset slightly from the domains that lie above. In summary, four domains are evident in the Koala area, although at this time only the upper two radial divisions and the elevation division are well delineated.

Similar procedures were carried out on both the Koala North and Panda mining areas. Results are plotted in Figure 5-6 and Figure 5-7.

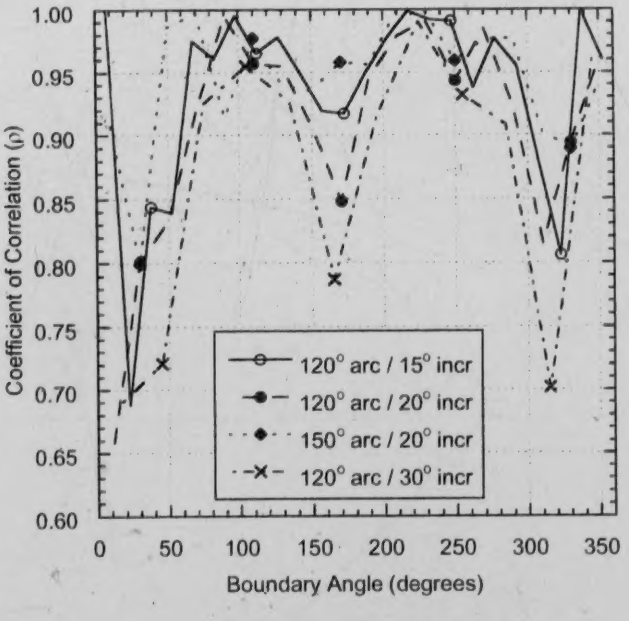

Figure 5-6 Koala North Radial Correlations

At Koala North, three boundaries are evident, occurring at 45°, 165° and 315°. Due to lack of data at depth, these domains will simply be extrapolated downwards for future analysis. The correlations are 0.40, 0.45 and 0.72 for the three domain boundaries. The correlation of 0.72 is across the 315° boundary and is obviously less significant than the others, though it is still sufficiently different to warrant separate treatment.

At Ekati™, Koala North surface operations divided the open pit into roughly north and south sections and treated these areas as separate domains. This delineation is quite different from the findings above. Unfortunately, it is not known if these domains are currently being employed at Koala North by underground operations. In summary, three domains are evident in the Koala North area.

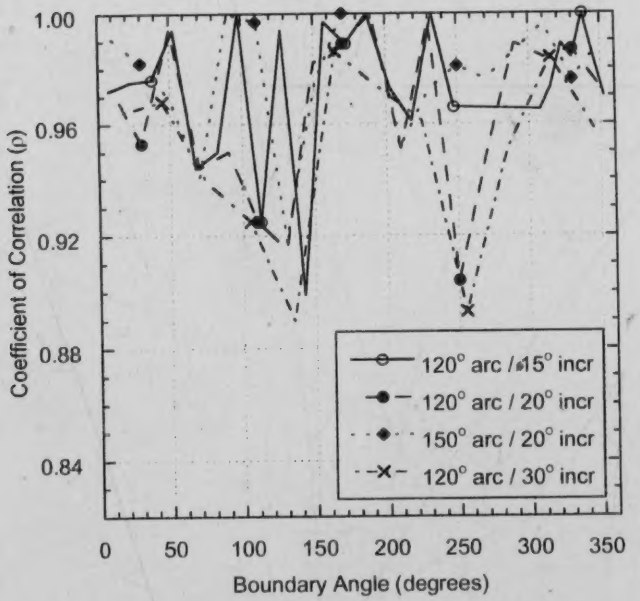

Figure 5-7 Panda Radial Correlations

Analysis for Panda consisted only of data from the upper domain (i.e. Z > 200 m). Insufficient information is available to analyze the lower domain at this time. In the Panda upper area, two domains are quite evident, occurring at approximately 130° and 255°. The correlation between these two areas is 0.86. This is perhaps high enough to justify combining the areas such that one domain sufficiently describes the entire Panda area. For now, the two areas will be considered separate, unless additional findings in the next chapter further support their amalgamation.

Domain divisions currently in use at Panda are located at 22.5°, 157.5° and 247.5°. From Figure 5-7, the domain boundaries should be located at 130° and 255°. There is some agreement between the two systems, although by the correlation method the domain boundaries at Koala and Panda are actually quite similar (both have a 255° boundary), perhaps indicating that emplacement of the kimberlite pipes occurred along the same plane of weakness and thus created similar jointing patterns radially. In summary, at least three domains have been found in the Panda mining area, although at this time only the upper two are well delineated.

Domain boundaries for all pits are identified in Figure 5-8. Stereonets of each domain are located at the end of Chapter 6.

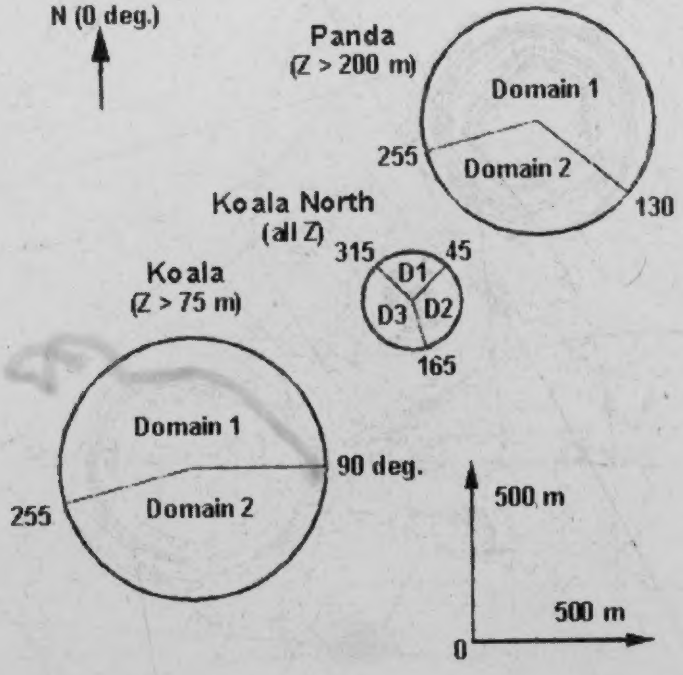
N (0 deg.)
Panda
(Z > 200 m)
Domain 1
Domain 2
255
130
Koala North
(all Z)
315
45
D1
D2
D3
165
Koala
(Z > 75 m)
Domain 1
Domain 2
255
90 deg.
500 m
500 m
0

Figure 5-8 Summary of Quantified Structural Domains

5.4.4 Prediction of Structural Domains at Distant Locations

Eventually structural domains will be needed below existing open pit operations for analysis of future underground workings. These areas at depth are currently sampled sparsely or not at all. As a result a prediction must be made until more exploration drilling occurs.

In the Ekati™ environment, there are a limited number of dominant joint sets within each structural domain. When aspects dealing with underground mining need to be analyzed the surface domains of the appropriate overlying area will be assumed to be continuous and simply extrapolated down. At Ekati™ where dominant structural features have been found to be fairly continuous this is an acceptable practice.

Not all mines have such dominant joint sets and identifiable domains. Simply extrapolating a near surface domain to greater depth may not be acceptable. Another potential drawback of this simple extrapolation method is that it does not make use of all the structural data in the region, only the data in the overlying domain.

Estimation may also be needed if a new kimberlite pipe was discovered in the immediate vicinity. It might be desired to predict any structural domains there by data available from the other three operations. As delineation of structural features via diamond drilling is quite expensive, statistical prediction of domains could represent a significant cost savings if feasible.

Geostatistics could be used for statistical prediction purposes. More specifically a procedure known as block kriging could be employed. In this procedure, directional variograms are needed such that the spatial continuity can be assessed and proper weighting assigned to data points. Figure 5-9 depicts a set of directional correlograms, which provide a descriptive summary of the spatial continuity for the Koala area.

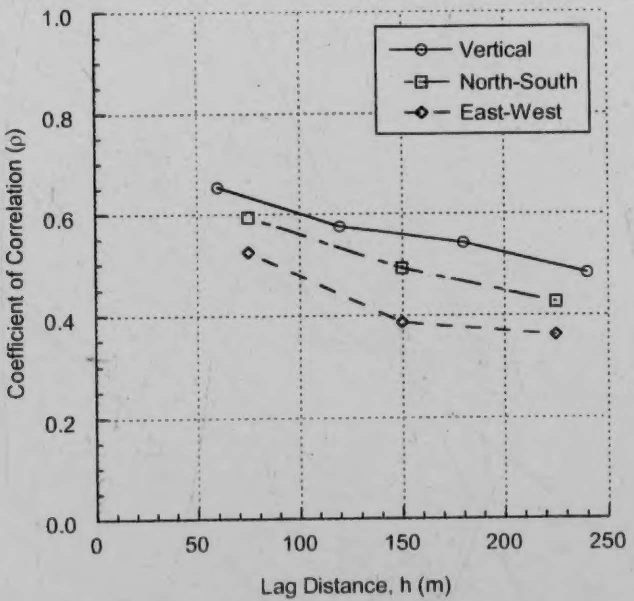

Figure 5-9 Koala Directional Correlogram

The relation given in Eqn 5-2 converts the information in Figure 5-9 into a variogram, which is the traditional measure of spatial information in geostatistics.

$$\gamma(h) = C(0) - C(h) \qquad \text{Eqn 5-2}$$

C(0) is the variance, *C(h)* the covariance and *γ(h)* the variogram value. From this information, a model is created such that a variogram value can be computed over any possible distance or orientation, not just along the three directions shown in Figure 5-9.

The region is then divided into blocks (i.e. pie pieces), each containing 100 values. These values are the joint frequencies for the 100 stereonet windows that represent the block. Block sizes would be determined based upon data spacing and quantity, and the desired size of the estimation area.

With the variogram model constructed, appropriate weights are calculated which respect the spatial continuity of the dataset. The formula is given in Eqn 5-3.

$$w = C^{-1} \bullet d \qquad \text{Eqn 5-3}$$

The vector *d* consists of the covariance values between any particular sample and the point being estimated. Generally, this covariance decreases as the sample gets farther away from the point to be estimated. This can be seen in Figure 5-9, where as the lag distance (or distance between samples) increases the correlation coefficient decreases.

The *C* matrix records the covariance values between each sample and every other sample, thus providing information on the clustering of the sample data. If two samples are very close to each other, this will be recorded by a large covariance in the *C* matrix. If two samples are far apart, this will be recorded by a low covariance. This phenomenon is also observed in Figure 5-9.

The vector *w* consists of the set of kriging weights that will produce unbiased estimates. The multiplication of *d* by the inverse of *C* adjusts the raw inverse statistical distance weights in *d* to account for possible redundancies between the samples (Isaaks and Srivastava, 1989). In essence, the net result is that some of the weight allocated to samples very close to the estimated location is redistributed to other samples that are farther away yet less redundant. It is now possible to estimate the values for a desired block via Eqn 5-4.

$$\hat{v}_o = \sum_{i=1}^{n} w_i \bullet v_i \qquad \text{Eqn 5-4}$$

All blocks have spatial coordinates; thus, any block in the area can be simulated and a stereonet constructed from the 100 values. Many realizations could be performed by geostatistical simulation in order to assess the level of uncertainty in the estimations.

From the simulated stereonets of various blocks, comparing and possibly grouping adjacent blocks could again roughly delineate structural boundaries. From this output dominant joint sets in the simulated area could be identified and used for stability analysis.

The above procedure may be useful in further predicting structural domains below existing open pit operations at the Ekati™ Diamond Mine, but is beyond the scope of this thesis.

In summary for this chapter, initially data collected from four different sources was compared. While the data generally supported one another, sufficient differences existed to warrant the separate treatment of each type.

As diamond drill hole (DDH) data are by far the most abundant, they were used as input when structural domains in the region were determined. It is recommended that the surface mapping data be used to supplement the DDH findings. For instance, when working in a certain area of an open pit it will be in a certain structural domain determined from DDH data. Cell mapping represents additional knowledge and can be used to help make decisions in the vicinity of where the mapping occurred. Also note that with the DDH data, joint sets are considered to be ubiquitous within the domain. Another strength of cell mapping is in identifying discrete planes or joint intersections along which failure is probable.

At this point, the use of the virtual mapping would not be recommended for everyday mapping purposes until sufficient improvements have been made whereby features occurring perpendicular to the rock face can be easily identified. However, value may still be found when performing back analysis on failure planes. The identification of a discrete plane is done quite easily and the orientation could then be used for kinematic failure analysis and back calculation of strength parameters. The only disadvantage here is that the open pit photos must be kept up to date in order for a recent failure to be analyzed within an acceptable period of time.

Finally, a method was proposed with which to delineate structural domains given joint orientation data. The method is more quantitative, unbiased and applicable than other methods discussed in the beginning of this chapter. The structural domains are then used to structurally model various regions at the Ekati™ mine. The next chapter deals with joint set characteristics of the structural domains found in this chapter.

Chapter 6

Joint Set Spacing and Shear Strength Properties

6.1 Review of Joint Set Identification

6.1.1 Importance of Joint Sets

A joint set represents a planar, sub-parallel group of discontinuities; often displaying spatial and orientational relations with folds, anticlines, synclines and faults formed during the same period of tectonic activity (Priest, 1993). Correlation of joint sets with past tectonic activity is not the focus in this thesis, identification of dominant joint sets is.

The recognition of major joint sets in a particular structural domain within a rock mass is required before any failure analyses can be carried out. Thus, representivity of and confidence in the gathered structural geologic data is key to conducting an effective analysis and having sufficient confidence in the results. Chapter 4 and Chapter 5 dealt with issues of data collection and domain identification respectively, such that now joint set identification can proceed.

It is most common to characterize joints by their orientations; however, recall from Priest (1993) that the discontinuity properties that have the greatest influence at the design stage are: orientation, size, frequency, surface geometry, genetic type, and infill material. Generally, joints created during the same tectonic event will share similar properties in all these areas (Priest, 1993). Later tectonic events may create similarly oriented joints, but with different spacing, surface geometry and infill characteristics. It is speculated that differentiation of joints based on characteristics other than orientation is difficult; it is generally observed that only one joint set is assigned over a particular orientation range.

6.1.2 Tests of Similarity

A variety of statistical techniques have been developed over the years with the intention of aiding in the identification of joint sets within a structural domain. Traditionally joint sets were determined from analyzing joint orientations plotted on a stereonet and subsequently grouping areas where a high clustering of joint poles occurred. While this subjective approach may still be appropriate for domains that contain a few distinct and segregate clusters, when joint orientations appear dispersed and random on the plots, visual comparisons are often not sufficient to determine where one joint set begins and another ends.

Mahtab and Yegulalp (1982) developed an approach for clustering fracture orientation data based on a randomness test. The first step involved identifying clusters of poles on a series of stereonets. The identification of clusters is somewhat subjective, as the user has to provide a threshold value above which classifies a grouping of poles as significantly dense enough to be considered a cluster. The second step involves looking at these clusters on all stereonets to see if they occur over the same orientation range, if so they can be called a set. Again, the procedure is subjective as user input is required to determine how close clusters have to be to be considered the same. The third step involves assigning previously unassigned points to clusters, and is iterative. Note that the final joint sets defined using this method are mutually exclusive (i.e. no overlap between joint sets).

It is recognized that there may be overlap in pole clusters between joint sets. As a result, it may be beneficial to assign a probability to a joint indicating which set it may belong to. This clas~~sification is better for~~ reliable estimates of set distribution functions because it provides gradual transitions between sets, a feature more in line with the continuous shape of distribution functions (Marcotte and Henry, 2002). In addition to having overlapping joint sets, Dershowitz et al. (1996) emphasized inclusion of geological information such as termination modes, displacements, striation, and mineralization when defining sets.

While the latter methods would all be appropriate for identifying joint sets within the structural domains present at the Ekati™ Diamond Mine they are unnecessary. As will be seen shortly, dominant joint sets present at the mine are quite obvious and distinct from one another. Thus, a traditional subjective approach will be sufficient for classification purposes at Ekati™ and for this thesis.

6.2 Joint Sets at Ekati™ Mine

6.2.1 Joint Set Identification and Characteristics

Initially poles to joints were plotted on a stereonet and within each structural domain major and minor joint sets visually identified. Each joint set is discrete and there is no overlap. Once the set window is defined, average parameters (i.e. mean orientation, roughness, infill, spacing) for the joint sets were established.

A set window is defined by two trend values and two plunge values. The exceptions are sub-horizontal joint sets that may be defined at the centre of a stereonet simply by the plunge of their poles. Figure 6-1 depicts both types of set windows on a pole plot overlaid with contours for the first structural domain in Panda pit. Poles are plotted to ensure that no relevant ones are left outside the set windows since in the contour view individual poles are not identifiable. However, there may be more than one pole at a location, thus the contour view is still necessary to see the relative density or clustering of poles. Stereonets of pole clusters and of joint sets for all domains may be found at the end of this chapter.

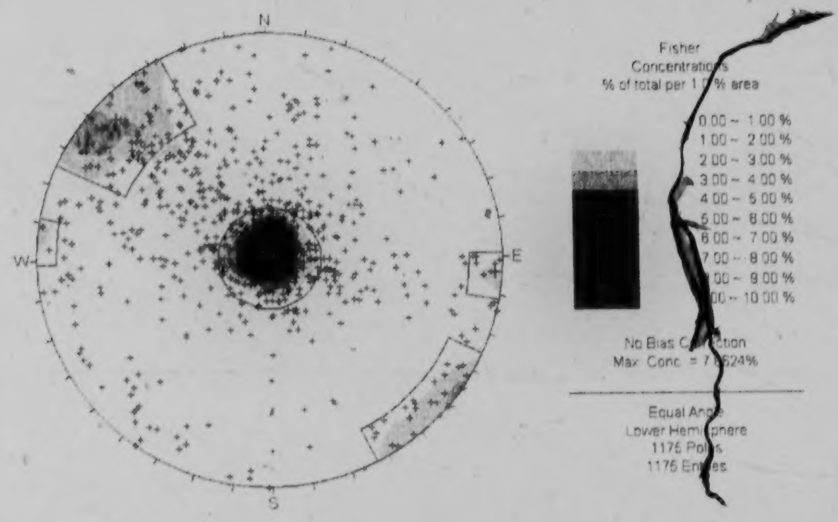

Figure 6-1 Pole Plot Overlaid with Contour Plot Depicting Set Windows

For each set window, a mean orientation is calculated. In order to quantify the uncertainty around the mean pole orientations of joint sets, the Fisher distribution was employed. This model assumes that a population of orientation values is distributed around some true value, thus the model can be used to describe the distribution of discontinuity normals (i.e. poles) around the true value of a joint set.

Note that the Fisher distribution is symmetric. Other models may be more appropriate when dealing with asymmetric data. From Figure 6-1, it is seen that the selected joint sets are not truly symmetric. Because the asymmetry is not too pronounced, the model is deemed adequate to describe orientation uncertainty at Ekati™.

From the Fisher distribution two parameters will be used to characterize the joint orientation data, the confidence limit and the variability limit. The confidence limit is interpreted as being *X*% certain that the true mean orientation of the joint set lies within about *Y*° of the given mean pole orientation (Priest, 1993). The variability limit is interpreted to mean that *X*% of the data will likely fall within *Z*° of the given mean pole orientation.

Poles outside the set windows are considered random and are only taken into account when assessing the overall degree of brokenness of the rock mass. Table 6-1 summarizes mean joint set orientations along with their uncertainty. Recall that the structural domains are depicted in Figure 5-8.

Table 6-1 Joint Set Orientations

Mining Area			Joint Sets						
			Set (#)	Major/ minor (M/m)	Mean Pole Orient		Mean Pole Uncertainty		
					Trend (deg)	Plunge (deg)	1 Std Dev (X%)	Conf. (Y deg)	Var. (Z deg)
Koala	Structural Domain	1	1a	M	34	76	68.26	0.6	17.1
			2a	m	222	85	68.26	0.8	9.4
			3a	M	174	3	68.26	0.8	11.3
			4a	M	143	5	68.26	0.6	13.8
			5a	m	203	6	68.26	0.8	9.5
		2	1b	M	226	88	68.26	0.6	20.3
			2b	M	346	6	68.26	0.7	10.7
			3b	m	208	0	68.26	0.8	7.3
			4b	m	55	1	68.26	0.7	5.5
			5b	m	316	2	68.26	0.7	4.5
			6b	m	328	37	68.26	1.0	16.3
			7b	m	279	53	68.26	0.8	8.6
Koala North	Structural Domain	1	1c	m	301	88	68.26	1.9	9.9
			2c	M	190	68	68.26	2.2	16.1
			3c	M	352	59	68.26	2.1	19.8
			4c	m	261	44	68.26	1.7	8.3
			5c	M	342	4	68.26	1.4	6.2
			6c	m	122	0	68.26	1.7	6.6
			7c	m	81	6	68.26	2.0	8.2
		2	1d	M	13	87	68.26	1.4	15.8
			2d	m	359	39	68.26	2.4	17.7
			3d	m	61	5	68.26	2.0	10.6
			4d	m	287	16	68.26	1.9	8.0
			5d	m	135	40	68.26	2.1	9.7
			6d	m	160	14	68.26	1.3	4.7
			7d	m	50	30	68.26	2.2	9.5
		3	1e	M	305	86	68.26	1.2	22.7
			2e	M	267	0	68.26	1.4	12.6
			3e	m	301	2	68.26	1.4	9.4
			4e	M	141	4	68.26	1.2	9.0
Panda	Structural Domain	1	1f	M	335	88	68.26	0.8	15.9
			2f	M	314	6	68.26	1.1	14.2
			3f	m	94	2	68.26	1.2	5.8
		2	1g	M	186	85	68.26	1.1	18.1
			2g	M	324	3	68.26	1.7	8.7
			3g	m	323	38	68.26	2.1	17.7
			4g	m	307	10	68.26	1.6	6.0

The confidence and variability limits given in Table 6-1 are for the first standard deviation (68.26%), thus it is encouraging that the confidence of the given mean orientation for a joint set is at most 2° from the expected value. The variability limit reflects the spread of the joint set; this has implications for analysis where it must be realized that a joint set with orientations fluctuating over 20° could mean the difference between rock mass stability and instability.

After the joint set windows are defined, their characteristics can be extracted from the dataset. Joint surface roughness represented by the Laubscher (1990) B parameter and joint filling represented by the D parameter are two important values that need consideration when determining strength properties of the joints. Joint spacing is also an important property that is required when assessing stability and modes of failure within the rock mass. These aforementioned values are determined for all joint sets. For some minor joint sets, the spacing characteristics could not be determined due to a lack of appropriately spaced measurements.

The Laubscher (1990) B parameter was converted to the Barton (1985) JRC value using Eqn 4-2 rewritten to solve for JRC. This format is desirable as in the next section an empirical shear strength equation will be used to back calculate a JRC value based on laboratory test results from a direct shear apparatus. A summary of measured roughness values and calculated spacing values are given in Table 6-2. For joint sets with adequate data, the standard deviation of the measurements is provided.

Table 6-2 Joint Set Spacing and Roughness Characteristics

Joint	Spacing		Roughness			Infilling	
			Laubscher B		JRC	Laubscher D	
Set (#)	Mean (m)	S.D. (m)	Mean	S.D.	Mean	Mean	S.D.
1a	1.16	1.3	77	8.5	11.0	89	11.7
2a	1.55	1.6	79	8.3	12.0	88	12.1
3a	1.57	1.5	74	9	9.5	86	11.3
4a	1.32	1.5	77	9	11.0	85	12.7
5a	2.00	1.90	74	10.2	9.5	87	11.7
1b	1.00	1.20	79	8.9	12.0	92	10.8
2b	1.63	1.4	75	8.3	10.0	85	14.6
3b	1.60	1.60	75	7.1	10.0	79	15.5
4b	1.94	1.2	78	7.9	11.5	80	18.8
5b	-	-	77	-	11.0	90	-
6b	1.97	1.8	77	8.9	11.0	90	11.1
7b	1.96	1.8	80	8.3	12.5	94	8.4
1c	1.26	1.1	89	3.1	17.0	100	1.1
2c	0.63	0.7	89	2.9	17.0	98	3.4
3c	1.01	1.2	89	4	17.0	99	2.2
4c	-	-	89	-	17.0	99	-
5c	-	-	89	-	17.0	95	-
6c	-	-	90	-	17.5	99	-
7c	-	-	87	-	16.0	99	-
1d	0.58	0.7	89	5.3	17.0	96	7.8
2d	0.78	0.8	88	7	16.5	92	11.6
3d	1.02	1.5	78	8.4	11.5	87	12.4
4d	-	-	83	-	14.0	98	-
5d	-	-	82	-	13.5	95	-
6d	-	-	84	-	14.5	98	-
7d	1.61	1.3	89	5	17.0	98	2.4
1e	0.71	1	86	6.3	15.5	96	0.5
2e	1.76	1.3	85	4	15.0	96	3.7
3e	1.75	1.6	83	4.9	14.0	96	3.7
4e	1.95	1.8	83	4.3	14.0	94	3.7
1f	0.67	0.8	81	7.6	13.0	91	9.7
2f	1.21	1.3	82	7.8	13.5	92	8.5
3f	-	-	87	-	16.0	92	-
1g	0.67	0.7	73	11.2	9.0	85	11.1
2g	-	-	69	-	7.0	79	-
3g	0.60	1.10	72	10.2	8.5	91	11.3
4g	-	-	71	-	8.0	85	-

The large variability shown by the standard deviations represents in part the inconsistency introduced by utilizing many core loggers. The changing recording systems used over the years at Ekati™ add to this variability. Lower variability's at Koala North can be partly attributed to less data and more consistent logging within one system. Extremely low variability cannot be expected simply due to the inherent variability of the geologic structures in question.

Future deterministic analyses will use the mean values for both joint set orientations and roughness characteristics; however, variability in the parameters must be kept in mind. It may also be beneficial to perform probabilistic analyses such that this variability can be quantitatively captured. This type of probabilistic analysis, while extremely useful, is beyond the scope of this thesis.

6.2.2 Using Coefficients of Correlation to Help Identify Spatial Continuity of Joint Sets

Section 5.3.1 discussed the concept of the correlation coefficient, which was then applied to quantitatively assess the similarity between two stereonets. The same procedures may be used to assess the similarity between more than two variables.

For instance, a rock mass may be divided up into slices and stereonets generated of each slice. Each stereonet contains 100 windows, as before, which are representative of a specific orientation range. The correlation of one window throughout these multiple stereonets can then be assessed.

A region in space (i.e. rock mass) is divided up into n slices. Thus n stereonets are generated and a particular orientation range represented by window Z is analyzed. The frequency values within window Z for slices 1 to $n-1$ represent the X values in Eqn 5-1, and frequency values within window Z for slices 2 to n represent the Y values. The coefficient of correlation can now be calculated.

In this method, the values of window Z are compared over multiple slices. A high correlation would indicate that the joint set is present over all slices, and thus is found throughout the rock mass. Low correlations would indicate a discontinuous jointing pattern (i.e. randomness), or the presence of that set in some slices but not others. If the latter scenario is encountered cell mapping can be used to fill in the blanks regarding localized jointing patterns within the rock mass.

It may be possible to determine the continuity of a joint set by simply analyzing contoured stereonets of the slices; the drawback to this method is that being subjective, it is not quantifiable. The correlation method is perhaps more useful when determining if a cluster of poles is worthy of being classified as a minor joint set, or are simply some pseudo-random discontinuities present over a limited area. In addition, the method can be used to see how extensive minor joint sets are, or whether a certain joint set is encountered throughout adjacent structural domains.

At Ekati™ all major joint sets are obvious, as are any that traverse multiple domains. The above procedure would be very useful in further delineating minor joint sets, but is beyond the scope of this thesis.

6.2.3 Determination of Structural Domain RQD

From the joint data, an average value for the rock quality designation (RQD) over each structural domain was calculated. RQD was proposed by Deere (1964) as a measure of the quality of borehole core and can be calculated via Eqn 6-1, where the numerator represents the length of core greater than a threshold value (typically 100 mm) and the denominator is the total length of all core.

$$RQD = 100\sum_{i=1}^{n} \frac{\overline{X}_{n}}{L} \qquad \text{Eqn 6-1}$$

Core sizes from BQ to PQ with core diameters of 36.5 mm to 85 mm, respectively, are generally acceptable for measuring RQD as long as proper drilling techniques are used that do not cause excess core breakage or poor recovery, or both (ASTM D6032-96). The Ekati™ drilling program utilized core that was primarily of HQ size, which has a diameter of 65 mm. Some NQ sized core (nominal 50 mm diameter) was drilled as well.

While logging, the total length parameter in the RQD equation is typically taken to be the length of a run, 10 ft or 3.048 m. When calculating RQD over a domain, the length consisted of segments of orientated diamond drill core. The average RQD over all segments is used as a representative value for the domain.

Note that the RQD value calculated is based solely on oriented fractures. Consequently, poor areas in the rock mass where orientation was lost are not captured in the value. Thus, the RQD calculation should be treated with caution, as it will give artificially high values. Also, note that the calculated RQD values are averages over all sections of drill hole at any orientation that lie within a given structural domain. No efforts to account for spatial variance were made. Table 6-3 gives the RQD value over the structural domains of each area.

Table 6-3 Structural Domain RQD Values

Mining Area	**Structural Domain**	
	Number (#)	**RQD (%)**
Koala	1	96
	2	97
Koala North	1	89
	2	93
	3	95
Panda	1	96
	2	98

The RQD is quite high in all areas. Relative to other values in the table, Koala North appears to be the most broken-up region as the three lowest RQD values all correspond to this area. Table 6-2 seems to support this finding, as Koala North has more domains, more joint sets, and lower joint set spacings than the Koala and Panda areas. These factors would seem to contribute to the formation of smaller block sizes within the Koala North area.

From visual observations, certain areas of Koala North (particularly along the south wall) appear to have the most closely spaced joints and hence smallest block size. However, depending on the orientations of the discontinuities the true spacing is not observed (Figure 4-7) and thus visual observations are not always the most reliable.

6.3 Shear Strength of Joints

6.3.1 Empirical Analysis of Joint Shear Strength

The shear strength of a joint is a function of effective normal stress σ'_n and friction angle ϕ. This relation is given in Eqn 6-2 and is known as the Mohr-Coloumb shear strength failure criterion (Priest, 1993).

$$\tau = \sigma'_n \tan\phi \qquad \text{Eqn 6-2}$$

The friction angle itself can be considered to be the sum of two values: the residual or basic friction angle ϕ_r for an apparently smooth surface of the rock material, and a roughness angle i due to surface irregularities of a joint (Priest, 1993). This relationship is given in Eqn 6-3.

$$\phi = \phi_r + i \qquad \text{Eqn 6-3}$$

The roughness angle may also be broken down into two components, a geometrical component and an asperity strength component. Thus, there are three components of shear strength – a basic frictional component, a geometrical component controlled by surface roughness, and an asperity failure component (Brady and Brown, 1993). Asperity failure occurs at large normal stresses when shear will not occur over the asperities; instead the asperities will be sheared through.

Total frictional resistance is very difficult to ascertain but it is possible to estimate its individual components. The basic friction angle is determined from a rock specimen that has a very smooth surface; a simple tilt test is all that is needed for approximate estimation. Stimpson (1981) suggests a technique using rock core, something readily available at Ekati™. Note that a wet sample may have a lower friction angle due to pore water pressures reducing the normal stresses on the joint face.

The asperity geometry contribution to total roughness can be captured by estimating the Laubscher (1990) small-scale joint expression parameter (B) when logging core. The joint roughness coefficient (JRC) from Barton et al. (1985) is another such method and was the procedure employed during cell mapping.

The asperity failure component of total roughness is portrayed by the Laubscher (1990) joint wall alteration parameter (C). Similarly from Barton et al. (1985) the joint wall compressive strength (JCS) in another way to quantify this parameter. At the Ekati™ mine the joint walls are generally considered unaltered and thus their strength is simply taken to be that of the host rock.

Barton proposed that the peak shear strength of joints could be represented by the empirical relation given in Eqn 6-4 (Brady and Brown, 1993).

$$\tau = \sigma'_n \tan\left[JRC \log_{10}\left(\frac{JCS}{\sigma'_n}\right) + \phi_r \right] \qquad \text{Eqn 6-4}$$

At the Ekati™ mine the depth of overlying rock is used to approximate the effective normal stress acting on a joint surface. The JRC parameter is not known from logging drill core but the B parameter is; the conversion can be accomplished via Eqn 4-2. The validity of this conversion will be established shortly.

As stated previously, the JCS is simply the uniaxial compressive strength of the host granite rock, which is approximately 150 MPa. The basic friction angle for the host rock is approximately 31° (Priest, 1993), a typical value for granite rock types. These are all the parameters required to estimate joint shear strength empirically.

The existence of joint infill can have both a positive and negative impact on strength, depending on the properties of the infill material. A healed joint bonded by calcite will introduce an apparent cohesion into Eqn 6-2 and Eqn 6-4, thus increasing the shear strength of the joint. Effects of cohesion will be more significant at low normal stresses, where failure is still occurring over the asperities and not through them.

A low friction material such as clay infilling a joint will often decrease the shear strength (Priest, 1993). The infill must be thick enough when compared to the height of asperities to effect shear behaviour. As well, certain clay families swell upon hydration and can cause high pressures if dilation is inhibited. This serves to reduce normal stress on the joint and therefore decreases shear strength. If joint sets exist with clay infilling (i.e. low joint infill values represented by the Laubscher (1990) D parameter), the JCS value could be lowered to reflect that the clay would dominate the shear strength of the joint as it's thickness is greater than the height of the asperities.

As can be seen in Table 6-2, no joint sets seem to be dominantly clay filled, which would be indicated by Laubscher values around 50. Not accounting for joints dusted with clay or having thin layers of calcite (D values in the 80 to 90 region) likely introduces some error, which is not conservative. However, logging practices at Ekati™ were somewhat inconsistent (i.e. infill thickness not always recorded, discrepancies over years as to what value to assign to clay dusting) so it was thought better to leave the JCS value unaltered. Note from Table 6-2, all joint surfaces are quite rough (B parameter > 80), and therefore any infill will dominate behaviour only if the thickness is greater than the asperity height; this is not the case for the joint sets at Ekati™.

6.3.2 Lab Results and Comparison from Joint Shear Strength Testing

Mathis (1998) reported direct shear laboratory test results for samples of open joints (i.e. not healed) taken from both the Koala and Panda mining areas. These results will be used to substantiate JRC data collected from diamond drill core logging. A sample specimen is shown in Figure 6-2; image A is a side view of a joint before testing and image B is an overhead view of both joint surfaces after shear testing.

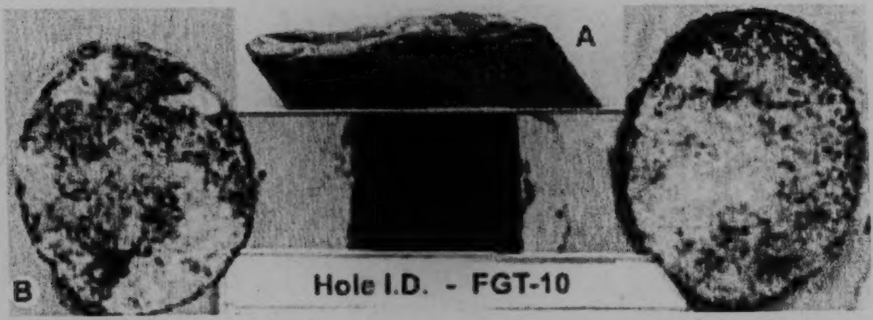

Figure 6-2 Direct Shear Testing of Joints (modified from Mathis, 2002)

The peak shear strength results along with associated applied normal stress are given in Table 6-4. Also included in this table are additional calculations used to help establish the degree of confidence in the measurements made during core logging (average measured JRC values from Table 6-2).

Table 6-4 Direct Shear Test Results

Project	Hole ID	Domain	Sample Depth (m)	Peak Normal Stress (kPa)	Peak Shear Strength (kPa)	Equiv. Depth (m)	Back Calc. *i* (deg)	Back Calc. JRC	Ave. Back Calc. JRC	Ave. Meas. JRC
Koala	Kgt-03	1	116.74	810	1424	30.6	29	13	11	11
	Kgt-03		134.25	503	806	19.0	27	11		
	Kgt-03		145.68	150	1032	5.7	*51*	17		
	Kgt-05		174.85	321	256	12.1	8	3		
	Kgt-06	2	121.13	522	787	19.7	25	10	10	11
Panda	Pgt-01	1	81.50	140	95	5.3	3	1	5	14
	Pgt-02		47.90	280	494	10.6	29	11		
	Pgt-03		195.35	448	379	16.9	9	4		
	Pgt-04		154.30	742	571	28.0	7	3		
	Pdc-09	2	312.22	141	314	5.3	35	12	11	8
	Pdc-09		319.04	280	462	10.6	28	10		

The structural domains from which the samples were taken correspond to those determined in Chapter 5. The equivalent depth was calculated from the peak normal stress and is the thickness of overlying granite that would create such a stress. The equivalent depths range from 5 to 31 metres; representative of possible locations of joint failure planes within a bench.

Given peak shear strength, the equivalent JRC parameter is back calculated using Eqn 6-4. The average over the structural domain is then calculated and compared to the average of JRC values measured via core logging (from Table 6-3). Based on the limited number of lab tests carried out, the agreement between back calculated JRC values and measured JRC values is quite good. This provides confidence that Eqn 4-2 is adequate in relating the B and JRC joint roughness parameters.

However, a large discrepancy occurs in Domain 1 of the Panda area where measured JRC values are significantly higher than were found from test results. As only two tests were done in this area, they may not be representative of the domain. As well, the uniaxial compressive strength of granite was used as a value for JCS, thus joint infilling is not adequately captured. In Figure 6-2, calcite can be seen on the surface of the joint; this would result in lower shear strengths than if the joint was clean. As the thickness of these calcite layers is not specifically recorded during core logging, it is not possible to reliably degrade the JCS value from the default value of granite.

Recall that in Chapter 5 two upper domains were determined for Panda, though the correlation between them was relatively high. As the measured JRC values in Table 6-4 are quite different between the upper domains, they will be kept separate.

It was also of interest to calculate the roughness angle i of Eqn 6-3, as many computer software programs do not use JRC values but instead require Mohr-Coloumb parameters when calculating shear strengths of discontinuities. Priest (1993) recommends that for design purposes the total friction angle should not exceed 70°; use of an angle greater than 70° may lead to unrealistic results. As the basic friction angle is 31°, any back calculated roughness angles in Table 6-4 should be truncated to a maximum of 39°.

In general, the level of agreement between fieldwork and laboratory test results establishes the validity of the data collected during the core logging process. Due to the limited amount of laboratory testing performed, the results measured from core logging will be used in future analyses.

6.4 Summary of Structural Domains and Major Joint Sets at the Ekati™ Diamond Mine

The structural domains are defined at the Ekati™ site, as well as the joint sets and their characteristics prevalent within these domains. The following figures are contoured stereonet pole plots of all structural domains with identified joint sets. The figures are equal-area, lower hemisphere projections. Table 6-5 provides a summary of the information.

For Koala South, in Figure 6-3 (A) and Figure 6-4 (A) the shading represents Fisher concentrations % (0 to 5) of total per 1% area. Mean joint set orientations are indicated in Figure 6-3 (B) and Figure 6-4 (B).

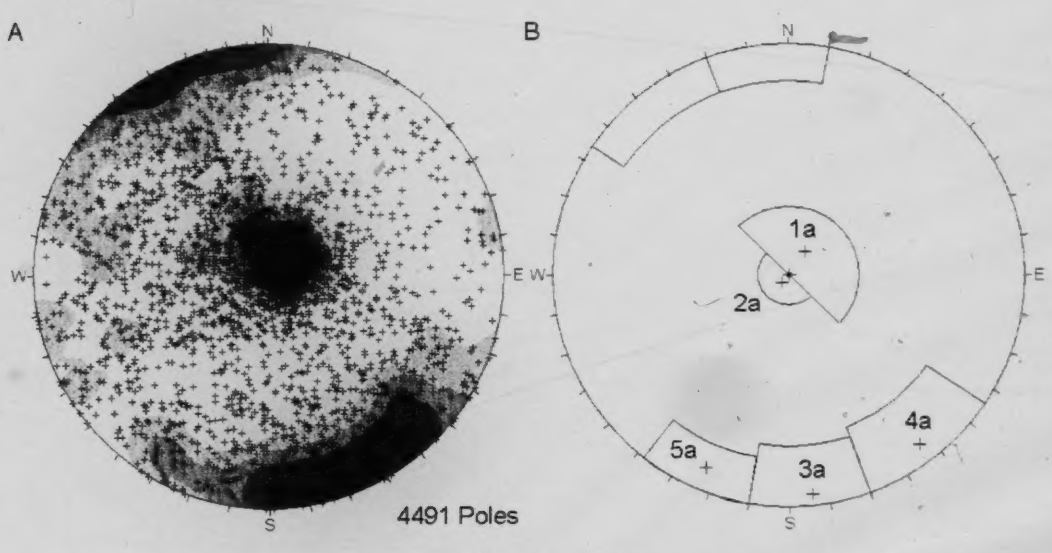

Figure 6-3 Stereonet of Contoured Joint Poles (A) and Joint Set Windows (B) in Koala Structural Domain 1

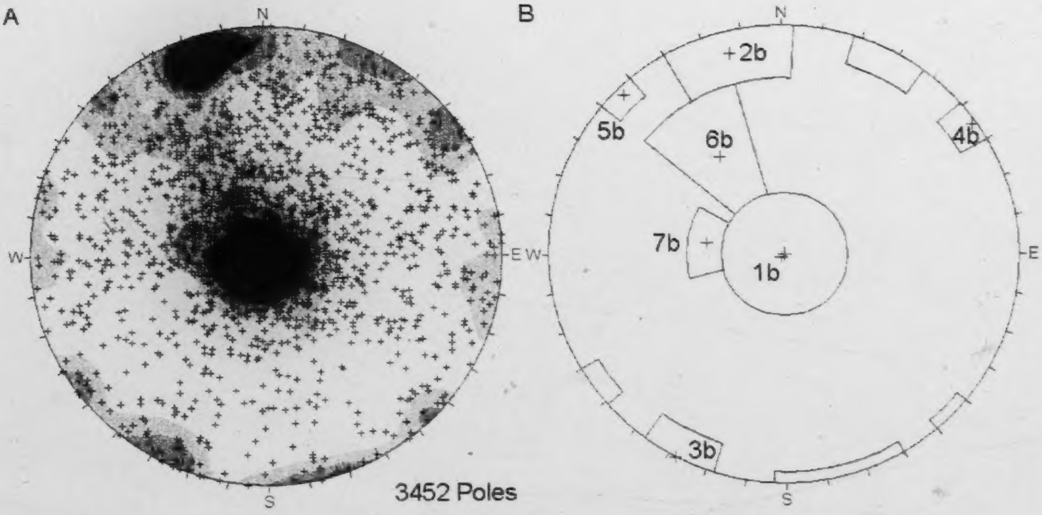

Figure 6-4 Stereonet of Contoured Joint Poles (A) and Joint Set Windows (B) in Koala Structural Domain 2

For Koala North, in Figure 6-5 (A), Figure 6-6 (A) and Figure 6-7 (A) the shading represents Fisher concentrations % (0 to 5) of total per 1% area. Mean joint set orientations are indicated in Figure 6-5 (B), Figure 6-6 (B) and Figure 6-7 (B).

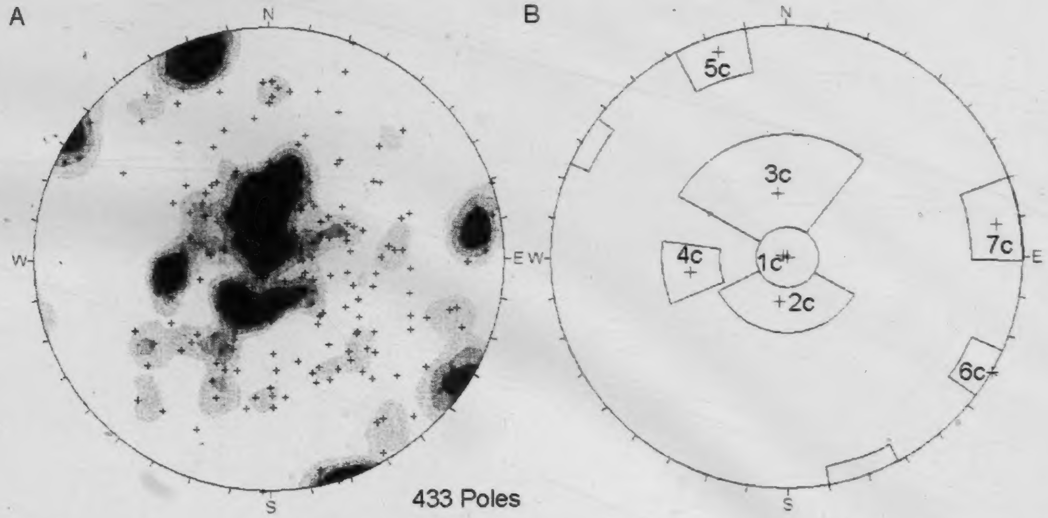

Figure 6-5 Stereonet of Contoured Joint Poles (A) and Joint Set Windows (B) in Koala North Structural Domain 1

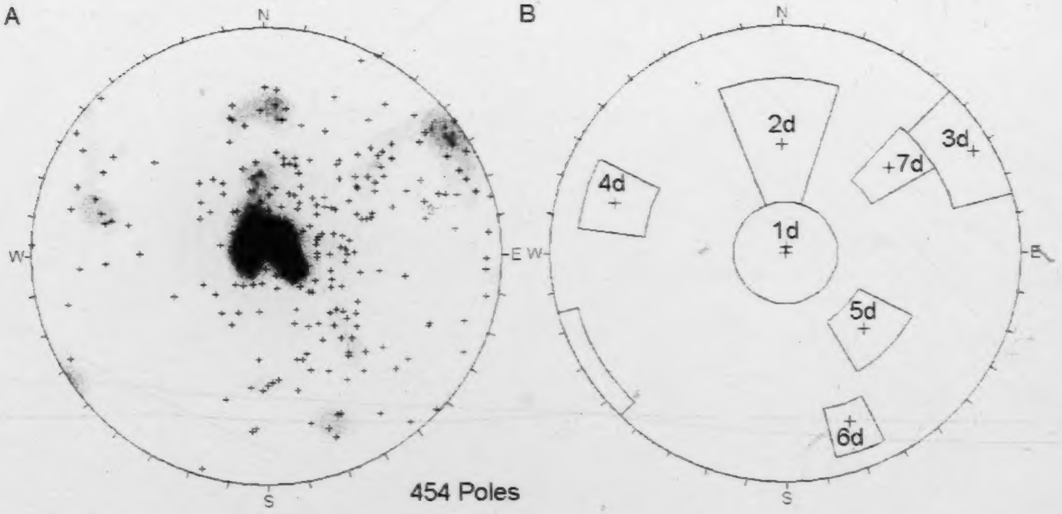

Figure 6-6 Stereonet of Contoured Joint Poles (A) and Joint Set Windows (B) in Koala North Structural Domain 2

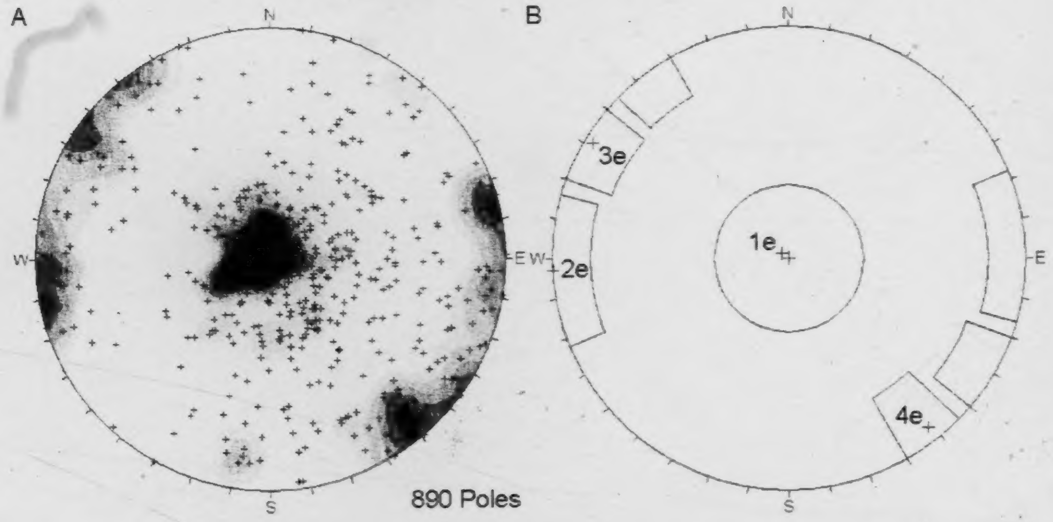

Figure 6-7 Stereonet of Contoured Joint Poles (A) and Joint Set Windows (B) in Koala North Structural Domain 3

For Panda, in Figure 6-8 (A) and Figure 6-9 (A) the shading represents Fisher concentrations % (0 to 10) of total per 1% area. Mean joint set orientations are indicated in Figure 6-8 (B) and Figure 6-9 (B).

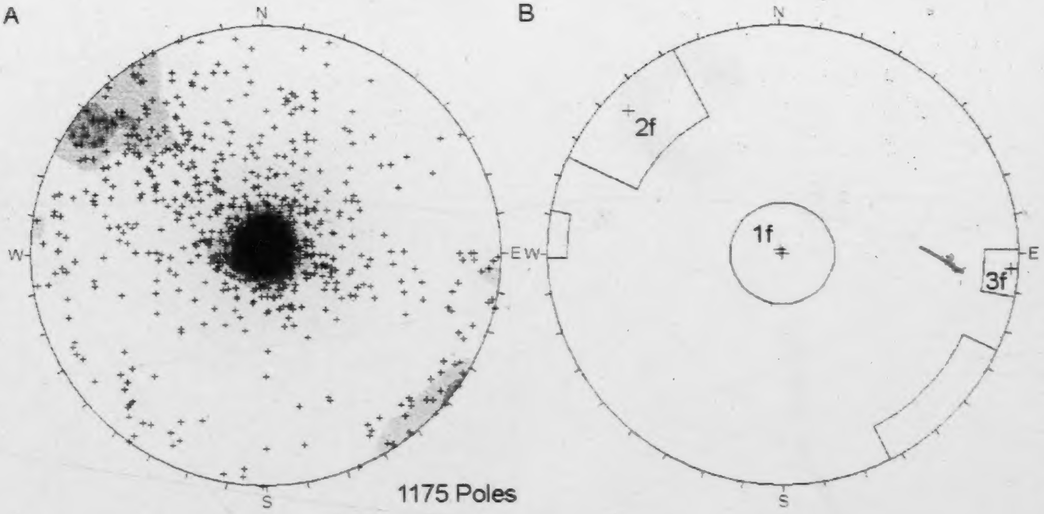

Figure 6-8 Stereonet of Contoured Joint Poles (A) and Joint Set Windows (B) in Panda Structural Domain 1

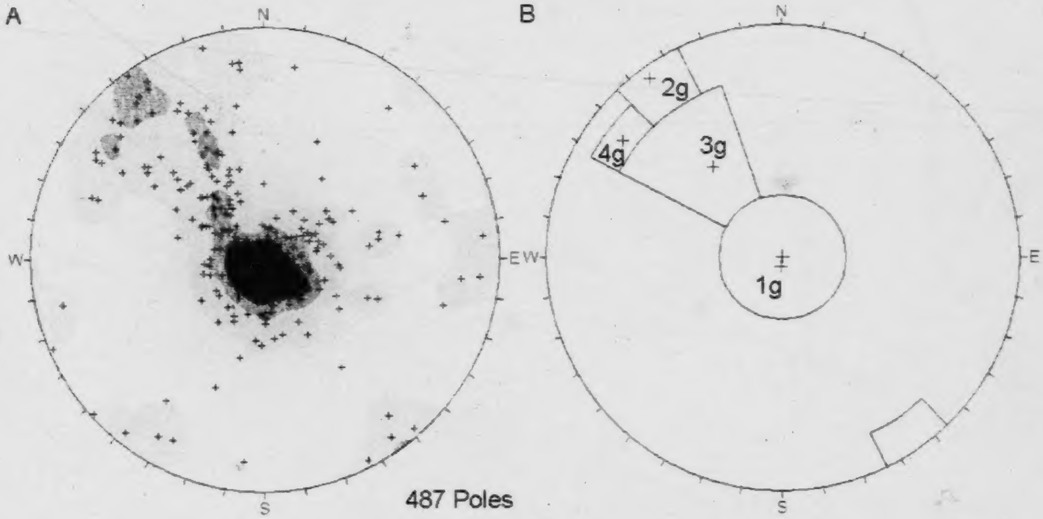

Figure 6-9 Stereonet of Contoured Joint Poles (A) and Joint Set Windows (B) in Panda Structural Domain 2

Table 6-5 Summary of Structural Domains and Joint Sets at Ekati™ Mine

Mining Area	Structural Domains				Joint Sets				
	Num. (#)	Radial (deg)	Elev. (m)	RQD (%)	Num. (#)	Plane Orient.		Spacing (m)	Rough. (JRC)
						Dip (deg)	Dip Dir. (deg)		
Koala	1	255-090	>75m	96	1a	14	214	1.16	11.0
					2a	05	042	1.55	12.0
					3a	87	354	1.57	9.5
					4a	85	323	1.32	11.0
					5a	84	023	2.00	9.5
	2	090-255	>75m	97	1b	02	046	1.00	12.0
					2b	84	166	1.63	10.0
					3b	90	028	1.60	10.0
					4b	89	235	1.94	11.5
					5b	88	136	-	11.0
					6b	53	148	1.97	11.0
					7b	37	099	1.96	12.5
Koala North	1	315-045	all	89	1c	02	121	1.26	17.0
					2c	22	010	0.63	17.0
					3c	31	172	1.01	17.0
					4c	46	081	-	17.0
					5c	86	162	-	17.0
					6c	90	302	-	17.5
					7c	84	261	-	16.0
	2	045-165	all	93	1d	03	193	0.58	17.0
					2d	51	179	0.78	16.5
					3d	85	241	1.02	11.5
					4d	74	107	-	14.0
					5d	50	315	-	13.5
					6d	76	340	-	14.5
					7d	60	230	1.61	17.0
	3	165-315	all	95	1e	04	125	0.71	15.5
					2e	90	087	1.76	15.0
					3e	88	121	1.75	14.0
					4e	86	321	1.95	14.0
Panda	1	255-130	>200m	96	1f	02	155	0.67	13.0
					2f	84	134	1.21	13.5
					3f	88	274	-	16.0
	2	130-255	>200m	98	1g	05	006	0.67	9.0
					2g	87	144	-	7.0
					3g	52	143	0.60	8.5
					4g	80	127	-	8.0

With this information, it is now possible to analyze specific stability issues that were introduced in Chapter 3. In Chapter 7, particular areas of concern pertaining to mining operations are elaborated upon. Methods available for managing these potential structurally controlled failures will be proposed at this time; then analysis can proceed.

Chapter 7

Potential Rock Mass Instabilities at Ekati™ Mine

7.1 Surface to Underground Transition

Bench failures occurring while surface mining is still ongoing will obviously have an impact on the operating area and movement of surface equipment. Currently diligent monitoring by on-site geotechnical engineers as well as field personnel discover many unstable areas before failure has a chance to occur. The area may then be coned off and allowed to fail, initiated to fail, or stabilized.

These small bench failures may perhaps have a more significant impact once underground mining starts and a gloryhole is formed. The planned mining method leaves no crown pillar at the base of the open pit. As no material will be left over the drawpoints, the mining area will be left exposed to any highwall failures that might occur. In fact, the layout of the open bench method is such that any overhead material coming loose will be funnelled into the drawpoints. In addition, the area will be exposed to weathering effects, further adding to issues of instability. For open benching to be successful at Koala North, the stability of the open pit highwall and gloryhole walls must be ensured.

Akin to bench failures in surface operations, in underground excavations the stability of the decline, ramp, development drifts, and cross-cuts also pose a threat to the operation of the mine. In the well-jointed Ekati™ rock mass, wedge failures will be the foremost concern.

In order to evaluate stability in either surface or underground mining areas, an understanding of the local jointing conditions is necessary. The transition from surface mining to that of underground is illustrated in Figure 7-1.

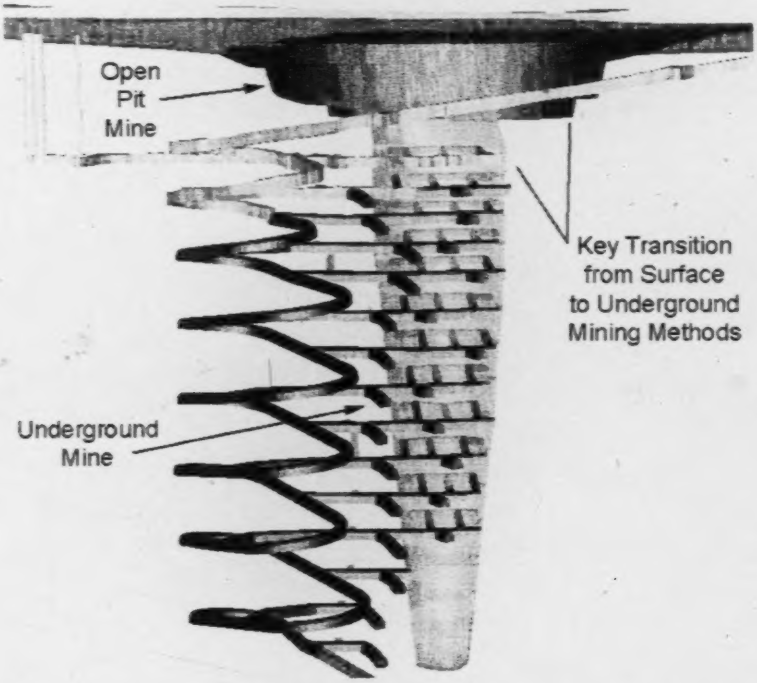
Open
Pit
Mine
Key Transition
from Surface
to Underground
Mining Methods
Underground
Mine

Figure 7-1 Surface to Underground Transition at Koala North

Figure 7-1 illustrates the fact that surface mining activities will directly impact future underground operations. Potential problems stemming from the activities of both surface mining and underground mining methods and their influence on underground operations are discussed next.

7.2 Causes of Instability and Consequences of Failure

7.2.1 Effects of Surface Mining on Underground Operations

Instability in the open pit is caused by unfavourable fault or joint orientations with respect to the pit wall. These types of failures would not likely traverse multiple benches, although cases of larger scale failures are possible, as is shown in Figure 7-2.

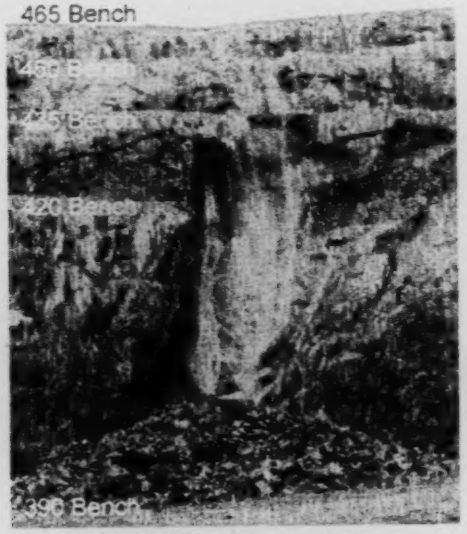

Figure 7-2 Multiple Bench Planar Failure in Koala Pit, Spring 2002 (photo courtesy of Gary Baldwin)

As noted previously, perhaps of greater importance is the impact that a reduced catchment width from a bench failure will have on underground operations. Recall that current surface mining operations are designed with 14 m wide catch benches, 3 m of which are allowable spall. Excessive spall off the bench crest will reduce the width below the desired 11 m; below 8 m is critical. Also reducing catchment widths are large bench toes that are not removed. In both cases, blasting practices coupled with structural features in the area will determine how successful the operation is in reaching the targeted 11 m bench width. Figure 7-3 is a plan view of a bench in Panda pit, with the degree of shading indicating achieved catchment width.

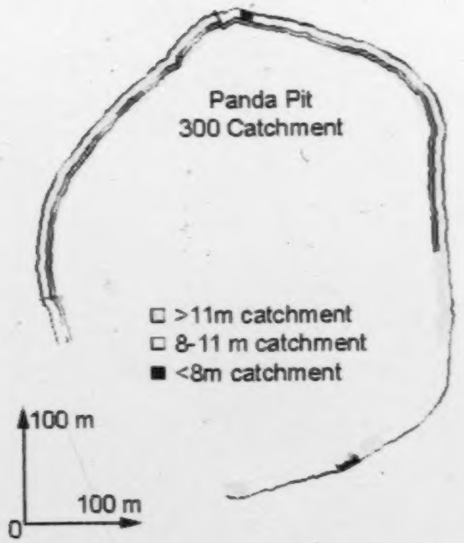

Figure 7-3 Catchment Width Achievement on Panda 300 Bench

As can be seen, two small areas are below the critical threshold. These areas having catchments of less than 8 m will be potentially hazardous to future underground operations.

The primary purpose of catch benches is to intercept falling rock and prevent it from causing damage to people and equipment. The benches must be designed such that they adequately dissipate the kinetic energy from a rock fall. Rock debris must then be periodically removed such that the catch bench remains functional.

A narrow catch bench will not perform its intended duties on three fronts. First, it is not wide enough to intercept all of the falling rocks. Second, it does not provide adequate run-out to dissipate the kinetic energy of any rocks that do manage to fall on it; thus they continue down to the pit bottom. Third, a bench may be so narrow that equipment is prohibited from cleaning the bench surface. As debris is built up, the already ineffective bench becomes even less efficient. Figure 7-4 depicts such a zone in Koala pit.

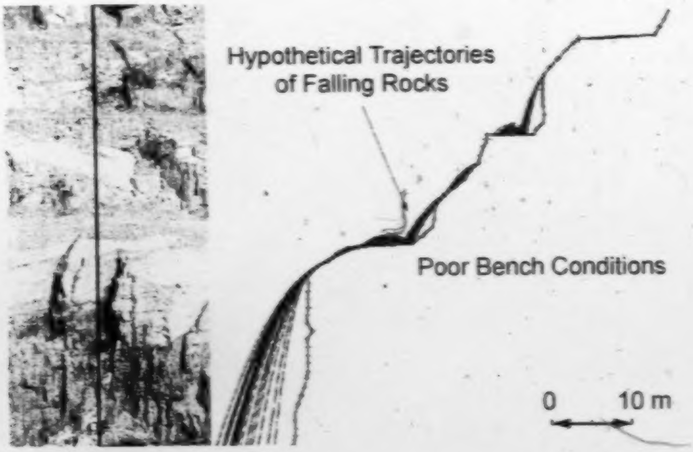

Figure 7-4 Unstable Section in Koala Pit West Wall

The right side of the figure is a cross section through the vertical line in the left and illustrates how poor wall control and ineffective catchments may allow falling rock to enter the gloryhole. The hypothetical rock trajectories were generated using the RocScience program Rocfall (Tannant and Wang, 2003).

Concerning bench failures, it is possible to stabilize these problem areas while the open pit is still in operation. Once surface mining is completed, stabilization of these zones will be far more difficult as direct access to the area may no longer be admissible if narrow bench widths prevent mobilization of equipment.

Failures of the highwall will therefore affect both the safety and economics of surface and underground operations. In surface operations, bench failures may damage equipment, restrict access to areas and require clean-up and possible remedial measures such as stabilization and monitoring. For underground operations, these failures have the potential to damage equipment such as scoops operating below in the gloryhole. Large-scale wall failure would obviously have a huge impact on underground operations. Economics would dictate whether the material should be mucked out, or the operation converted to sub-level caving in the case of a large amount of material overlying the drawpoints.

7.2.2 Gloryhole Conditions

Failures occurring in the gloryhole walls are also caused by unfavourable joint orientations. Wedge failures will be the primary concern but cases of toppling failure may exist as well. In either case, joint set spacing and trace length will play an important role, as these factors influence the size of wedges that can fall to the drawpoints below.

Unlike bench failures in the open pit region, direct access to gloryhole walls is not possible, as shown for a South African diamond mine in Figure 7-5. Thus, any support method to be carried out, such as cable bolting, must originate in underground workings such as the development and cross-cut drifts.

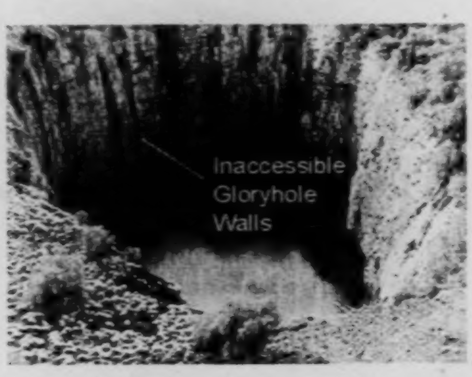

Figure 7-5 Kimberley Gloryhole, South Africa (modified from Aviation Adventure Tours, 2002)

The geometry of the kimberlite pipes may help to alleviate wedge failure concerns. Due to the carrot-shaped nature of the pipe, the area to perimeter ratio (hydraulic radius) decreases with depth. Increased wall curvature with depth should result in relatively even walls, thus allowing natural confining stresses to stabilize loose wedges. However, only the relatively small Koala North pipe, where the hydraulic radius ranges from 18 near suface down to 10 in the lower levels (Harvey, 2003), should benefit from this geometric stabilization. The other kimberlite pipes that are planned to be mined using underground methods are much larger than Koala North; thus, wall irregularities where failure is prone to initiate will be more likely.

Gloyhole wall failures will have much the same effect as overlying bench failures, causing potential damage to equipment such as scoops operating below. Restricting scoop access past the brow will minimize, but not completely eliminate, the risk of equipment damage, as brow failure is a possibility. Even if equipment is not damaged in the event of a failure, large blocks of granite can choke the drawpoints, thus delaying production and necessitating secondary blasting procedures. Dilution should be minimal as the granite chunks can be easily distinguished from the kimberlite ore, thus they can be separated before reaching the processing plant.

Large-scale gloryhole wall failure would obviously have a huge impact on underground operations. A large volume of rock falling to the bottom of the gloyhole would create a damaging airblast that could affect personnel and equipment working underground. In this case, the consequences of instability would extend far back from the drawpoints and affect a wide area of the underground development. As already stated, after a large-scale failure economics would dictate whether the open benching operation should be converted to sub-level caving as it may be difficult to re-establish open benching again.

Also note that due to the explosive emplacement of kimberlite pipes, the contact zone between host granite and intruded kimberlite ore may contain a higher degree of jointing. Once underground mining has exposed the gloryhole walls, sloughing of this broken zone of granite into the draw points may be a concern. The extent this zone penetrates back into the waste rock must be determined from exploratory diamond drilling. Ground support may be required to stabilize the draw points.

Sloughing of the contact zone will primarily affect economics by diluting the ore. This becomes more critical the deeper the mine progresses as the hydraulic radius is decreasing and hence for a given volume of waste rock, the dilution ratio will be higher. If problems do arise with dilution from the pipe wall then it may be desirable to make a conversion to sub-level caving (SRK, 2000). It should also be noted that if these contact zones do exist, they are likely quite permeable. Potential instability would then be maximized during freeze/thaw cycles when blocks are worked loose via ice-jacking.

7.2.3 Underground Development

Of primary concern to underground developments will be stability of the sidewalls and back (or roof). Wedge failures are the mechanism of failure in this environment. The size and nature of wedges created will depend on the orientation of structural features in the area with respect to the orientation and shape of the drifts. Given that the structural domains in the region are now known it is possible to determine an optimum orientation. Note that the optimal orientation of cross-cuts will also be affected by the stability of the brow, which was discussed in the previous section.

Figure 7-6 depicts a situation where mining personnel are required to work quite close to the brow. In this instance the presence of ice formations and of a curving granite/kimberlite contact contribute to possibilities of instability. Note the presence of an arched back, useful for improving stability, used this situation.

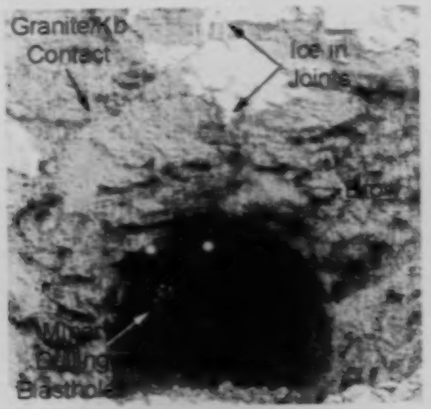

Figure 7-6 Cross-cut Drawpoint

The intersection of each development drift on a level with the cross-cut drifts is a critical area as well, and one where wedge formation may be more likely to occur due to the greater area of exposed back. The shape and size of developments can have an important role in minimizing failures, although these parameters are often established by operational constraints.

Wedge failures occurring in underground developments will have much the same effects as small bench failures do in surface operations. Namely, failures may damage equipment, restrict access to areas and require clean-up and remedial measures such as stabilization and monitoring.

Stabilization of potential wedge failures may be achieved by a variety of means. Wire mesh, rock bolts and shotcrete are primary lines of defence. Also under investigation is the use of spray-on liners for use in the cross-cuts. These liners are still in the developmental stage, as the challenges of adhering to a very friable material (kimberlite) in potentially sub-zero temperatures have not yet been overcome. Controlled blasting and a properly arched back will also improve stability, and may eliminate some of the need for additional artificial support.

7.3 Hazard Mitigation

Protective measures are required in order to control hazards associated with instituting the open bench underground mining method at Ekati™. I have proposed that through well-engineered development, adequate artificial support and proper instrumentation, these hazards can be kept in check and the operation maintained successfully. The following chapters address specific stability concerns in the context of the Koala North underground mine.

7.3.1 Gloryhole Stability

Gloryhole wall stability is critical to the success of underground mining operations. Wall orientations in conjunction with structural domains, and therefore the joint sets contained within, dictate what types of failure mechanisms are likely to occur. A kinematic failure analysis coupled with joint strength information and an understanding of the local stress conditions is required to determine an optimal direction from which to access the kimberlite pipe.

Given the well-jointed rock mass at Koala North, a cable bolting system may be useful in potential problem areas for gloryhole wall stabilization. In order to protect underground mining operations from gloryhole wall failure and the associated airblast, an advance warning system is desired such that adequate warning can be given to mine personnel before failure occurs.

7.3.2 Development Stability

Design of underground workings at Koala North should be approached with the structural geology of the area in mind. By carefully considering the shape and size of access drifts, it will be possible to reduce artificial support requirements, minimize production interruptions, and enhance the safety of the workplace. Concerning artificial support, rock bolting may be necessary to ensure safe working conditions.

Chapter 8

Stability Analysis of Koala North Gloryhole

8.1 Relevant Failure Mechanisms and Required Input

At Koala North, stability of the exposed gloryhole walls must be assessed in order to determine if large blocks of host granite have the potential to fall suddenly into the mining area, thus posing a safety hazard and possibly rendering the open bench mining method ineffective. Wall failures near the brow will be particularly detrimental to the underground mine as damage to the scoops or blockage of the drawpoints will halt production.

In Chapter 5, three structural domains were identified at Koala North. Although actual data sampling did not progress much below the 240 m elevation at Koala North, the structural domains will be assumed to be continuous and so apply down to the 100 m elevation, which is currently the lower limit for planned underground mining. Chapter 6 identified the dominant joint sets within the structural domains. Strength and spacing characteristics were determined for all joint sets.

The structural domains and joint set characteristics will be used to analyze gloryhole wall stability at Koala North. Wedge failures and toppling failures will be the two modes of failure analyzed, as these failure types are most commonly observed at the mine. From the results, it will be possible to recommend optimal orientations and support mechanisms for the cross-cuts accessing the kimberlite orebody. The findings will be compared to what is currently being done at Koala North (recall this depiction in Figure 3-7).

8.2 Analysis Methodology

8.2.1 Wedge Failures

The stability of the gloryhole wall in each structural domain will be analyzed. In most structural domains at Ekati™, the most dominant joint set is sub-horizontal. As joints generally have little to no tensile strength, it is predicted that the tops of wedges would open up along these sub-horizontal joints.

Thus, wedge failures in the gloryhole walls may be analyzed in a fashion similar to wedge failures occurring along bench faces in an open pit environment. An example of horizontal joint relief causing mid-bench wedge failures is shown in Figure 8-1.

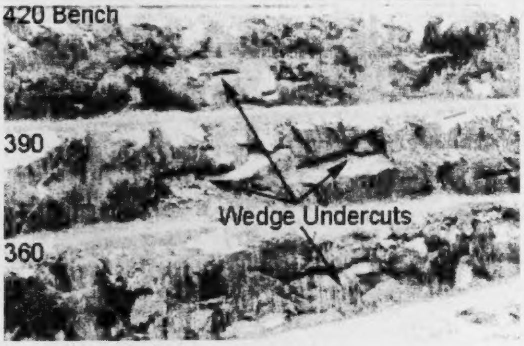

Figure 8-1 Wedge Undercutting in Panda Pit NW Wall

Note that the undercuts were formed via the horizontal joint set in conjunction with a moderately dipping northeast trending joint set and another subvertical set. These sets were identified earlier, and lend further credence to the structural domain delineation and joint set identification procedures employed in earlier chapters. Stereonets for Panda pit Domain 1 are located at the end of Chapter 6 and depict the aforementioned joint sets.

In many instances, cable bolting was required to stabilize the overhanging rock mass left by the undercutting wedge. Improper blasting practices against the final wall tend to exacerbate these failures; particular attention should be paid to the geologic structure in the area of a blast.

This opening up of the sub-horizontal joints will also affect the stresses on the joints near the gloryhole wall. Effectively, the normal stresses acting on the joint planes forming the wedge will be due solely to the weight of the wedge itself, and not of any overlying rock mass. A wedge formed in this fashion is illustrated in Figure 8-2, where discontinuity C represents the sub-horizontal joint set.

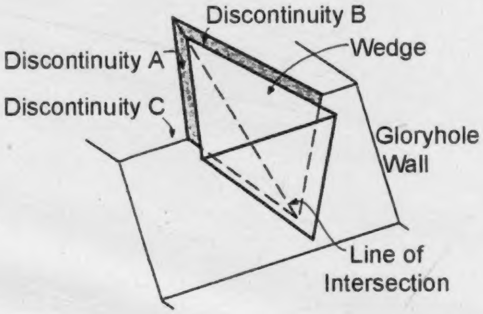
Discontinuity B
Wedge
Discontinuity A
Discontinuity C
Gloryhole Wall
Line of Intersection

Figure 8-2 Wedge Formed by Intersection of Three Discontinuities with Gloryhole Wall (modified from Norrish and Wyllie, 1996)

Plotting the joint sets and range of gloryhole wall orientations on a stereonet enables the identification of kinematically feasible modes of failure. Wedge identification via a stereonet is depicted in Figure 8-3. Note that for clarity the sub-horizontal joint set has not been plotted.

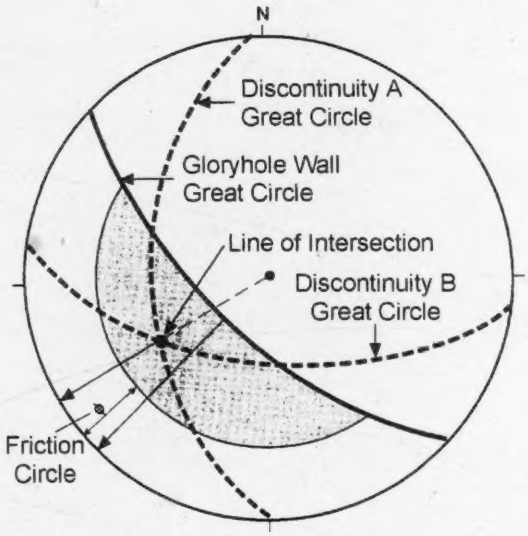
N
Discontinuity A
Great Circle
Gloryhole Wall
Great Circle
Line of Intersection
Discontinuity B
Great Circle
Friction
Circle
φ

Figure 8-3 Stereonet Wedge Failure Identification (modified from Norrish and Wyllie, 1996)

Lines of intersection occurring in the shaded area of Figure 8-3 represent wedges that are potentially unstable. The conditions for wedge failure are as follows (Norrish and Wyllie, 1996):

1) The trend of the line of intersection must approximate the dip direction of the slope face (i.e. the gloryhole wall).

2) The plunge of the line of intersection must be less than the dip of the slope face (i.e. must daylight on the gloryhole wall).

3) The plunge of the line of intersection of discontinuity planes A and B must be greater than the average angle of friction of the two discontinuities.

After identification of critical joint sets, it is necessary to determine the strength parameters along these planes. While stereonet analysis identifies kinematically feasible wedges (conditions 1 and 2), strength information (condition 3) is required to quantify, via a factor of safety, the likelihood of failure.

Strength parameters for the joints were determined as discussed in Section 6.3. Briefly, JRC values for all joint sets were available (Table 6-5), and the JCS was taken to be the strength of granite (150 MPa). Using Eqn 6-4 with a normal stress on the joints equivalent to a 10 m high column of granite on a 1 m^2 base, the roughness angle was back calculated and added to the base friction angle (31°) to get the total friction angle. Although most wedges formed will likely not be as large as a 10 m column of granite, it was felt prudent to be conservative because possible damaging effects from blasting have not been incorporated.

Wedges defined by their three discontinuity planes (or joint sets) and associated total friction angles were input into the RocScience program SWedge to calculate a factor of safety. If inadequate, the factor of safety can be increased by applying external forces (i.e. cable bolts) to the wedge. Note that the wedge analyses assume that the wedges, defined by three intersecting discontinuities, are subjected to gravitational loading only. Therefore, the stress field in the rock mass surrounding the excavation is not taken into account, although its effects will be discussed later on in this chapter. While this assumption leads to some inaccuracy in the analysis, the error is generally conservative, leading to a lower factor of safety (RocScience geomechanics software and research, 2003).

8.2.2 Toppling Failures

Toppling failure is another failure mechanism that is possible in the walls of the gloryhole. Flexural toppling, block toppling and block-flexural toppling are primary modes of this type of failure. Block toppling is depicted in Figure 8-4. Due to spacing characteristics of the joint sets and strength parameters of the intact rock, block toppling is the most likely mode to be encountered at Ekati™.

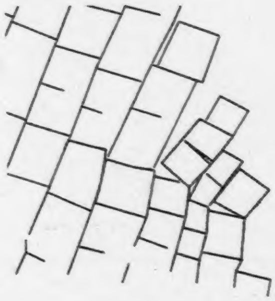

Figure 8-4 Block Toppling in a Hard Rock Mass with Widely Spaced Orthogonal Joints (modified from Hudson and Harrison, 1997).

Plotting the joint sets and range of gloryhole wall orientations on a stereonet enables the identification of kinematically feasible modes of failure. Joint strength information is added to the stereonet (i.e. angle of friction) to further define potential failures. Toppling identification via a stereonet is depicted in Figure 8-5.

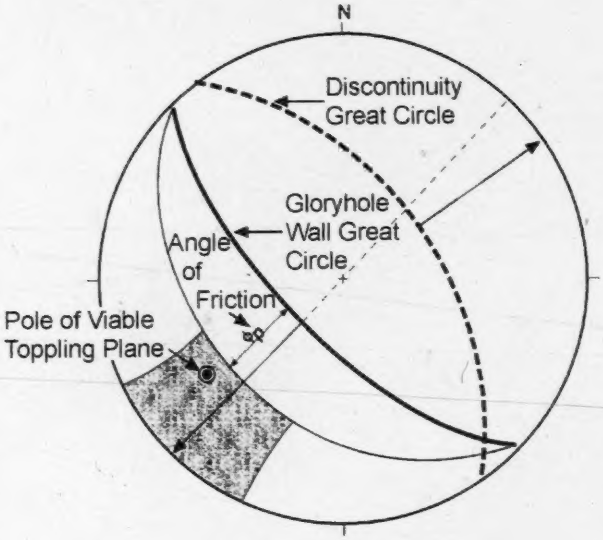
N
Discontinuity Great Circle
Gloryhole Wall Great Circle
Angle of Friction
ϕ
Pole of Viable Toppling Plane

Figure 8-5 Stereonet Toppling Failure Identification (modified from Norrish and Wyllie, 1996)

Poles plotted in the shaded region of Figure 8-5 represent possible toppling modes of failure. The conditions needed to satisfy toppling failure may be described as follows:

1) The discontinuities must have a dip direction within +/-20° of the slope face dip direction, and must dip into the slope face (Norrish and Wyllie, 1996).

2) The pole of the discontinuity plane must have a plunge less than the inclination of the slope face less the friction angle of the discontinuity (Norrish and Wyllie, 1996).

3) There must be a set of discontinuity's to form the bases of the toppling blocks (Hudson and Harrison, 1997).

In addition to the above three points, which may be determined via a stereonet, joint set spacing characteristics and trace lengths must be known in order to determine if the centre of gravity of the block falls outside the dimension of its base, a necessary condition for toppling failure. Recall that Ekati™ joint spacing information is given in Table 6-5.

With the above in mind it is possible to perform a simple direct toppling instability analysis, which relates only to the geometry of the rock and does not include strength parameters (Hudson and Harrison, 1997). In reality, strength parameters are important as significant horizontal movements at the crest and very little movement at the toe characterize toppling failures. In order to accommodate this differential movement between the toe and crest, interlayer movement must occur. Thus, shear strength between layers is crucial to the stability of a slope that is structurally susceptible to toppling (Norrish and Wyllie, 1996).

The analytical procedures for toppling failure analysis are not as clear-cut as for other methods of rock slope failure, particularly the concept of factor of safety (Norrish and Wyllie, 1996). Simultaneous toppling and sliding behaviour of the blocks further complicate an accurate failure prediction and factor of safety. With this in mind, only the possibilities of toppling failure will be assessed, no effort is made to quantify a factor of safety.

8.3 Stability Investigations

8.3.1 Structural Domain 1 Analysis

The joint sets and friction circle for structural Domain 1 were plotted on a stereonet and feasible wedge and toppling modes of failure identified. The stereonets are shown in Figure 8-6 A and B. Only relevant joints contributing to the failure modes are plotted.

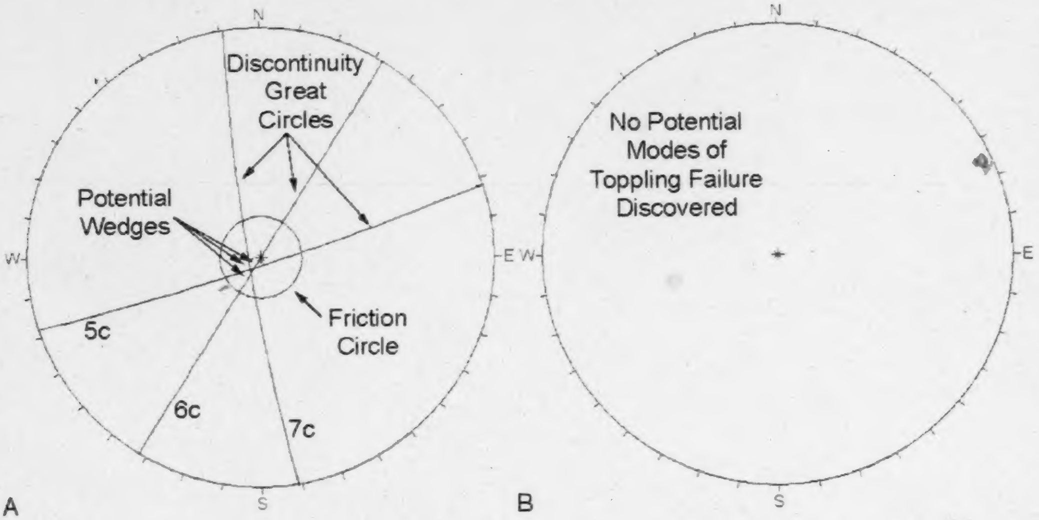
N
Discontinuity Great Circles
Potential Wedges
W
E
5c
Friction Circle
6c
7c
S
A
N
No Potential Modes of Toppling Failure Discovered
W
E
S
B

Figure 8-6 Stereonet Identification of Failures in Koala North Domain 1 (A – Wedge Failures, B – Toppling Failures)

From the relevant joint sets, the formation of three possible wedges is indicated. The gloryhole wall orientation in Domain 1 is from 315° to 45°. As all three lines of intersection depicted in Figure 8-6 fall within this range, condition 1 for wedge failure is satisfied.

The dip of the gloryhole walls is generally 85° as shown in Figure 7-1, but in certain sections may be vertical. When possible a wall dip of 85° will be used in analysis, but if the plunge of the line of intersection of joint planes is greater than this, a wall dip of 90° will be used. Condition 2 for wedge failure will always be satisfied.

The plunges of all three lines of intersection are located within the friction circle. Recall that the joint set total friction angle can be a maximum of 70°. Thus, unless the JRC value for a joint set is less than 14, the roughness angle will be truncated to 39°. As all joints in this domain have JRC values greater than said threshold, the friction circle has been set to 70°. Condition 3 for wedge failure is satisfied.

The last input parameter needed for analysis is joint trace lengths. As discussed previously, this is one parameter that cannot be determined from logging diamond drill core. Cell mapping may provide indications of trace lengths. Unfortunately, the quantification of this parameter from cell logging performed at Ekati™ is extremely limited. Consequently, a 10 m trace length for all joints has been assumed. Even though joint features at Ekati™ have been noted to be planar and continuous, a trace of 10 m represents the upper realm and is likely somewhat conservative for stability analyses.

As all input parameters are now known, each of the three wedges was created in SWedge and a factor of safety calculated. The three wedges likely to form as Domain 1 is traversed clockwise are shown in Figure 8-7 A, B and C. Note the joint sets contributing to wedge formation are listed in the bottom right of each illustration. Clearly all the potential wedges are tall and thin.

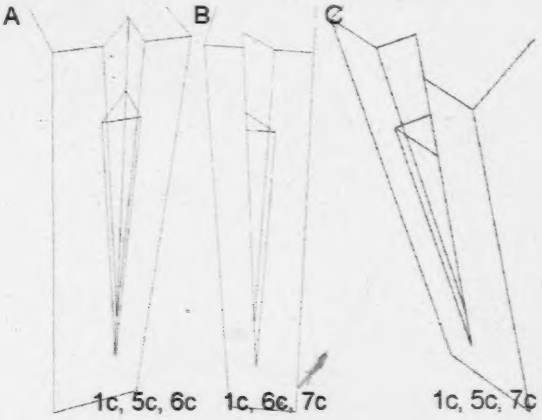

Figure 8-7 Wedge Failures in Domain 1

Table 8-1, located at the end of this section, summarizes wedge features such as volume, mass, apex angle, line of intersection and factor of safety. Toppling possibilities in all domains are summarized in Table 8-2, although none were found within Domain 1.

8.3.2 Structural Domain 2 Analysis

An analysis identical to that performed on Domain 1 is applied to the joint set information of Domain 2. Stereonets depicting wedge and toppling failure possibilities are shown in Figure 8-8 A and B.

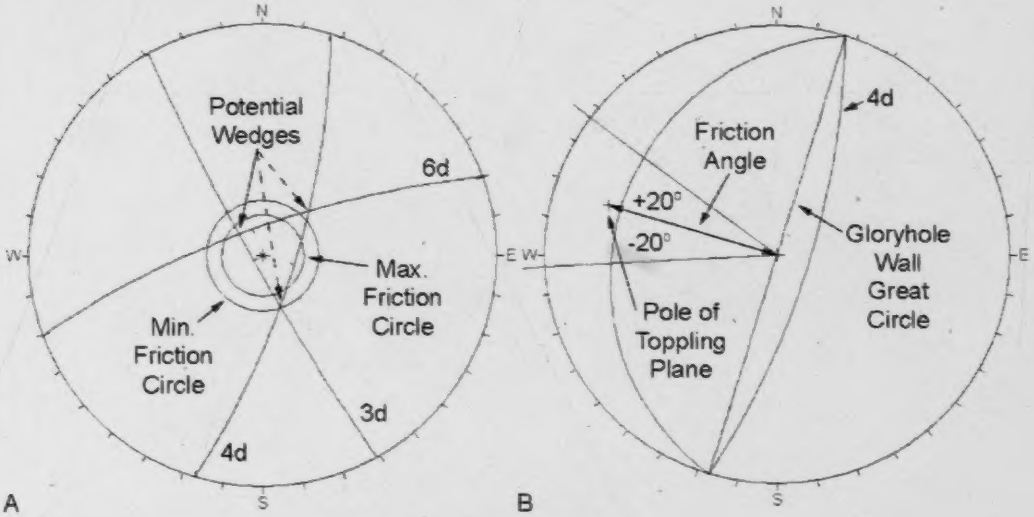
N
Potential Wedges
6d
W
E
Max. Friction Circle
Min. Friction Circle
3d
4d
S
A
N
4d
Friction Angle
+20°
-20°
W
Gloryhole Wall Great Circle
E
Pole of Toppling Plane
S
B

Figure 8-8 Stereonet Identification of Failures in Koala North Domain 2 (A – Wedge Failures, B – Toppling Failures)

Joints 3d and 5d (Table 6-2) of Domain 2 are below the JRC threshold value of 14, roughness angles of 32° and 37° have been calculated for these joint sets respectively. Both a minimum friction angle of 63° and a maximum angle of 70° (see Figure 8-8 A) were used for analysis.

The three conditions necessary to ensure kinematically possible wedge failures were analyzed in the same manner as was done for the Domain 1 wedge possibilities. It was found that three wedges occurred in the shaded region of Figure 8-3. However, the lines of intersection of two of these (represented by dashed lines in Figure 8-8 A) do not approximate gloryhole wall orientations in this domain. Thus, only one wedge is likely to form and is depicted in Figure 8-9.

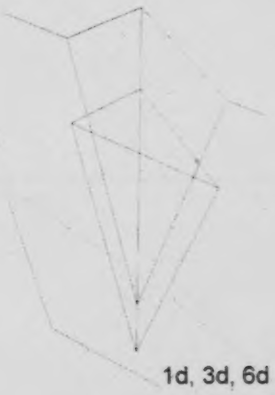

Figure 8-9 Wedge Failure in Domain 2

Concerning toppling failure, one instance was found (Figure 8-8); with the sub-horizontal joint set within Domain 2 able to form the base of the toppling blocks. The last step in the evaluation of toppling is to ensure that the centre of gravity of the block falls outside the dimension of its base. Given the joint spacing and trace lengths at Ekati™, toppling instability is a possibility if the conditions are right, as illustrated in Figure 8-10.

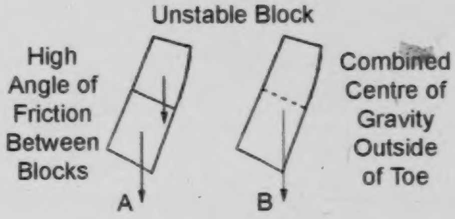
Unstable Block
High Angle of Friction Between Blocks
Combined Centre of Gravity Outside of Toe
A
B

Figure 8-10 Centre of Gravity Influence on Stability

Joint strength properties, set spacing and trace lengths will all influence the size of blocks and whether they behave as discrete units or group together and behave as a single structural feature. Thus, it is very difficult to accurately predict a factor of safety for toppling.

8.3.3 Structural Domain 3 Analysis

An analysis identical to that performed on Domains 1 and 2 is applied to the joint set information of Domain 3. Stereonets depicting wedge and toppling failure possibilities are shown in Figure 8-11.

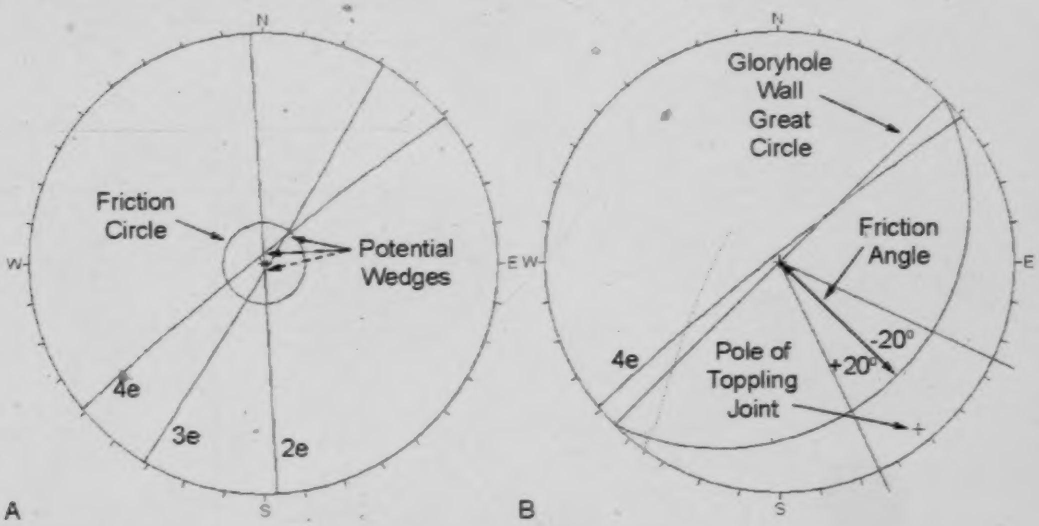
N
W
E
S
Friction Circle
Potential Wedges
4e
3e
2e
A
N
W
E
S
Gloryhole Wall Great Circle
Friction Angle
-20°
+20°
4e
Pole of Toppling Joint
B

Figure 8-11 Stereonet Identification of Failures in Koala North Domain 3 (A – Wedge Failures, B – Toppling Failures)

For all joints, the maximum friction angle of 70° was applicable. Three possible wedges were identified, one of which had a line of intersection not close to that of the gloryhole wall. Thus, the two kinematically possible wedge failures are depicted in Figure 8-12, proceeding clockwise around Domain 3.

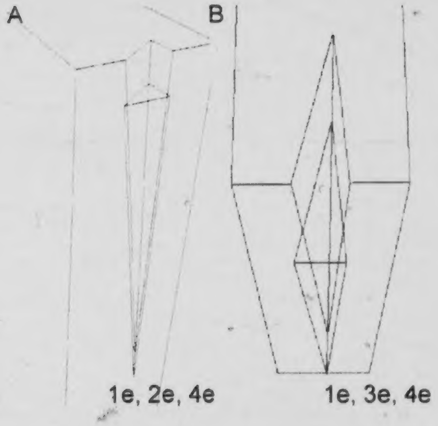

Figure 8-12 Wedge Failures in Domain 3

One instance of toppling failure was found, with the sub-horizontal joint set within Domain 3 able to form the base of the toppling blocks. As before, the complex interaction of factors such as the joint strength properties, set spacing and trace lengths will determine whether or not toppling will actually occur. As before, only the possibility of failure is addressed and no factor of safety will be calculated for the toppling failure case.

8.3.4 Summary of Kinematic Failures

Locations and characteristics of all kinematically potential wedge failures found throughout the three Koala North structural domains are given in Table 8-1. The locations of possible toppling failures are summarized in Table 8-2.

Table 8-1 Summary of Wedge Failures in Koala North Gloryhole Wall

Failure Location			Wedge Characteristics						
Domain	Wall Orientation		Defining Joints	Line of Inter.		Apex Angle (deg)	Volume (m^3)	Weight (tonnes)	Factor of Safety
	Dip (deg)	Dip Dir (deg)		Trend (deg)	Plunge (deg)				
1	90	212	1c, 5c, 6c	212	84	40	1.6	4.4	0.82
1	85	221	1c, 5c, 7c	221	82	82	0.7	1.9	0.57
1	85	212	1c, 6c, 7c	212	81	41	0.7	2.0	1.17
2	85	313	1d, 3d, 6d	313	74	83	11.9	32.0	1.08
3	90	357	1e, 2e, 4e	357	85	54	1.7	4.6	0.47
3	85	038	1e, 3e, 4e	038	73	21	2.4	6.4	4.58

Table 8-2 Summary of Toppling Failures in Koala North Gloryhole Wall

Failure Location			Toppling Block
Domain	Wall Orientation		Defining Joints
	Dip (deg)	Dip Dir (deg)	
2	90	286	4d
3	90	135	4e

A discussion of these gloryhole wall wedge and toppling failures is undertaken in the next section. Possible effects of these failures on underground developments are considered.

8.4 Discussion of Potential Failure Mechanisms

8.4.1 Failure Sizes

Predominantly small, narrow, steep-sided wedges are predicted to form in the Koala North gloryhole. This is because the gloryhole walls are quite steep and the joint friction angles quite high, thus only wedges with steep lines of intersection can fail. The gloryhole wall dip direction given in Table 8-1 is equal to the trend of the line of intersection of a wedge failure where possible. It is realized that wedges will likely occur along +/-20° of this gloryhole wall orientation, as long as a different structural domain is not entered. The shape and size of wedges over this range will vary slightly from those depicted. A real wedge occurring at the top of Koala North pit within domain 1 is pictured in Figure 8-13.

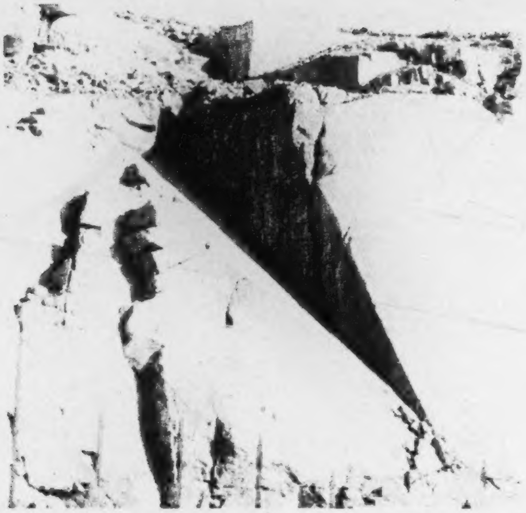

Figure 8-13 Koala North Wedge in North Wall

The wedges were also formed based on the maximum joint trace length of 10 m, therefore representing possibly the largest wedge failures that are likely to occur. However, the average joint set spacing in the region is in the order of 0.5 to 2 m. Thus, it is possible that any large wedges formed would be truncated by this lower spacing before failure occurred. Truncations due to other joint sets not forming the wedge are also likely.

Recall from Chapter 7 that due to the explosive emplacement of kimberlite pipes the contact zone between host granite and intruded kimberlite may be highly fractured in areas. This increases the likelihood that large wedges may not immediately form; instead a gradual spalling or ravelling of the gloryhole wall would occur. Appropriate drill hole data was not available which would allow determination of the extent that this zone penetrates back into the host rock.

Two instances of toppling failure were deemed likely. Due to the spacing characteristics of the joint sets this failure mode is unlikely, unless a situation such as depicted in Figure 8-10 arises. If this is the case, progressive ravelling of the gloryhole wall could be expected.

It appears that wedge and toppling failures will not pose major threats to the operation of the gloryhole. Wedges predicted to form from joint set data are all quite small and should not pose a significant danger to underground operations. However, the joint set database does not contain information on faults. The presence of these features may allow much larger failures to occur. Small wedge failures that do occur will pose a nuisance as they can become mixed in with the kimberlite ore. Multiple small failures occurring in one area may lead to progressive undermining of a potentially much larger wedge failure from above.

8.4.2 Groundwater

Hydrologic conditions will affect both wedge and toppling stability. Precipitation falling over the area of the open pit and surrounding local drainage basin will make its way to the gloryhole. Water may easily infiltrate the gloryhole walls if the rock mass is highly jointed and hence highly permeable. When water becomes trapped within a joint, the normal forces on the plane are reduced, thereby reducing the available resisting force (shear strength). If the shear strength is reduced below the driving force (shear stress), failure will occur. A good dewatering program will eliminate much of this concern.

Hydraulically induced problems are exacerbated when coupled with the thermal regime of the area. Every season, water trapped within joints expands by approximately 9% upon freezing (Andersland and Ladanyi, 1994), thus increasing the driving force and encouraging the tipping over or sliding out of blocks into the gloryhole. This phenomenon is known as ice-jacking.

Unfortunately, infilled joints may be affected much more. Wash out of material may undercut a block and initiate toppling failure. Clay infill may swell upon hydration, creating high forces that tend to push out wedges.

8.4.3 Blasting

As mentioned previously, blasting practices can have a negative impact on the stability of wedges and toppling blocks. Large vibrations and heaving due to gas penetration into the joints may initiate failure in otherwise stable blocks.

8.4.4 Implications of Stress

The previous stability analysis was based upon the assumption that blocks were subjected to gravitational loading only. While ignoring in-situ stresses makes the analysis conservative, the influences of stresses on gloryhole wall stability still warrant consideration as an overly conservative analysis may have negative economic implications.

The impact of stress on gloryhole wall stability will be discussed. Actual quantification of the stress state in the Ekati™ region is beyond the scope of this thesis, thus a hydrostatic stress state will be assumed to exist in the horizontal plane. Vertically, stresses are likely roughly equal to the mass of overlying rock. Near surface the horizontal stresses are likely greater in magnitude than their vertical counterpart due to past glacial erosion. Since underground mining is occurring at relatively shallow depths, stresses will not approach the compressive strength of granite.

Figure 8-14 depicts in 2D plan view all stresses acting on an element within a rock mass some distance away from a circular excavation. The area is in a hydrostatic stress field (i.e. far field stresses are equal and therefore $K=1$ in the figure).

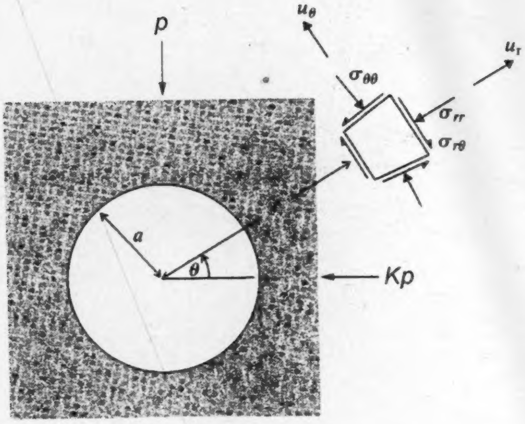

Figure 8-14 Elemental Stress Distribution about a Circular Excavation (modified from Brady and Brown, 1993)

Given that the excavation is nearly circular, Kirsch equations could be used to determine the stresses on any element in the surrounding rock mass. This would be useful if a fault was known to be in the region and it was desired to determine if movement would occur when the local stress fields change due to excavation. An analysis of faults is beyond the scope of this thesis.

The immediate area of concern at Koala North is the gloryhole wall and surrounding zone. Figure 8-15 depicts the stresses around a circular excavation from the boundary and proceeding outwards into the rock mass until stresses return to far field conditions.

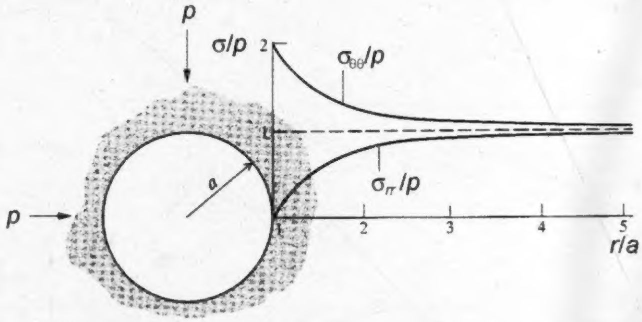

Figure 8-15 Boundary Stress Distribution around a Circular Excavation in a Hydrostatic Stress Field (modified from Brady and Brown, 1993)

Normal stresses at the free face are zero, while tangential stresses at the boundary double under hydrostatic conditions. This stressed zone around the opening serves to effectively clamp any potential wedges or toppling blocks that have small apex angles in place. Resultant normal stresses developed across the discontinuities bounding the rock wedge enable a higher shear resistance of the discontinuity to be mobilized and the rock wedge to become wholly or partially self-supporting (Crawford and Bray, 1983).

Unfortunately, Koala North is not completely circular in shape; this is seen in Figure 3-7, where the kimberlite pipe is in fact slightly elongated in the north-south direction. Under hydrostatic conditions the distribution of tangential stresses around a non-circular boundary is not uniform. Stresses concentrated around the apexes of the ellipse may be over double that of hydrostatic conditions, whereas stresses along the long axis walls of the ellipse will be reduced. This is illustrated in Figure 8-16.

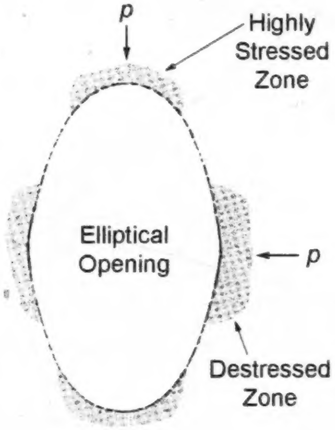

Figure 8-16 Stressed Zones around an Elliptical Opening in a Hydrostatic Stress Field

Depending on the exact geometry of the ellipse, stresses along the long wall may be greater or even less than hydrostatic. Fortunately, stresses much less than hydrostatic are not expected, as the Koala North kimberlite pipe is only slightly elliptical and is assumed to be under hydrostatic stress conditions. Obviously, wedge and toppling failures would occur more readily in the gloryhole walls along the long axis of the excavation due to lower tangential stresses in this area.

It has been determined that access to the slightly elliptical kimberlite pipe is best accomplished parallel to the long axis (i.e. from the north or south), as tangential stresses will be higher in these areas, thus providing additional confinement to the brow area.

Various analytical solutions are available that take in-situ stresses into account for factor of safety determination. Unfortunately these are difficult to apply in practice, as the interaction between stress redistribution and joint dilation during failure of tapered wedges is a complex problem that is neither well documented nor understood (Elsworth, 1986). A simpler approach will be used to provide a rough estimate of wedge stability at Ekati™.

Initially assumptions that the wedge shaped block is two dimensional, symmetric and has a horizontal applied resultant force are made. These assumptions, shown in Figure 8-17, are reasonable given the conditions at Ekati™. Note that while this approach was initially created for the analysis of horizontal openings underground, the same principles are still effective given a vertical excavation orientation.

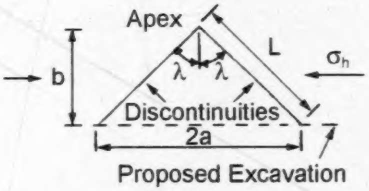

Figure 8-17 Model of a 2D Rock Wedge

MacLaughlin (2002) then found that if half of the wedge apex angle was less than or equal to the angle of friction of the joint surfaces, the wedge would be stable. Table 8-1 shows that the largest half apex angle (λ) is approximately 43°, while joint friction angles were generally 60° to 70°. It is concluded from this criteria that all potentially unstable wedges identified from a kinematic strength analysis are likely to be stabilized by stress effects. Wedge failure is only likely if the apex angle exceeds 120°.

8.5 Structural Implications for Development in Koala North

8.5.1 Recommended Cross-Cut Orientations for Kimberlite Pipe Access

Based on the kinematic and strength analysis, the optimal route for cross-cut access to the kimberlite pipe is not immediately clear. The apex angle of all wedges in Table 8-1 is less than 120° and it is unlikely that significant wedge failures will occur due to the beneficial confining stresses around the pipe boundary. However, due to the detrimental effects of ice-jacking it may be desirable to avoid Domain 2, as within this domain by far the largest wedge will form.

Considering the local stress fields, it was noted that the long axis of Koala North is in a north-south direction and therefore the areas of maximum confinement occur in the north and south walls. It appears that access to the kimberlite orebody is best accomplished from one of these two directions, as this will ensure the best brow stability.

If the kimberlite pipe is accessed from the north, all cross-cut development occurs within Domain 1; if accessed from the south, cross-cut development must take place in both Domains 2 and 3. Recall that it may be desirable to avoid Domain 2. As well, toppling modes of failure may occur in Domains 2 and 3 but not in Domain 1.

From a quantified kinematic and strength approach coupled with a qualitative stress analysis, it seems that access from the north is slightly preferential. Visual observations of the Koala North open pit highwalls also tend to support this finding; the south wall appears much more broken and ravelled than the north wall.

Additional visual and mapping observations should be performed in order to identify any faults in the area; these features are not easily identifiable from core logging data. The presence of fault features may enable much larger failures to occur than are possible from jointing alone.

8.5.2 Gloryhole Support Issues

In most sections of the gloryhole support will not be needed, as any possible wedge failures will be quite small and easily handled by the equipment underground. Given the tall thin shape many potential wedges have, it would be difficult to support these with cable bolts.

Domain 2 contains the largest potential wedge (potentially in the order of 10 m^3). This wedge is not likely to fail because the factor of safety is greater than 1 and tangential boundary stresses further stabilize the wedge. However, environmental conditions (i.e. ice-jacking), improper blasting practices and the presence of fault structures could initiate failure in otherwise stable wedges.

Upon failure, a wedge would likely fall to the gloryhole floor and break up into pieces capable of being mucked out by a remote scoop. In the event that the wedge does not break up secondary blasting may be necessary. As this delays production, it may be desirable to support the problem area in Domain 2 in advance. The problem area is shown dotted in Figure 8-18; it lies within the hatched area, which is Domain 2.

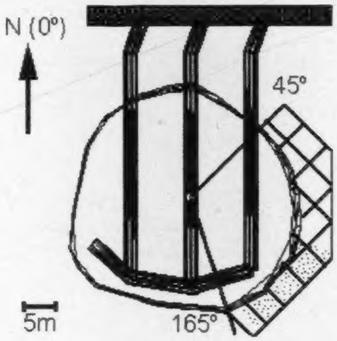

Figure 8-18 Plan View of Area in Domain 2 Possibly Requiring Artificial Support

Installation of cable bolts from the easternmost cross-cut and slot drift could be used to provide support for the unstable section of wall. Two options would be available for installation: stabilizing the wall of the current level or stabilizing the level below. The stabilization options could be combined for greater effect; this is depicted in Figure 8-19.

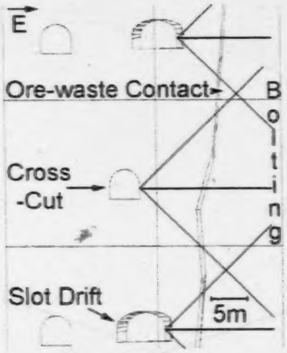

Figure 8-19 Section Depicting Cable Bolt Gloryhole Wall Support

Tension or untensioned grouted cable bolts could be used to support the gloryhole wall. After blasting the ore, the cables would be left hanging against the wall. Kinematically, the optimal bolt orientation should trend roughly 180° to the trend of the wedge line of intersection and be inclined at the angle of friction from the line of intersection. It should be realized that operationally it would be hard to meet these criteria in most cases due to operational constraints. Aspects dealing with optimal bolt length and orientation as related to factor of safety are discussed in further detail in Chapter 9.

8.5.3 Gloryhole Monitoring Issues

8.5.3.1 Access

The nature of open benching in conjunction with environmental conditions at the Ekati™ mine create a situation where monitoring of the gloryhole wall is exceedingly difficult. Monitoring is required to provide advance warning of possible failures.

As personnel access is not permissible in the gloryhole itself, the condition of the walls is difficult to assess. It is likely that upon completion of a level, the cross-cuts are back-filled or sealed in some way. This is necessary to maintain the integrity of the underground ventilation circuit. A secondary benefit of reduced waste transportation costs is realized if the cross-cuts are back-filled. With this in mind, even visual observations to assess the integrity of the walls may not be possible.

If visual observations are physically possible, they are not always feasible due to environmental interference from factors such as rain, fog and snow. The diameter of the Koala North pipe is small enough that optical instruments may still be operable; this is discussed further in the following section. Visibility will be more severely affected in the larger Koala and Panda pipes, perhaps rendering optical instrumentation ineffective.

Installation of instrumentation along the north wall could be done quite easily as all development occurs in that region; along the other three directions it is much more difficult, as underground workings are not located within these regions. Figure 8-20 illustrates possible locations for installation of instrumentation.

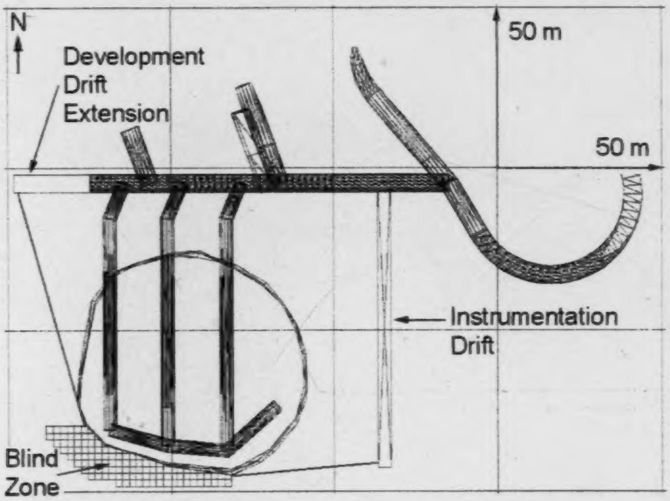

Figure 8-20 Plan View of Instrumentation Drift

Note the presence of a dedicated instrumentation drift in Figure 8-20. With such a drift monitoring of the east wall and parts of the south wall are possible. Recall that the southeast wall was the location of the largest potential wedge failures (shown in Figure 8-18). Extension of the development drift to the west would allow coverage of a good portion of the west wall.

With the two aforementioned extensions, pipe coverage is quite good, with only a small blind zone existing in the southwest corner. In order to eliminate this blind zone it may be desired to wrap the instrumentation drift around the south end of the pipe.

Alternatively, it may be possible to install instrumentation vertically, down from the floor of the open pit into the gloryhole walls below.

Driving an instrumentation drift would be rather costly, and thus would only be considered if a suitable instrumentation method could not be found which would render the aforementioned unnecessary. The next section will evaluate suitable rock mass instrumentation methods that can be installed horizontally from developments, as well as vertically from the surface.

8.5.3.2 Instrumentation

Personnel access is not permissible in the gloryhole itself, thus some form of remote data collection is necessary. It is also extremely desirable that the instrumentation forms an automated continuous monitoring system. In this way deformation magnitude thresholds can be set; once exceeded, warnings can be automatically sent to the appropriate personnel.

Advance warning is particularly important as rates of deformation could climb quite suddenly due to a few days of cold or warm temperatures. Cold temperatures may initiate ice-jacking while hot weather may introduce an influx of melt-water and therefore increased water pressures. Continuous monitoring allows plots of deformation to be created in real-time. In this way, rates can be calculated, since a critical rate may occur before a threshold magnitude is reached.

As previously mentioned, environmental conditions such as fog may preclude the use of optical instrumentation at Koala North. Due to the underground ventilation circuit, airflow is likely to be positive pressure with respect to the outside. In other words air will flow out of the cross-cuts and into the gloryhole, reducing an incursion of snow into the developments. This pressure may create a slight updraft, which in turn may help retard fog development in the gloryhole and increase the success of employing an optical instrument. Figure 8-21 is a section view of the underground workings.

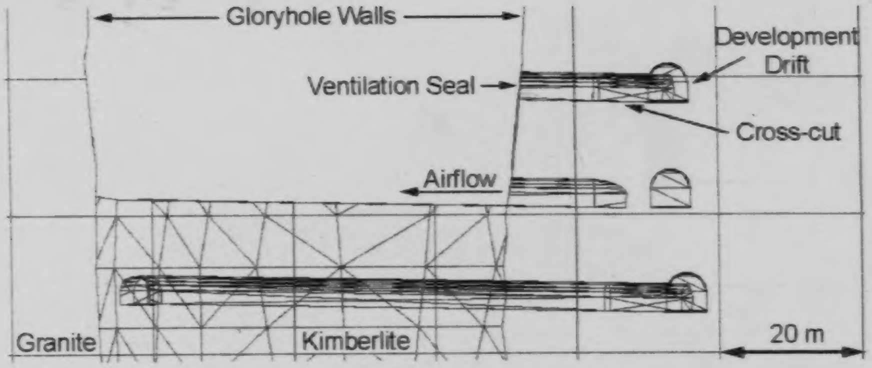

Figure 8-21 Section of Instrumentation Installation

Certain optical instruments (Mah et al., 1995) can be extended just past the brow; they then take a 360° picture of the gloryhole walls. Various plots over time can then be superimposed to distinguish any changes taking place. One drawback of this method is that snow-cover on the gloryhole walls may mask rock mass movement. As well, mined out cross-cuts cannot be completely back-filled; sufficient room must be left to extend the instrument past the brow.

As the success of optical methods is not guaranteed, it is necessary to discuss other forms of instrumentation as well. Fortunately, many forms of instrumentation are available with which to monitor the deformation of rock masses. These include, but are not limited to: extensometers, inclinometers, smart cables, ground penetrating radar, time domain reflectometry (TDR), and optical TDR (OTDR).

TDR is relatively new method for monitoring rock mass deformations, but has been used in a variety of locations, including Ekati™. Laboratory studies have indicated that under ideal conditions it is possible not only to quantify the magnitude of deformation but also, in some cases, to distinguish shearing from tensile failure (O'Connor and Dowding, 1999). Note that quantification of displacement in the field is not exact as it is highly dependent on the type of cable employed. As well, due to the complex relationship between shear movement and normal dilation, quantification between shear and tensile failure in the field is not yet sufficiently reliable for practical use. TDR is also limited in that a failure near the collar effectively cuts off any communication with the remainder of the cable.

Additionally, in order to adequately monitor an area for suspected movement quite a course grid of TDR instrumentation is needed. The drilling costs would tend to make this method uneconomical as a general monitoring tool. Thus, optical methods are considered superior for this application.

However, even considering all the drawbacks, TDR instrumentation is recommended for monitoring a discrete plane or over a limited area where future problems are suspected. As long as problem areas can be identified in advance, TDR can be a relatively cheap and reliable monitoring method.

In summary, the stability of the Koala North gloryhole has been evaluated. It was found that wedge and toppling failures based on joint set data would not pose a significant threat to the underground mining operation since size of any failures would be small (only a few m^3 at most). Based on a kinematic and joint strength stability analysis coupled with the effects of stresses an optimal orientation has been recommended with which to access the kimberlite pipe. The optimal direction was found to be from the North, which is the direction used in practice at Koala North. Possible gloryhole support (cable bolting) and instrumentation (optical, TDR) methods were recommended and briefly discussed.

Chapter 9

Koala North Underground Development Stability

9.1 Relevant Failure Mechanisms and Required Input

The previous chapter addressed the stability of the gloryhole walls at Koala North. It was found that access to the pipe from the north was desirable from a kinematic stability analysis and an examination of stress. Access from the north would entail development of underground workings within structural Domain 1; the stability of these development drifts and cross-cuts must now be established.

Of particular concern will be failures occurring in the back, or roof, of the excavation. Wedge failures occurring in the sides of developments are easily supported and will not be focused upon. Concerning the back, wedge and slab-like formations will be the relevant modes of failure.

Chapter 6 identified the dominant joint sets within the structural domains. Strength and spacing characteristics were determined for all joint sets. This information will be used in conjunction with the RocScience program UnWedge to evaluate the stability of wedges located in the excavation back.

As before, note that the wedge analyses will be based upon the assumption that the wedges are defined by three intersecting discontinuities, plus the back of the excavation, and are subjected to gravitational loading only. The stress field in the rock mass surrounding the excavation is not quantitatively taken into account. While this assumption leads to some inaccuracy in the analysis, the error is generally conservative, leading to a lower factor of safety (RocScience geomechanics software and research, 2003).

9.2 Stability Analysis

9.2.1 Methodology

The stability of the back where the development drift intersects the cross-cut will be analyzed. As this development occurs within Domain 1, there are 7 joint sets that must be taken into account. Combinations of 3 joint sets will be looked at to determine if a wedge failure is likely.

Two forms of wedge failure are possible: failure by falling and failure by sliding. Using stereonets it is possible to identify which mode is likely for a given wedge. Identification of a falling wedge via a stereonet is shown in Figure 9-1.

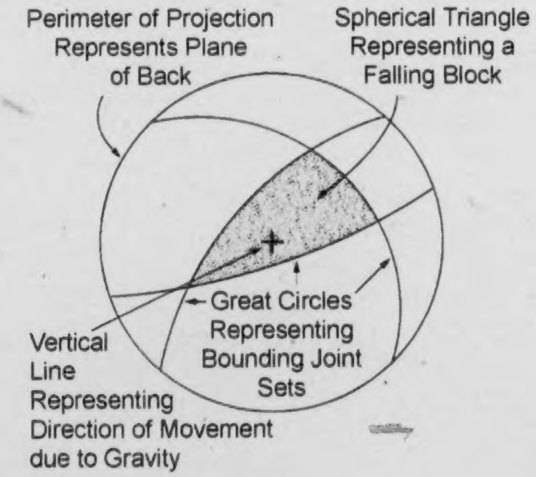
Perimeter of Projection Represents Plane of Back
Spherical Triangle Representing a Falling Block
Great Circles Representing Bounding Joint Sets
Vertical Line Representing Direction of Movement due to Gravity

Figure 9-1 Kinematic Identification of a Falling Wedge (modified from Hudson and Harrison, 1997)

As falling does not involve movement on any of the joint surfaces, it is not necessary to introduce a strength criterion into the analysis. Due to gravitational loading, the wedge detaches from its bounding planes and moves vertically downwards.

Two modes of failure by sliding are possible: failure along the line of maximum dip of a joint surface or failure along the intersection of two joint surfaces. The difference between these two modes may also be detected with a stereonet, and is shown in Figure 9-2.

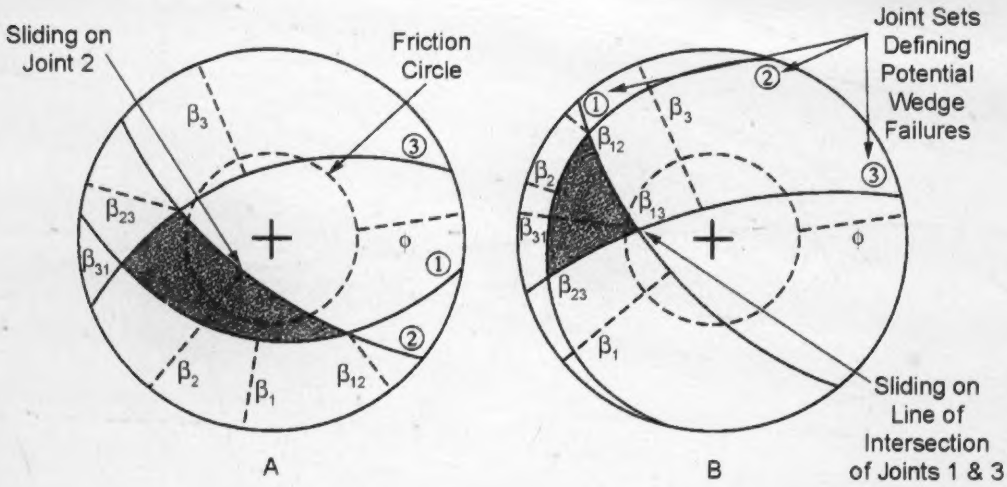
Sliding on Joint 2
Friction Circle
β_3
③
β_{23}
β_{31}
ϕ
①
②
β_2
β_1
β_{12}
A
Joint Sets Defining Potential Wedge Failures
②
①
β_3
β_{12}
③
β_2
β_{13}
β_{31}
ϕ
β_{23}
β_1
Sliding on Line of Intersection of Joints 1 & 3
B

Figure 9-2 Kinematic Identification of Sliding Wedges (modified from Hudson and Harrison, 1997)

In the case of a sliding failure, the strength of the bounding joints must be known. For failure to be possible in both sliding cases, the direction of sliding must plunge steeper than the angle of friction of the joint surfaces.

In most structural domains at Ekati™ the dominant joint set is sub-horizontal. As joints generally have little to no tensile strength, it is predicted that relief of these joints could occur once a drift has been developed. In combination with sub-vertical joint sets a dangerous situation may arise where large slabs drop from the back, as illustrated in Figure 9-3.

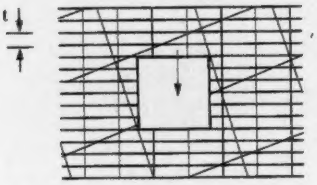

Figure 9-3 Slab Failure Due to Relief Along Sub-Horizontal Joint Set (modified from Hudson and Harrison, 1997)

The hidden danger is that joint sets forming the slab may not be visible on the back, thus failure may be sudden and unexpected. This type of failure mechanism is particularly sensitive to the spacing (*t*) of the sub-horizontal set.

The failure mechanisms discussed so far have dealt solely with the excavation back. Inclined hemispherical projection methods (i.e. stereonets) may be used to evaluate the walls of the excavation as well. However, as mentioned previously, stability of the back is the primary concern and will be the focus of analysis.

The RosScience program UnWedge will be used in conjunction with orientation, dimensional, and strength data to determine falling and sliding modes of wedge failure in the back.

The UnWedge program is simply an automated way of performing the stereonet procedures for failure analysis described above. The program also ties in physical dimensions, allowing the geometry of a development drift and cross-cut to be analyzed. Realistic wedge sizes may be generated, which in turn will help when establishing artificial support requirements.

Joint set orientations and spacing will be examined to determine if slab failures are a possibility at Koala North. Factors of safety will not be computed for this failure mechanism.

9.2.2 Investigation

From Figure 3-7 the geometry of an intersection between a development drift and cross-cut is known. This area is the most critical as it is the location of the largest unsupported back span, or width. A view of the area analyzed is shown in Figure 9-4.

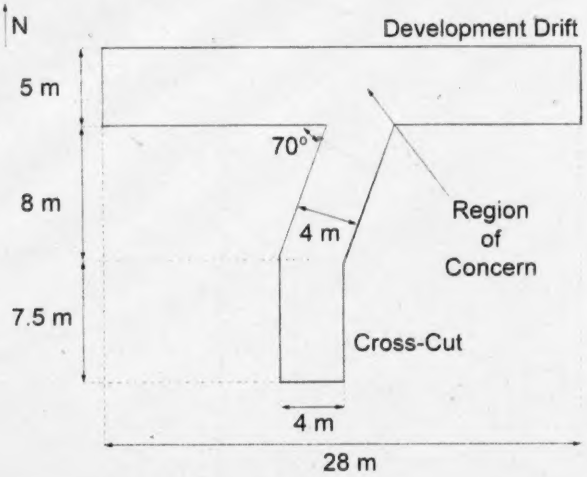

Figure 9-4 Plan View of Development Drift and Cross-Cut Intersection

The orientations of joint sets and their associated strength parameters were also input into UnWedge. Due to the high JRC values within Domain 1, a total friction angle of 70° was used. Potential wedges may be truncated by the joint spacing of the sliding plane; as a worst-case scenario was desired, this was not done.

A total of 35 possible wedge failures were analyzed. The cases resulting in kinematic factors of safety less than 1 are given in Table 9-1. Note that all joints were truncated to a maximum trace length of 10 m in order to obtain realistic results.

Table 9-1 Potential Wedge Failures in Excavation Back

Back Wedge (#)	Bounding Joints	Failure Mode	Sliding Plane(s)	Wedge Characteristics				Factor of Safety	Stress Effect on FofS
				Face Area (m^2)	Vol. (m^3)	Apex Height (m)	Wt. (t)		
5	1c 2c 7c	Fall	-	31.7	2.21	4.08	5.95	0	no
7	1c 3c 5c	Slide	5c	7.3	0.46	4.4	1.25	<1	-
8	1c 3c 6c	Slide	6c	0.86	0.002	3.37	0.01	0	+
13	1c 5c 6c	Slide	6c	0.9	0.002	3.4	0.01	0	+
14	1c 5c 7c	Slide	5c	21.3	1.06	2.85	2.86	<1	-
15	1c 6c 7c	Slide	6c	0.9	0.002	3.2	0.01	0	+
17	2c 3c 5c	Slide	5c	5.7	0.86	1.53	2.32	<1	-
18	2c 3c 6c	Slide	6c	12.8	2.93	3.18	7.90	0	+
19	2c 3c 7c	Fall	-	14.6	3.49	3.17	9.41	0	no
23	2c 5c 6c	Slide	6c	16.3	9.89	4.93	26.70	0	+
24	2c 5c 7c	Fall	-	22.5	12.99	3.94	35.06	0	no
25	2c 6c 7c	Fall	-	33.5	40.16	6.8	108.45	0	no
26	3c 4c 5c	Slide	5c	8.6	2.81	2.71	7.57	<1	-
27	3c 4c 6c	Slide	6c	12	7.49	2.34	20.21	0	+
29	3c 5c 6c	Slide	5c & 6c	7.3	2.67	4.19	7.20	<1	?
30	3c 5c 7c	Slide	5c & 7c	8.6	3.15	3.78	8.51	<1	?
32	4c 5c 6c	Slide	6c	12.4	19.35	5.84	52.23	0	+

There are 17 potentially unstable wedges, four of which may fall out of the back and the rest will fail by sliding. Figure 9-5 depicts examples of the falling and sliding forms of failure previously discussed.

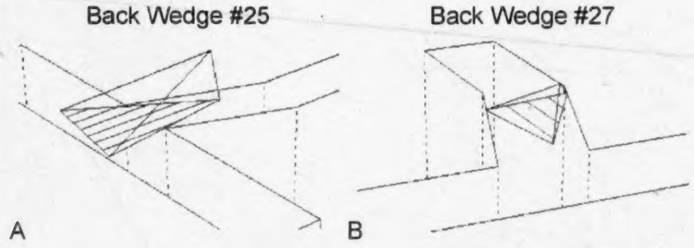

Figure 9-5 Modes of Failure (A - Falling, B - Sliding)

Not shown in Table 9-1, slab failures may also occur in the back, although these will be dependent upon the spacing of the sub-horizontal joint set. A slab failure is depicted in Figure 9-6.

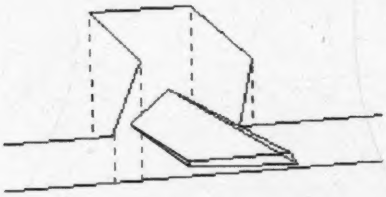

Figure 9-6 Slab Failure Example

As traces of all three boundaries are visible on the back, the failure shown in Figure 9-6 is not as dangerous as it potentially could be. With joint set spacing in the order of 1 m, and with the presence of sub-horizontal and sub-vertical sets, slab-like failures in the back are a distinct possibility.

9.2.3 Discussion of Results

Based on a kinematic analysis of joint features, wedge failures (both falling and sliding) are likely to occur in the back. These wedges represent the largest size likely to form as no joint set spacing truncation has been applied; instead, the maximum trace length (10 m) of joints was used.

Additional visual and mapping observations should be performed in the developments to identify any faults in the area, as these features are difficult to identify by logging core. The presence of fault features may enable larger and more persistent failures to occur than are possible from jointing alone.

Implications of stress have not been considered. It is probable that wedges with small apex angles will be self-supporting if the influences of stress were considered. Due to the degree of underground development and the proximity of this development to the gloryhole, the local stress fields are difficult to predict. Some form of numerical modelling would be necessary to obtain an accurate depiction of the stress regime; this is beyond the scope of this thesis.

It is possible to qualitatively assess the implications of stress. As discussed in Chapter 8, cross-cuts will access the gloryhole from the north. High tangential stresses in this region will thus tend to close off joints striking north-south. At the same time, stress relaxation will occur in the radial direction from the pipe once the kimberlite is mined out on a level; this tends to open up joints striking east-west.

The kinematic stability of sliding wedges in the back will be affected by whether the sliding joints have been stressed or destressed. By taking into account the orientations of joints (from Table 6-5), the effect of stress on the kinematic stability of sliding wedges has been shown in Table 9-1 as an increase (+), no effect (no), decrease (-) or unquantifiable (?) change in the factor of safety.

Environmental implications must also be discussed. As introduced in Chapter 2, the underground development may traverse the permafrost boundary. Due to ventilation in the summer months, degradation of the permafrost will occur. Thus, water may permeate into open joints thereby increasing driving forces and hence instability. During subsequent winter months, an influx of sub-zero temperature air into developments could initiate ice-jacking instability mechanisms.

Optimal drift design and artificial means of support will be required to increase the factor of safety against wedge failures. Both topics are elaborated upon next.

9.3 Development Optimization

9.3.1 Drift Shape and Size

Within the UnWedge program, development drifts were approximated as rectangular cross-sections. Currently, the width and height dimensions for a cross-cut are desired to be nominally 3.8 m wide by 4 m high with an arched back. The width and height ? dimensions of a cross-cut are set by minimum operational constraints such as scoop dimensions and required space for ventilation and service lines.

The arched back is created in order to optimize the redirection of stresses around the excavation; in this way loose, non-supporting material is not located on the back and does not pose a safety hazard. In a blocky discontinuous rock mass, this arch-like redirection of stresses is essentially operating on the principles of a voussoir arch.

Improper blasting practices may widen the drift and destroy the arch, resulting in a flat back. Consequently, much larger wedge failures may occur than have been planned for, as the back span is now increased. As well, intersection corners tend to get cut off by equipment turning corners; hence, it is better to design for a larger span during planning.

Accordingly, a flat back was used in analysis along with a 4 m wide cross-cut. Thus, the analysis is conservative and will still be applicable even if challenges are encountered in achieving the nominal cross-cut dimensions. Artificial means of support will be designed based on the conservative parameters.

9.3.2 Drift Support

From Table 9-1, it is evident that some means of artificial support will be needed to control wedge failures occurring in the back. Rock bolts, shotcrete and wire mesh are standard forms of support found in underground mining developments and will be suitable for use at Koala North.

It was stated in Chapter 8 that the optimal cable bolt orientation should trend approximately 180° to the wedge line of intersection and plunge at the angle of friction relative to the line of intersection; this will now be shown to be true.

Note that there is a fundamental difference between some cable bolts and rock bolts. Tensioned cable bolts are active support mechanisms and provide a positive resisting force at the time of application, which may increase as further deformation occurs.

Grouted and untensioned rock bolts are passive support mechanisms, meaning that rock deformation and displacement is needed in order for the bolt to generate or apply a resisting force. Figure 9-7 depicts the support of a wedge by rock bolting.

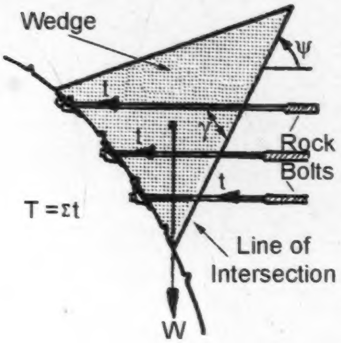

Figure 9-7 Rock Bolt Wedge Reinforcement (modified from Brady and Brown, 1993)

From the parameters shown in Figure 9-7 a factor of safety can be calculated as the sum of resisting forces divided by the sum of disturbing forces. Assuming the Mohr Coulomb shear strength law applies, the factor of safety equation against sliding, as it applies to passive rock bolts, is given in Eqn 9-1 (water forces have been neglected).

$$FS = \frac{(W\cos\psi + T\sin\gamma)\tan\phi + T\cos\gamma}{W\sin\psi} \qquad \text{Eqn 9-1}$$

In order to optimize the bolt angle (γ), it is necessary to differentiate $\delta T/\delta\gamma=0$ to find the maximum. While Eqn 9-1 is slightly different for active support mechanisms such as tensioned cable bolts, upon differentiation the same conclusion for an optimal bolt orientation is reached; that is that $\gamma=\phi$, the friction angle.

While bolting with the optimal orientation angle is ideal and will minimize support requirements, it is simply not practical on an operational basis; time and equipment constraints preclude such an arrangement. As the joint sets at Koala North are ubiquitous, wedges may form anywhere and it is therefore necessary to have a regular pattern of rock bolting for protection.

Many factors influence the design of a ground support system, including: general stress state, rock mass conditions, groundwater conditions, possible failure modes, support pressure required, time for support action, cost and availability, and temporary or permanent reinforcement requirements (Stillborg, 1994). An in-depth analysis of these parameters as they pertain to rock bolts is beyond the scope of this thesis, thus empirical parameters and knowledge of common practices will be used to select an appropriate rock bolt pattern for the back.

The development drift intersections with the cross-cuts are located quite close to the production blasts in the kimberlite. Mechanically anchored rock bolts are not recommended in these conditions, as tension in the bolt may be lost if blasting vibrations loosen the bolt anchor.

Grouted rebar rock bolts are proven, effective, and cheap. Some joints in the area are likely wet; this factor coupled with the relatively long set time for cement prohibits its use as a grouting agent. Resin, although more costly than cement, is an acceptable grout if it can adequately set in ground temperatures of -4°C.

Friction anchored rock bolts may be a viable alternative to resin grouted rebar's. Split sets are not recommended as they are of limited load capacity and are only suitable for installation in shorter holes. Swellex rock bolts are subject to corrosion, although protective coatings are available at extra cost. Normal Swellex bolts may be acceptable in the cross-cuts as they are only needed for a short time period. However, recall that it may be desirable to keep some of the cross-cuts open for instrumentation purposes.

Based on a preliminary analysis it is recommended that resin grouted rebar rock bolts be used underground due to their simplicity and effectiveness. If a detailed analysis indicates that resin is too costly or is unsuitable for sub-zero temperatures, purchase of Swellex installation equipment is proposed. Characteristics of the rock bolts and pattern details are summarized in Table 9-2. Note that suggested bolts are for use in granite only, quite likely a different type of bolt would be used for support of the cross-cuts in kimberlite.

Table 9-2 Rock Bolt Support Attributes

Bolt Properties		**Units**
Type	Resin grouted rebar	-
Diameter	19	mm
Capacity	12	tonnes
Length	2.4	m
Orientation	vertical	-
Spacing (long)	1.2	m
Spacing (traverse)	1.2	m

A rebar diameter of 19 mm is a standard size available in Western Canada; this has a yield load of 12 tonnes. Lengths of 1.8 m, 2.4 m and 3.6 m are available. A 2.4 m length was chosen as some of the wedges are formed from joints that dip quite steeply into the back and a 1.8 m bolt would not adequately penetrate into stable rock. This case is illustrated in Figure 9-8. The 1.8 m bolts are probably sufficient for the cross-cut drifts but longer bolts are beneficial in the wider spans of the development drifts and the drift intersections. A 3.6 m bolt requires more resin and more time to install; given the dimensions of the drifts and the unstable blocks it is not required.

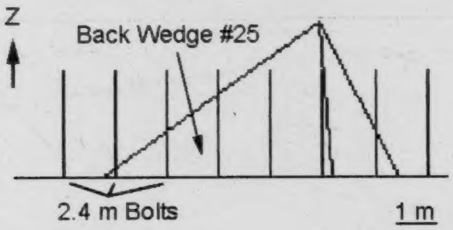

Figure 9-8 Long Section of Development Drift Showing Rock Bolt Support of Wedge

Vertical orientations for the bolts are not optimal in most cases, but from an operational perspective, this orientation will be easier to install. Depending on the equipment utilized, it may be desirable to fix the boom location and drill the centre bolt hole vertical; the remaining holes would fan out at angles from this fixed position.

Bolt spacings are commonly approximated to be half the bolt length. Given the joint spacings in the domain (~1 m), this spacing is appropriate. As well, 1.2 m bolt spacing will work nicely with the 1.5 m by 3.4 m welded wire mesh sheets the rock bolts will pin to the back. The completed pattern is shown in Figure 9-9. A pattern of bolts at 1.2 m spacing is consistent with practice at other mines (Choquet, 1991) and will provide more than enough bolts to hold the deadweight of any wedges that may occur in intersections between drifts.

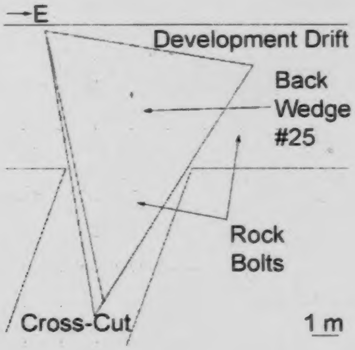

Figure 9-9 Plan View of Rock Bolt Pattern

For additional safety, welded wire mesh should be used with the rock bolts to catch and hold smaller pieces of loose rock. If zones of poor quality rock mass are encountered a thin coating of shotcrete can be applied over the pattern of bolts and mesh for additional support.

Secondary spot bolting should be utilized if visual observations identify potential blocks that the pattern bolting does not support. Spot bolting should also be performed on any steeply dipping wedges in the side walls. If a particularly poor section of wall is encountered it may be necessary to pattern bolt the side walls. Proper blasting practices will greatly alleviate the amount of secondary and tertiary bolting required.

In summary for this chapter, wedge failure mechanisms in the back at the development drift and cross-cut intersection have been identified. Utilization of proper artificial support mechanisms will control these failures and allow the operation of underground mining activities to occur safely.

Chapter 10

Summary and Recommendations

10.1 Summary

The main purpose of this thesis was to use structural geology data to delineate structural domains and then to characterize the joint sets found within structural domains at the Ekati™ Diamond Mine. From the outcome of this analysis, proper design, monitoring and stabilization methods could be recommended for use at the Koala North underground mine. As such, the main objectives accomplished in this thesis were:

1) Collection and amalgamation of existing structural geology data at the Ekati™ mine into one database,
2) Use of statistical techniques to analyze the structural database to determine spatial boundaries (structural domains) between zones of rock mass possessing joints with different orientation characteristics,
3) Determination of the orientation and strength properties of dominant joint sets within each structural domain,
4) Use knowledge of the structural domains and associated joint set characteristics to analyze the stability of gloryhole walls created at Koala North by underground mining,
5) Use the structural model to assess stability of underground development drifts at the Koala North operation.

As described in the preceding chapters these primary objectives were achieved.

In Chapter 4 a database was constructed that consisted of information gathered from four different collection procedures: diamond drill core logging, large-scale cell mapping, small-scale cell mapping and virtual cell mapping. The database consisted primarily of joint orientations, but in some cases other parameters such as joint roughness and infilling were obtained.

Drill logs were the most numerous data source, also being the only method capable of providing information on structures at depth. These structures were characterized by the Laubscher (1990) mining rock mass rating system. Large and small-scale cell mapping provided information on localized jointing. The Barton (1985) joint roughness coefficient was used to characterize these structures. Virtual cell mapping, while not used extensively, was found to primarily identify the orientation of features which were sub-parallel to bench faces. Data was corrected for orientation bias such that the most accurate representation of the in-situ geologic environment was available.

In Chapter 5 a method was proposed with which to delineate structural domains from the joint orientation database. The basis of this method involves plotting stereonets for various regions in space; then, looking for significant changes between stereonets that can be attributed to a structural change between the physical areas they represent (i.e. a structural boundary). A 3-stage process was proposed for domain identification:

- Select data from a particular region in space. Regions may be selected using knowledge of local geology in conjunction with operational experience and desires at a mine site. At Ekati™, vertical slices and pie-shaped zones were selected.
- Plot joint orientation data on a stereonet. A plotting scheme was proposed whereby the stereonet was subdivided into 100 equal-area windows. A sensitivity analysis was carried out to ensure that results were not a function of the plotting format.

- Identify significant differences on the stereonets that indicate the existence of structural boundaries and therefore justify the creation of domains. By comparing a statistical function (the coefficient of correlation) between regions, areas of low correlation were identified, thus indicating the presence of a structural boundary.

Comparison of the four data types described in Chapter 4 was carried out. Virtual cell mapping was uncorrelated to all other types, and thus is only suitable for analysis of discrete planes. While similar, diamond drill core logging and cell mapping data could not be combined. Thus, only diamond drill core logging data was used as input for domain identification. Cell mapping may complement the core logging data and is useful in the identification of localized jointing patterns and fault zones.

The structural domains were then used to model various regions at the Ekati™ mine; in some cases there was good agreement with the more subjectively determined domains currently in use at the mine. It is felt that the proposed domain identification method is more quantitative, unbiased and applicable than other methods currently in use.

Chapter 6 determined the strength characteristics of joint sets within each structural domain. Four to seven joint sets were typically identified in each domain; Koala North in particular had many minor joint sets, lowering the overall RQD of the area. Joint set spacing in all areas was found to be around 1 m in most cases. Joints generally had an undulating shape and contained minor amounts of infilling.

From a strength perspective the joints were found to be quite strong, with the equivalent total friction angle approaching 70° in many cases. Between domains minimal differences in joint characteristics (excluding orientation) were discovered, the lone exception being the Panda domains, as one appears to have joints with lower JRC values.

Chapter 8 then addressed the stability of the Koala North gloryhole using the findings of Chapter 5 and Chapter 6. Wedge failure mechanisms were found to agree quite well with those that have occurred on bench faces. Instances of toppling failure were also addressed; toppling was found to be a possibility but is not expected to produce problems.

Based on a kinematic stability analysis coupled with the effects of stresses the optimal orientation for access to the kimberlite pipe was determined to be from the north, which is the practice of current operations at Koala North. Gloryhole wall support via cable bolting was discussed briefly; barring unforeseen difficulties, it is not expected to be necessary as the largest wedge failure predicted to occur is in the order of 10 m^3. From a geotechnical perspective, open benching is considered to be a viable mining method at Koala North.

Due to environmental conditions and the nature of the open benching underground mining method, monitoring of rock mass stability will be quite challenging at Koala North. Optical methods were recommended for general monitoring, while TDR instrumentation is recommended for the monitoring of discrete failure planes.

Chapter 9 dealt with the underground developments at Koala North; wedge and slab failure mechanisms in the back were identified. The largest wedge identified was 40 m^3 with a factor of safety of zero, as it would fall from the back. While stresses may keep this wedge in place, blasting effects may open joints and initiate failure.

A primary rock bolting pattern with wire mesh is recommended to support the back. Based on a preliminary analysis it was recommended that 2.4 m, 19 mm diameter resin grouted rebar rock bolts should be used due to their simplicity and effectiveness. This artificial support will control the failures and allow the operation of underground mining activities to occur safely and without interruption.

It should be restated that the structural database and modelled structural domains have been based solely on oriented joint data with a 10 m maximum trace length. Large-scale features such as faults have not been accounted for in any of the analyses. These discrete features may allow much larger failures to occur than are possible from jointing alone.

Blasting effects on stability have also not been characterized. Blasting practices can have a negative impact on the stability of wedges and toppling blocks. Large vibrations and heaving due to gas penetration into the joints may initiate failure in otherwise stable blocks.

It is hoped that results from the thesis objectives will allow a better understanding of the geologic structure and its implications for stability at the Ekati™ Diamond Mine.

10.2 Recommendations

Based on the work performed for this thesis some recommendations were noted which are thought to improve data collection processes and analysis procedures currently in use at the Ekati™ mine.

10.2.1 Data Collection and Processing

- Orientation information is critical for addressing stability issues in the Ekati™ environment. Accordingly, it is recommended that the clay bomb orientation technique be employed more often than every 3rd run, perhaps every 2nd run and as often as even every run (3.048 m or 10 ft) in poor ground conditions.
- Care must be taken to note which goniometer convention is being used. Use of computer software may require conversion to different systems. This must be done with care as an improper conversion may lead to serious errors in joint set characterization.
- Additional effort should be put forth to ensure the consistency of reported results between different individuals. Improved standardized training for new loggers would be beneficial.
- Most holes drilled to great depth have been used to establish the granite/kimberlite contact. The blind zone of drill holes at this orientation is such that potential structures contributing to wall instability are not captured. While expensive, it is recommended that some holes be drilled opposite or perpendicular the wall dip direction in order to delineate structures in the blind zones of the contact holes.

- When core logging and cell mapping, joints should be characterized by either the Laubscher (1990) mining rock mass rating (MRMR) system or the Barton (1985) joint roughness coefficient (JRC). Use of a common system will readily allow direct comparison between collection methods.
- Concerning cell mapping, more precision and detail is needed when approximating joint trace lengths, as it is not possible to estimate this parameter from core logging. This would allow a much more accurate prediction of failure volumes.
- Use of virtual cell mapping techniques should be limited to post failure analysis of discrete structures, until identification of joints perpendicular to bench faces is improved.
- Raw joint data should be entered into a similar spreadsheet, regardless of collection method; this eases data comparison and transformation.
- Calculation of true joint orientations from goniometer measurements should be performed in the spreadsheet; this removes dependency on secondary programs to complete the transformation. True orientations are required in spreadsheet form as input for structural domain delineation calculations.
- A comprehensive database containing all geotechnical data should be created and maintained.

10.2.2 Determining Structural Domains and Joint Sets

- Diamond drill core logging data should be used as input for the structural domain boundary delineation method proposed.
- Cell mapping should be used to supplement the domain results by providing additional information on localized jointing and instability issues.
- Cell mapping is particularly important for identifying large-scale features, such as faults. Features identified by cell mapping are also discrete, whereas joint sets within structural domains determined from diamond drill core logging data are considered to be ubiquitous.

- The Laubscher (1990) B parameter must be converted to an equivalent Barton (1985) JRC parameter in order to determine the equivalent joint roughness angle. A relation was proposed for this conversion.

10.2.3 Stability Analysis for Underground Excavations

- As mentioned in the summary, a total joint friction angle of 70° was the norm for sets at Ekati™. This angle is quite high and has no built-in factor of safety. It is therefore not recommended for use in design.
- Stability analysis was based on joint data with a maximum trace length of 10 m and did not take into account the existence of faults in the area. The presence of these features may allow much larger failures to occur. It is recommended that separate stability analyses on these discrete features be carried out.
- Instability effects due to blasting practices must be considered. As this aspect was not taken into account, the findings in this thesis are not conservative in that respect.
- Additional research should be done to determine the effectiveness of optical methods for large-scale rock mass movement monitoring.

Employing these recommendations will allow a better understanding of the geologic structure and its implications for stability at the Ekati™ Diamond Mine.

Chapter 11

References

Andersland, O.B. and Ladanyi, B. 1994. An introduction to frozen ground engineering. Chapman and Hall, New York.

Anonby, D. 2002. Personal Communication.

Ashton Mining of Canada Inc. 2002. The genesis of diamonds. (Online). Available: http://www.ashton.ca/fundamentals/thegenesis/genesis.html (Dec. 2002).

ASTM D 6032-96. 2001. Standard test method for determining rock quality designation (RQD) of rock core. American Society for Testing and Materials.

Aviation Adventure Tours. 2002. Kimberley and the big hole. (Online). Available: http://www.funflight.net/Africa/South_Africa/Kimberley.htm (Feb. 2003).

Barton, N., Bandis, S. and Bakhtar, K. 1985. Strength, deformation and conductivity of rock joints. International Journal of Rock Mechanics and Mining Sciences and Geomechanics Abstracts, **22**(3): 121-140.

Beer, A.J. 2002. JRC evaluation by visual comparison (stage 2). (Online). Available: http://www.ex.ac.uk/~ajbeer/geomechanics/jrctest.htm. (Dec. 2002).

Brady, B.H.G. and Brown, E.T. 1993. Rock mechanics for underground mining. 2nd edition. Chapman and Hall, Great Britain.

Call, R.D., Savely, J.P. and Pakalnis, R. 1982. A simple core orientation technique. *In* 3rd International Conference on Stability in Surface Mining. *Edited by* C.O. Brawner.

American Institute of Mining, Metallurgical, and Petroleum Engineers, New York, pp. 465-481.

Choquet, P. 1991. Rock bolting practical guide. Canada Communication Group – Publishing, Ottawa.

Cravero, M., Iabichino, G. and Mahtab, A. 1991. A comparison of procedures for defining orientation domains in jointed rock. *In* Proceedings of the 32nd U.S. Symposium on Rock Mechanics as a Multidisciplinary Science. *Edited by* J.C. Roegiers. A.A. Balkema, Rotterdam, pp. 1095-1103.

De Beers Canada. 2003. Canada: a diamond producing nation. (Online). Available: http://www.debeerscanada.com/files/canada-2.html (Feb. 2003).

Deere, D.U. 1964. Technical description of rock cores for engineering purposes. Rock Mechanics and Rock Engineering, **1**: 17-22.

Dershowitz, W., Busse, R., Geier, J. and Uchida, M. 1996. A stochastic approach for fracture set definition. *In* Proceedings of the 2nd North American Rock Mechanics Symposium on Rock Mechanics Tools and Techniques. *Edited by* M. Aubertin, F. Hassani and H. Mitri. A.A. Balkema, Rotterdam, pp. 1809-1813.

Deutsch, C.V. 2002. Geostatistical reservoir modelling. Oxford University Press, New York.

Dufresne, M.B., Olson, R.A., Schmitt, D.R., McKinstry, B., Eccles, D.R., Fenton, M.M., Pawlowicz, J.G., Edwards, W.A.D. and Richardson, R.J.H. 1994. The diamond potential of Alberta: a regional synthesis of the structural and stratigraphic setting, and other preliminary indications of diamond potential. Alberta Research Council. Open File Report 1994-10, p. 62-68.

Elsworth, D. 1986. Wedge stability on the roof of a circular tunnel: plane strain condition. International Journal of Rock Mechanics and Mining Engineering, **23**(2): 117-181.

Harvey, P.J. 2003. Starting Koala North – North America's first underground diamond mine. (Online). Available: http://www.cim.org (April 2003).

Hudson, J.A. and Harrison, J.P. 1997. Engineering rock mechanics: an introduction to the principles. Pergamon.

Hume, H.R., West, T.R. and Judd, W.R. 1982. A new technique for domain delineation of rock mass discontinuities. *In* Proceedings of the 23rd Symposium on Rock Mechanics. *Edited by* R.E. Goodman and F.E. Heuze. American Institute of Mining, Metallurgical, and Petroleum Engineers, New York, pp. 104-115.

Issaks, E.H. and Srivastava, R.M. 1989. An introduction to applied geostatistics. Oxford University Press, New York.

Kulatilake, P.H.S.W., Wathugala, D.N., Poulton, M. and Stephansson, O. 1990. Analysis of structural homogeneity of rock masses. Engineering Geology, **29**: 195-211.

Laubscher, D.H. 1990. A geomechanics classification system for the rating of rock mass in mine design. Journal of the South African Institute of Mining and Metallurgy, **90**(10): 257-73.

MacLaughlin, M.M., 2002. Roof wedge stability; a simple analytical model and numerical validation. *In* Proceedings of the 37th Symposium on Engineering Geology and Geotechnical Engineering. *Edited by* S. Sharma and J.H. Hardcastle. Pages 181-190.

Mah, S.G.L., Pakalnis, R.T., Poulin, R. and Clark, L.M. 1995. Obtaining quality cavity monitoring survey data. *In* Proceedings of the 3rd Canadian Conference on Computer Applications in the Mineral Industry. Pp. 400-407.

Mahtab, M.A. and Yegulalp, T.M. 1982. A rejection criterion for definition of clusters in orientation data. *In* Proceedings of the 22nd Symposium on Rock Mechanics. *Edited by* R.E. Goodman and F.E. Heuze. American Institute of Mining, Metallurgical, and Petroleum Engineers, New York, pp. 116-123.

Mahtab, M.A. and Yegulalp, T.M. 1984. A similarity test for grouping orientation data in rock mechanics. *In* Proceedings of the 25th Symposium on Rock Mechanics. *Edited by* C.H. Dowding and M.M. Singh. American Institute of Mining, Metallurgical, and Petroleum Engineers, New York, pp. 495-502.

Marcotte, E. and Henry, E. 2002. Automatic joint set clustering using a mixture of bivariate normal distributions. International Journal of Rock Mechanics and Mining Sciences **39**: 323-334.

Mathis, J.E. 1998. Panda pit slope design. URSA Engineering, Ellensburg.

Mathis, J.E. 1998. Koala preliminary pit slope analysis. URSA Engineering, Ellensburg.

Mathis, J.E. 2000. Koala north preliminary pit slope evaluation. URSA Engineering, Ellensburg.

Mathis, J.E. 2002. Fox pipe – preliminary pit slope evaluation. URSA Engineering, Ellensburg.

Mery, H. 2002. Metodo Sublevel Caving. (Online). Available: http://plata.uda.cl/minas/academicos/hmery/sub%20level%20caving.html (Dec. 2002).

Miller, S.M. 1983. A statistical method to evaluate homogeneity of structural populations. Mathematical Geology, **15**: 317-328.

Mining Technology. 2002. Ekati diamond mine, Canada. (Online). Available: http://www.mining-technology.com/projects/ekati/index.html#ekati1 (Dec. 2002).

Nicholas, D.E. and Sims, D.B. 2000. Collecting and using geologic structure data for slope design. *In* Slope Stability in Surface Mining. *Edited by* W.A. Hustrulid, M.K. McCarter and J.A.V.Z. Dirk. Society for Mining, Metallurgy, and Exploration, pp. 11-26.

O'Connor, K.M. and Dowding, C.H. 1999. Geomeasurements by Pulsing TDR Cables and Probes. CRC Press, Boca Raton.

Park, H.J. and West, T.R. 2002. Sampling bias of discontinuity origin caused by linear sampling technique. Engineering Geology, **66**: 99-110.

Pell, J. A. 1997. Kimberlites in the slave craton, Northwest Territories Canada. Geoscience Canada, **24**(2): 77-89.

Peterson, J.A. 2001. Blast damage mechanisms at Ekati™ mine. M.Sc. thesis, University of Alberta, Edmonton, AB.

Peterson, J., Tannant, D.D. and Todd, J. 2001. Wall control blasting practices at the Ekati™ diamond mine. Canadian Mining and Metallurgical Bulletin, **94**(1050): 67-73.

Priest, S.D. 1993. Discontinuity analysis for rock engineering. Chapman and Hall, London.

Roberts, G. and Poropat, G. 2002. Highwall joint mapping in 3-D at the Moura mine using SIROJOINT. CSIRO Exploration and Mining. (Online). Available: http://www.em.csiro.au/mine_environment_imaging/capabilities/index.html (April, 2003).

Rock, N.M.S. 1988. Numerical geology. Springer-Verlag, Berlin.

RocScience geomechanics software and research. 2003. DIPS help manual version 5.0. Toronto, Ontario.

Scheaffer, R.L. and McClave, J.T. 1995. Probability and statistics for engineers. Duxbury Press, Belmont.

Steffen Robertson and Kirsten Consulting Engineers. 1995. Preliminary evaluation of underground mining methods in NWT kimberlite Pipes. Report #B104207.

Steffen Robertson and Kirsten Consulting Engineers. 2000. Koala north underground feasibility phase I mining method selection and design. Report #2CB010.00.

Stillborg, B. 1994. Professional users handbook for rock bolting. 2nd edition. Trans Tech Publications, Germany.

Stimpson, B. 1981. A suggested technique for determining the basic friction angle of rock surfaces using core. International Journal of Rock Mechanics and Mining Sciences and Geomechanics Abstracts, **18**:63-65.

Tannant, D.D. and Wang C. 2003. Predictions of rock fall trajectories using discrete element and lumped mass modelling methods. *In* 3rd Canadian Conference on Geotechnique and Natural Hazards. On CD.

Terzaghi, R.D. 1965. Sources of error in joint surveys. Geotechnique, **15**: 287-304.

Norrish, N.I. and Wyllie, D.C. 1996. Rock slope stability analysis. *In* Landslides – Investigations and Mitigation. Special Report 247. Transportation Research Board. *Edited by* A.K. Turner and R.L. Schuster. National Academy Press, pp. 391-425.

Werniuk, J. 2003. Beneath the surface: get down – Canada's first diamond miner moves underground. Canadian Mining Journal, **124**(2): 17-20.

Chapter 12

Appendices

The Appendices provide figures and tables referred to, but not included in, the main body of the thesis.

12.1 Joint Roughness Table and Figures

Table 12-1 Alphanumeric to Numeric Laubscher Parameter Conversions (modified from Anonby, 2002)

A Parameter (Large-scale, shape)			
Symbol	Description	Numeric Range	Equiv. Value
P	Planar	70-79	75
C	Curved	80-84	80
W	Wavy	85-89	85
U	Undulating	90-94	90
S	Stepped	95-99	95
I	Irregular	100	100

B Parameter (Small-scale, roughness)			
Symbol	Description	Numeric Range	Equiv. Value
S	Smooth	60-84	75
K	Slickensided	85-94	85
R	Rough	95-99	95
V	Very rough	100	100

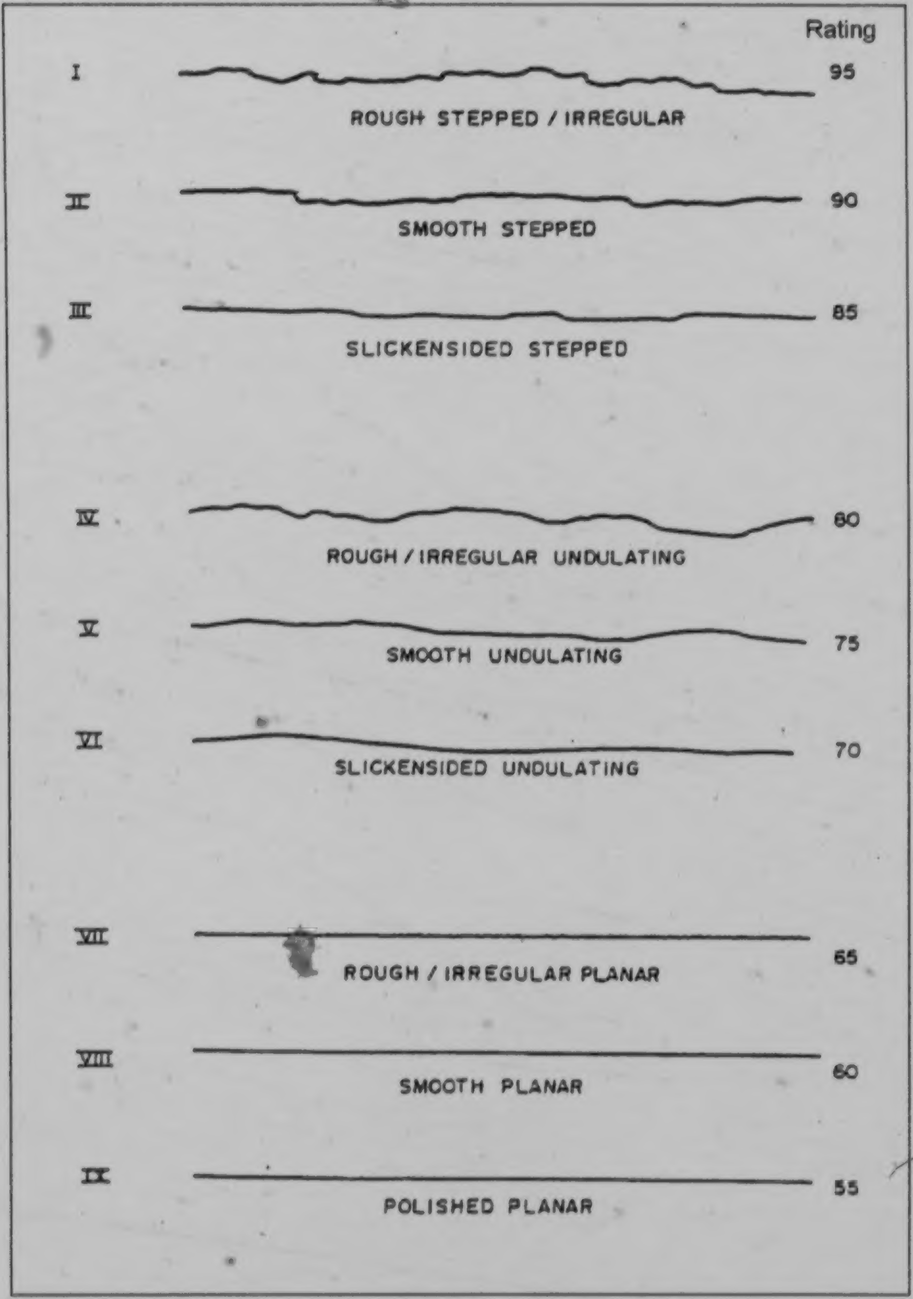
Rating
I
95
ROUGH STEPPED / IRREGULAR
II
90
SMOOTH STEPPED
III
85
SLICKENSIDED STEPPED
IV
80
ROUGH / IRREGULAR UNDULATING
V
75
SMOOTH UNDULATING
VI
70
SLICKENSIDED UNDULATING
VII
65
ROUGH / IRREGULAR PLANAR
VIII
60
SMOOTH PLANAR
IX
55
POLISHED PLANAR

Figure 12-1 Laubscher B Parameter Small-Scale Roughness Profiles (modified from Laubscher, 1990)

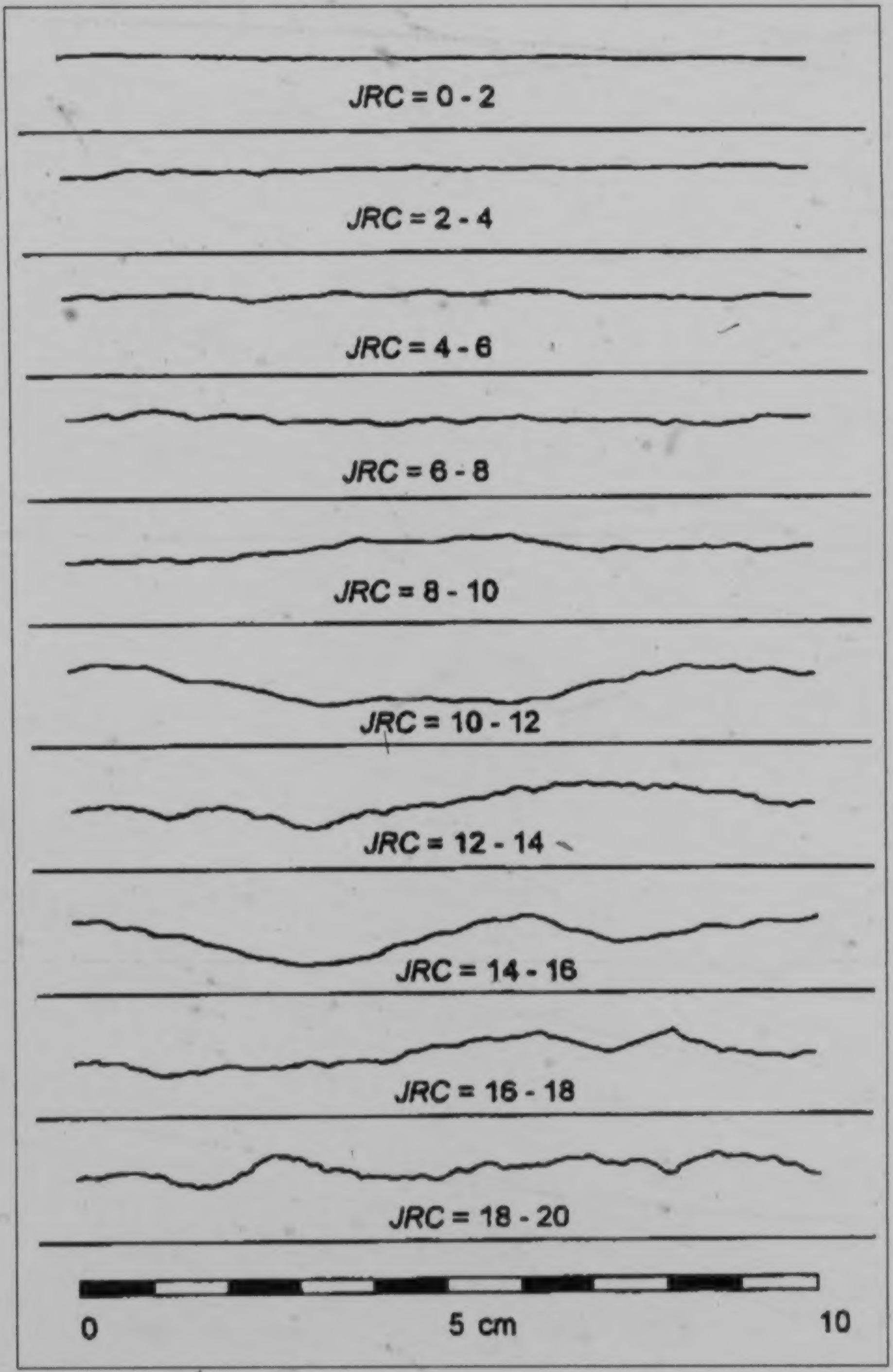
JRC = 0 - 2
JRC = 2 - 4
JRC = 4 - 6
JRC = 6 - 8
JRC = 8 - 10
JRC = 10 - 12
JRC = 12 - 14
JRC = 14 - 16
JRC = 16 - 18
JRC = 18 - 20
0
5 cm
10

Figure 12-2 Barton JRC Roughness Profiles (modified from Beer, 2002)

12.2Vector Mathematics for Joint Orientation Determination

Table 12-2 Vector Solution to Determine Fracture Orientation from Goniometer Measurements (from Call et al., 1981)

Determination of Dip Direction and Dip by Vector Solution

The input orientation data are

1) angle to core axis (α),
2) circumference angle (β),
3) bearing of drill hole (B), and
4) plunge of drill hole (P).

The circumference angle (β) would be the dip direction, if the hole were vertical and the top of the hole were north when the bottom end (B) of the core is inserted into the measuring box. If the top end (T) has been inserted, the circumference angle (β) must be subtracted from 360° before the conversions. The angle to the core axis (α) would be the complement of the fracture dip if the hole were vertical.

1) Conversion to lower hemisphere pole:

For bottom reading, $S = 180° + \beta$
For top reading, $S = 360° - \beta$
$D = 90° - \alpha$

2) Calculation of directional cosines:

$X = \cos S \sin D$
$Y = \sin S \sin D$
$Z = \cos D$

NOTE: The top of the hole is +X, east +Y, and down +Z.

3) Axis rotation for hole inclination:

$\phi = 90°$ - plunge of hole
$X' = X \cos \phi + Z \sin \phi$
$Y' = Y$
$Z' = Z \cos \phi - X \sin \phi$

4) Axis rotation for bearing of hole (Θ):

$X'' = X' \cos \Theta - Y' \sin \Theta$
$Y'' = Y' \cos \Theta + X' \sin \Theta$
$Z'' = Z'$

5) Conversion to dip direction and dip:

$A = \left| \mathrm{Tan}^{-1} \left(\frac{Y''}{X''} \right) \right|$

$Y'' > 0$ and $X'' \geq 0$ DDR $= A + 180$
$Y'' \geq 0$ $X'' \leq 0$ DDR $= 360 - A$
$Y'' \leq 0$ $X'' \geq 0$ DDR $= 180 - A$
$Y'' < 0$ $X'' \leq 0$ DDR $= A$

$\mathrm{Dip} = \cos^{-1} Z''$